universität wien

DISSERTATION

Titel der Dissertation

Neuronal circuitry for social behavior in female *Drosophila melanogaster*

verfasst von

Mag. Yang Wu BSc MSc

angestrebter akademischer Grad

Doctor of Philosophy (PhD)

Wien, 2013

Studienkennzahl lt. Studienblatt:	A 091 490
Dissertationsgebiet lt. Studienblatt:	Molekulare Biologie
Betreuer:	Dr. Barry Dickson

To my parents and Colleen, for their love and support.

Acknowledgements

This work could not have been completed without the support and help of many people.

Barry Dickson conceived the neuronal activation screen and ovipositor-extrusion project and provided constant support and supervision throughout my PhD.

Tianxiao Liu introduced me to fly basic husbandry and brain dissection and staining techniques. Anne von Philipsborn established the set-up for neuronal activation. Salil Bidaye initiated the activation screen with the VT library and afterwards shared the neuronal activation screen project. David Mahringer performed the epistasis screen to suppress female following behavior. Tianxiao Liu and Jai Yu helped in setting up the image registration system. Christian Machacek developed the Matebook tracking software. Attila maintained lab stocks and organized food orders every week. Katarina Bartalska helped with ordering and other stuff. Karin Panser helped with my fly work. Pawel Pasierbek from BioOptics helped with imaging and microscopes. Martin Columbini and David Kummerer from IMP workshop built different assay setups. Ines Ribeiro Martins Alves, Josh Lillvis, Tianxiao Liu, Anne von Philipsborn, Mark Palfreyman and Barry Dickson provided valuable feedback and comments on my thesis.

My PhD committee members, Simon Rumpel, Kristin Tessmar and Jürgen Knoblich monitored my progress throughout my PhD and provided helpful suggestions. All service departments of IMP/IMBA provided indispensible support. All current and past members of Dickson lab created a great working and social atmosphere with invaluable scientific discussions and support during my PhD.

Table of Contents

Synopsis

Social behavior is an evolutionarily advantageous strategy across different species ranging from single-celled microbes to human beings. Although various social behaviors have been well documented, the underlying neural substrates and mechanisms remain largely unknown. The objective of this thesis is to identify the neuronal circuitry for social behavior by exploiting the powerful genetics of *Drosophila melanogaster*. We are primarily interested in investigating the neural basis of two social behaviors displayed by female *Drosophila*: following (a common motif in both aggression and aggregation) and the rejection response (or ovipositor extrusion) during courtship. We performed a neuronal activation screen with an enhancer-bashing GAL4 library using a thermo-sensitive cation channel dTrpA1. GAL4 lines that induced various ectopic behaviors upon activation were identified. For the female following behavior, we used a stochastic labeling approach and intersectional genetics to identify the underlying neurons. We identified a female-specific neuronal cluster, named pMP8, and characterized it anatomically, molecularly and behaviorally. Furthermore, in order to identify the downstream partners of pMP8, we performed an epistasis screen by activating pMP8 with dTrpA1 while simultaneously silencing various neurons. Using intersectional approach, we obtained driver lines with more restricted expression pattern and observed an ellipsoid-body neuron commonly targeted by several lines. For ovipositor extrusion, three neuronal clusters were identified as candidates, including an ascending neuron, a local interneuron and a motor neuron. The ascending neuron seems to be required for female receptivity while the functions of the other two remained to be characterized. This study provides an entry point into the mapping and understanding of the neuronal circuitry for social behavior in *Drosophila* females.

Zusammenfassung

Soziales Verhalten ist eine evolutionär erfolgreiche Strategie und tritt bei diversen Lebewesen auf, von einzelligen Mikroben bis zum Menschen. Verschiedene soziale Verhaltensweisen sind gut dokumentiert, die ihnen zugrundeliegenden neuronalen Substrate und Mechanismen sind allerdings zum Großteil unbekannt. Das Ziel dieser Arbeit ist es, mit Hilfe genetischer Methoden in *Drosophila melanogaster* neuronale Schaltkreise für Sozialverhalten zu identifizieren. Wir sind hauptsächlich an zwei sozialen Verhaltensweisen interessiert, die das Drosophilaweibchen an den Tag legt: der Situation, in der eine Fliege der anderen während aggressiven Verhalten und dem Balzverhalten folgt (Folgeverhalten) und dem Ablehungsverhalten während der Balz (gekennzeichnet durch Ausstrecken des Ovipositors). Ziel war es, die neuronalen Grundlagen dieser Verhaltensweisen zu verstehen. Es wurde ein neuronaler Aktivierungsscreen einer enhancer tile GAL4 Bibliothek mit dem thermosensitiven Kationenkanal TrpA1 durchgeführt. Wir identifizierten GAL4 Linien, die in Neuronen exprimieren, deren Aktivität unterschiedliche künstlich hervorgerufene Verhaltensweisen auslösen. Für das weibliche Folgeverhalten wurden genetische Strategien (stochastische Markierung und intersektionale Methoden) angewandt, um die auslösenden Neuronen zu identifizieren. Es wurde die geschlechtsspezifische Neuronenklasse pMP8 identifiziert und anatomisch, molekular und verhaltensbiologisch untersucht. Um Neurone zu finden, die postsynaptisch mit pMP8 verbunden sind, wurde ein neuronaler Epistasisscreen durchgeführt, in dem pMP8 mittels dTrpA1 aktiviert wurde und gleichzeitig verschiedene Neurone inaktiviert wurden. Mit intersektionalen Methoden wurden driver Linien gefunden, die nur wenige Neuronen markieren. Mehrere dieser Linien exprimieren im selben Neuronentyp im Fächerkörper (ellipsoid body) des Gehirns. Drei neuronale Klassen wurden als Kandidaten für die Steuerung des Ausstreckens des Ovipositors gefunden: ein vom Ventralganglion ins Gehirn aufsteigendes Neuron, ein lokales Interneuron und ein Motorneuron. Das aufsteigende Neuron ist potentiell für die weibliche Rezeptivität erforderlich, die Funktionen der anderen Neuronen sind noch unerforscht. Die vorliegende Arbeit liefert wichtige Grundlagen, um neuronale Schaltkreise für soziales Verhalten in Drosophilaweibchen zu entschlüsseln und in ihrer Funktionsweise zu verstehen.

Chapter 1. Neuronal activation screen

1.1 Background

1.1.1 Studying neural basis of behaviors in *Drosophila melanogaster*

Animal behaviors are shaped by evolution to meet the challenges posed by environmental and physiological constraints. Behaviors are composed of observable actions that animals select to interact with their environment in response to external or internal stimuli based on individual experience. A major task of neuroscience is to understand how sensory information is processed, stored and integrated by neural circuits to guide animals appropriately for such action selection, and thus behavior. Although much progress has been made since the inception of modern neuroscience, this task is still far from accomplished.

The greatest obstacle that has hindered such understanding lies in the formidable inherent complexities of the nervous systems, which may soar to 10^{10} neurons and 10^{14}-10^{15} synapses in human (Herculano-Houzel, 2009). This raises technical challenges in identifying and characterizing individual neurons and their interconnections. So far, a complete mapping of neurons and synapses (connectome) has only been achieved by using electron microscopy in *Caenorhabditis elegans* which has only 302 neurons and around 5000 synapses (White et al., 1986). Although it is possible to restrict analyses to peripheral regions (i.e. sensory or motor circuits) or by investigating simpler organisms with reduced complexity, it narrows the range of questions that can be asked. Furthermore, once a neuron is identified, how one re-visits the same cell among so many other cells reproducibly remains demanding. One strategy that has emerged over the last two decades is to take advantage of genetic tools in model organisms to target specific neuronal populations. This, in theory, allows one to gain access to neural elements reproducibly at cellular level into the central nervous system and address questions regarding mechanisms underlying complex behaviors.

Drosophila melanogaster is a popular model organism and has been established for more than a century. It has a relatively small number of neurons but a rich reservoir

of behavior paradigms. With the rich armory of genetic toolbox available, *Drosophila* is ideally suited for studying the mechanisms of behaviors at molecular, cellular and circuitry levels, and has been successfully employed to advance our knowledge in this area (Simpson, 2009; Venken et al., 2011). Exogenous expression systems, such as GAL4-UAS system (Brand and Perrimon, 1993; Fischer et al., 1988), have been introduced into *Drosophila* and widely applied for expressing reporter or effector genes in neurons to visualize their morphology and to monitor or manipulate their activity. Spatial (e.g. GAL80 or split-GAL4 system) or temporal (e.g. MARCM or Flp-out) intersectional approaches allow further refinement of expression to specific populations (Lee and Luo, 2001; Luan et al., 2006; Suster et al., 2004). An array of behavioral assays have been established and well documented, such as courtship, aggression, and olfactory conditioning (Demir and Dickson, 2005; Siegel and Hall, 1979; Tully and Quinn, 1985; Yapici et al., 2008; Yurkovic et al., 2006).

1.1.2 Anatomy of the central nervous system in *D. melanogaster*

The central nervous system of *Drosophila melanogaster* is estimated to have about 100,000 neurons, equally distributed between two optic lobes, the central brain and the ventral nerve cord (VNC). Unlike vertebrates, the outside surface of the nerve tissues is occupied by the cell bodies and the inside is composed of synaptic neuropils formed by neurites projected from the surface and compartmentalized by glial sheaths and axon tracts. Canonical neuropeptides and neurontransmitters, such as acetylcholine, GABA, glutamate, histamine, serotonin, dopamine, tyramine, and octopamine, are used in flies (Simpson, 2009).

The brain and the VNC are the two main structures consisting of fused ganglia and are connected by descending and ascending fibers from around 3600 neurons. The central brain consists of the two optic lobes, the protocerebrum, and the subesophageal ganglion (SOG). Visual, olfactory, gustatory, and auditory inputs are sensed by respective sensory organs and sent to processing centers in optic lobe, antennal lobe (AL), SOG, and the antennal mechanosensory and motor center (AMMC), respectively (Figure 1.1A and B) (North and Greenspan, 2007). Further integration and processing centers are thought to happen in higher order structures such as the mushroom body (MB) and the central complex consisting of the fan-

shaped body (FB), the ellipsoid body (EB) and the paired noduli (NO) (Strauss, 2002a; Zars, 2000). The ventral nerve cord consists of the thoracic ganglion and the abdominal ganglion. The former can be further sub-divided into three pairs of neuromeres, the prothoracic, the mesothoracic (leg and wing), and the metathoracic ganglions which are innervated by sensory neurons corresponding to each pair of the appendages (Figure 1.1 C and D). Additionally, the VNC also contains muscle-innervating motoneurons, premotor neurons and various other interneurons.

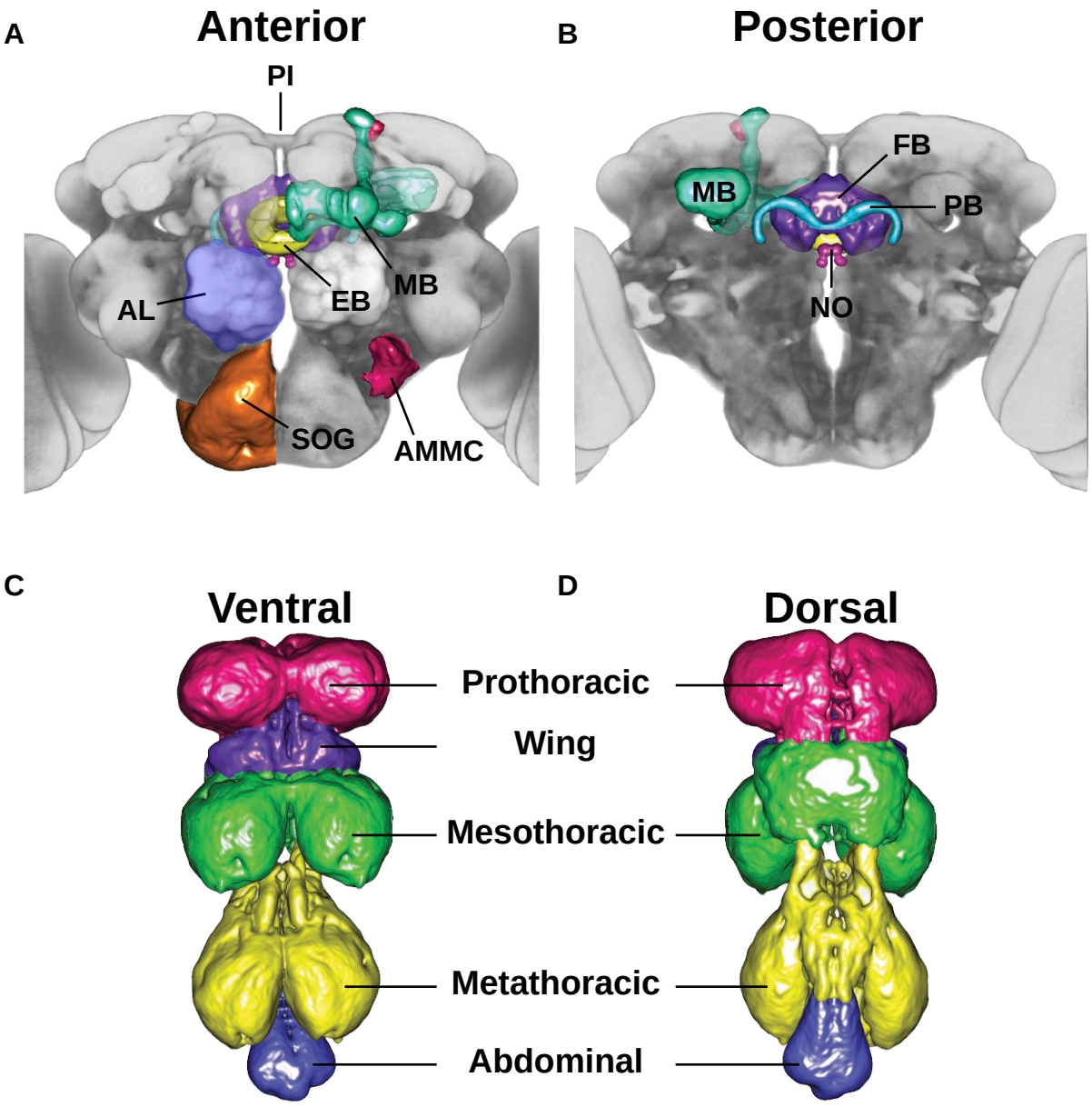

Figure 1.1 Organization of the nervous system of *D. melanogaster*
(adpated from Yu, J.Y., 2009)

1.1.3 Genetic resources for neuronal access in *D. melanogaster*

One of the biggest advantages of studying neural circuits underlying behavior in *Drosophila* is the extensive list of genetic tools available, which allows unprecedented genetic access to diverse neuronal classes and provides flexible means to character them. An initial step that paved ways for the development of such tools was the discovery of P-elements and their subsequent use in *Drosophila* transgenesis (Rubin and Spradling, 1982), which made random insertion of foreign genetic materials into *Drosphila* genome possible. Another essential advancement that allowed efficient site-specific transgenesis was the recent adoption of bacteriophage φC31 integrase (Groth et al., 2004), which catalyzes stable recombination between *attpB* and *attP* sites (Thorpe and Smith, 1998). This technique allows to control for the position effects, i.e. the influence that the local genomic environment exerts on transgene expression (Lewis, 1950; Wilson et al., 1990).

The use of genetic tools for providing access to defined neuronal populations started with the use of the binary GAL4-UAS (upstream activation sequence) system (Brand and Perrimon, 1993; Fischer et al., 1988). This system utilizes the yeast transcription factor GAL4's DNA binding specificity to an UAS and its transcription stimulating properties. By placing GAL4 under the influence of neuronally expressed enhancers and transgenes of choice under the control of an UAS, one can combinatorially express any gene of interest in a variety of neuronal populations targeted by respective GAL4 lines. The transgene of interest can be chosen for various applications, including visualizing a neuron, monitoring its activity, and silencing or stimulating it. This binary expression system eliminates the need for generating excessive fly stocks and proves to be extremely flexible and efficient. Thus, one can generate a large collection of different GAL4 lines to be used in different applications with an independent collection of UAS stocks.

Using similar strategy, several other binary expression systems have been developed, including the LexA-LexAop system from bacteria (Lai and Lee, 2006; Pfeiffer et al., 2010), the QF/QS-QUAS system from fungi (Potter et al., 2010), the Tet-On (Bieschke et al., 1998; Stebbins et al., 2001) and Tet-Off system from bacteria (Bello et al., 1998; Stebbins and Yin, 2001), and the Hap1-HBS system from

yeast (Hasemeyer, M. and Dickson, B.J., unpublished). These systems were developed with stringent specificity, thus allowing expression of different reporters or effectors in independent neuronal populations.

To allow GAL4 or other activators (LexA, QF, Hap1, ect.) to be expressed in different neuronal populations, two main strategies have been developed to generate driver lines: enhancer trap and enhancer bashing (Figure 1.2). The enhancer trap strategy was traditionally used to create large collections of GAL4 lines rapidly. It mobilizes and randomly integrates a modified P-element that contains the GAL4 coding sequence into different locations in the fly genome, thus bringing GAL4 under the control of various genomic enhancers (Brand and Perrimon, 1993). Although extremely efficient in creating large number of GAL4 lines, the method is limited by its broad expression due to the inability to control the numbers of enhancers that direct GAL4 expression. To alleviate this problem, the alternative enhancer bashing strategy was developed, in which small enhancer-containing genomic fragments are used to drive GAL4 expression and are integrated together in an enhancer-free genomic location with the help of φC31 integrase (Pfeiffer et al., 2008). By controlling the size of the genomic fragments, one can in theory adjust the numbers of enhancers that GAL4 is exposed to, thereby increasing or decreasing the spatial restriction of GAL4 expression. Additionally, because the enhancer-containing fragments are defined (i.e. DNA sequences are known) it is possible to subclone them into different vectors, such as alternative expression system, once a neuronal population of interest is identified.

Several methods have been developed to make use of the large collection of existing GAL4 lines to create drivers in alternative expression systems. The original P-element exchange method, which is based on the P-element's tendency to insert in excised P-element locus (Gloor et al., 1991; Sepp and Auld, 1999), can be used to replace GAL4 with a membrane marker (Berdnik et al., 2006) or other activators. Other systems that have developed for such purpose include MiMIC (**mi**nos-**m**ediated **i**ntegration **c**assette) (Venken et al.), G-MARET (**G**AL4-based **m**osaic-inducible **a**nd **r**eporter-exchangable **e**nhancer **t**rap) (Yagi et al.), InSITE (**in**tegrase **s**wappable **i**n vivo **t**argeting **e**lement) (Gohl et al., 2011) and recombineering method (Stowers, 2011).

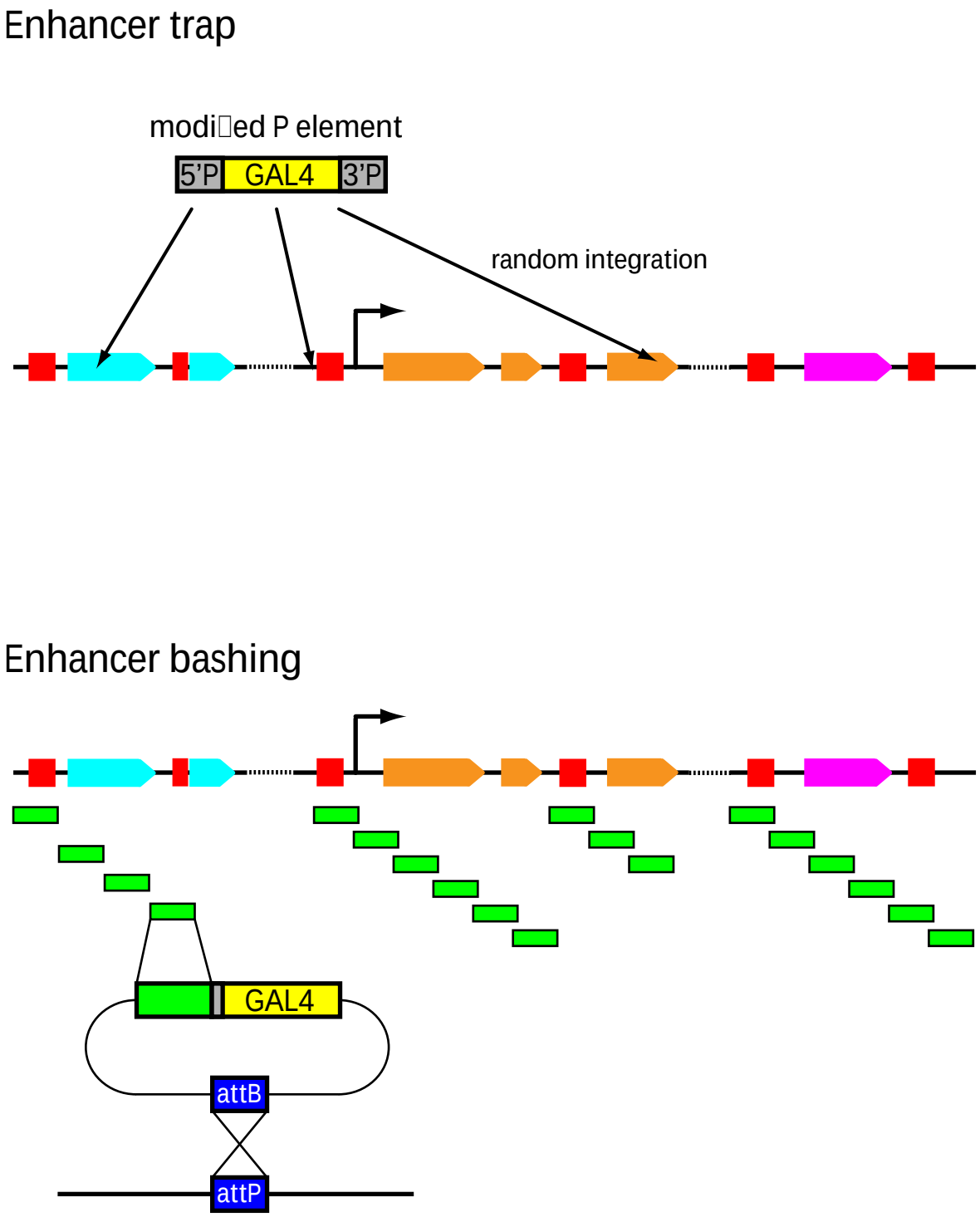

Figure 1.2 Generating GAL4 lines: enhancer trap vs. enhancer bashing

Further spatial refinement of expression is possible through intersectional strategies, such as the split-GAL4 system (Figure 1.3). The split-GAL4 system relies on the modular nature of GAL4 protein, which uses different functional domains for DNA-binding and transcription-activating activities (Brent and Ptashne, 1985). Therefore, the GAL4 protein can be separated into two independent polypeptides (Keegan et al., 1986) which can be associated to reconstitute GAL4 activity when facilitated by protein-protein interactions (Fields and Song, 1989). It has been demonstrated that by fusing a leucine zipper to the DNA-binding domain (ZpGAL4DBD) and the activation domain (ADZp) and expressing them under separate enhancers, one can restrict restored GAL4 transcriptional activity to the overlapping neurons where both domains are expressed (Luan et al., 2006). This system has been further optimized to enhance level of expression by using the p65 activation domain (Pfeiffer et al., 2010).

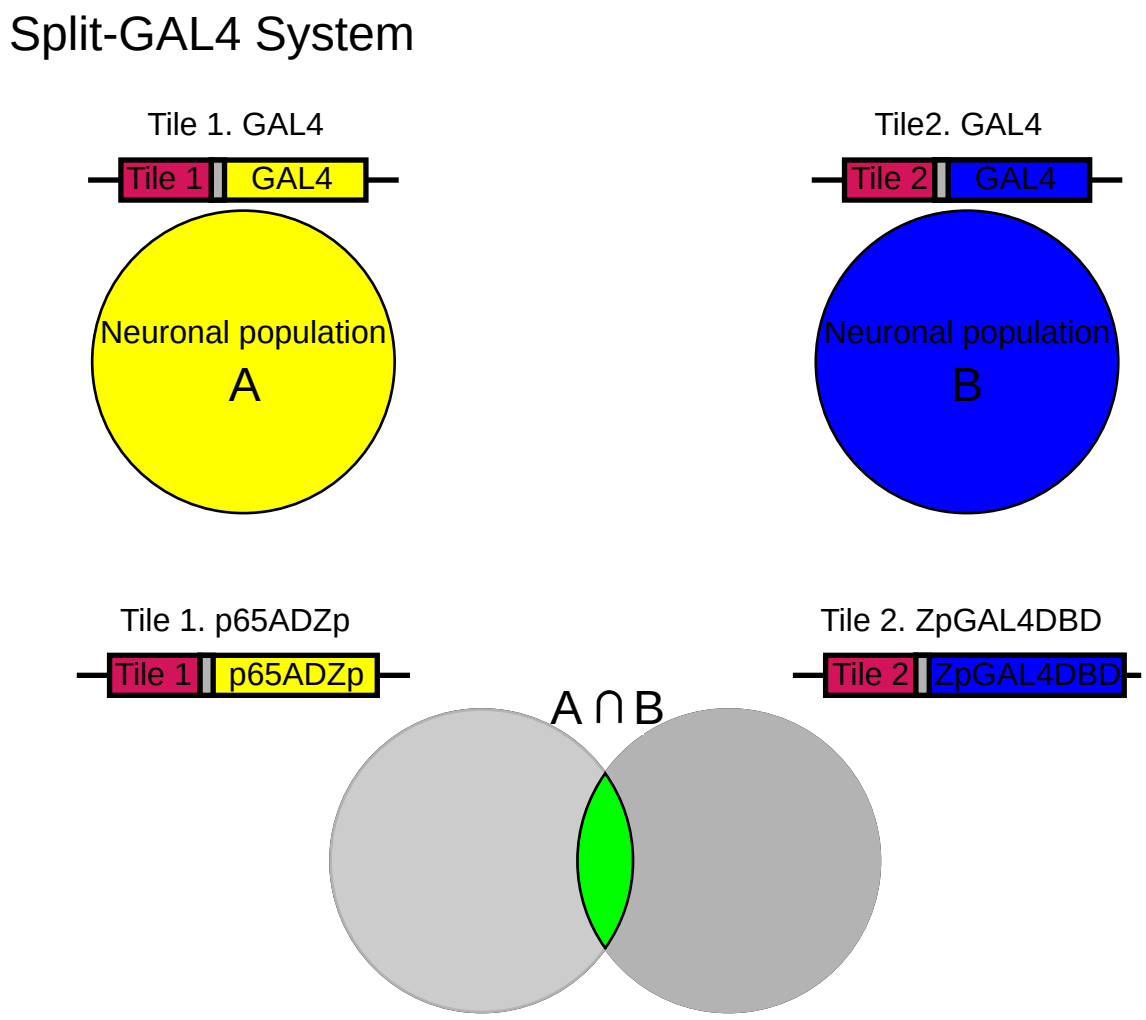

Figure 1.3 Intersectional genetics with Split GAL4 system

Another intersectional method is the targeted suppression of GAL4 activity by GAL80. The GAL80 protein inactivates GAL4 by binding to its activation domain and preventing its interaction with the transcription machinery in yeast (Traven et al., 2006) and does so in flies as well, presumably in a similar manner (Lee and Luo, 2001). Therefore, this allows targeted suppression of GAL4 activity in a subset of cells where GAL80 is expressed. By combining with GAL80 lines driven by different enhancers, expression of GAL4 drivers can be restricted to different subsets that can be used further for comparative analysis.

Utilizing the GAL4/GAL80 repressible system, the mosaic analysis with a repressible cell marker (MARCM) was developed by combining tub-GAL80 with hs-FLP/FRT (Figure 1.4 A). Initially designed for studying gene functions in neuronal morphogenesis in mosaic animals (Lee and Luo, 1999), this system permits neuronal lineage analysis and temporal refinement of GAL4 expression (Lee and Luo, 2001). In this system, GAL4 expression is constitutively suppressed by the ubiquitously expressed GAL80. Heat shock performed at different developmental stage induces expression of FLP which may recombine the chromosomes between two homologous FRT sites during mitosis. Being placed distal to the FRT site on the same chromosome, tub-GAL80 can be removed during mitotic recombination, thus creating GAL80-minus daughter cell(s) where suppression of GAL4 activity is relived (Lee and Luo, 1999). In *Drosophila*, neuroblasts (Nb) undergo asymmetric cell division to generate another neuroblast and a ganglion mother cell (GMC) which subsequently divides into two neurons (Goodman and Doe, 1993). Depending on which cell type contains GAL80-minus chromosomes after mitotic recombination, clones of multiple cells ($GAL80^-$ neuroblast), two cells ($GAL80^-$ ganglion mother cell) or one cell ($GAL80^-$ neuron) will be labeled (Lee and Luo, 2001) (Figure 1.4 A). A drawback of the MARCM system is that only one of the daughter cells will be marked after mitotic recombination. To bypass this problem, twin-spot MARCM (Yu et al., 2009a) and twin-spot generator (Griffin et al., 2009) have been developed to permit labeling of both daughters, in which two fluorescent proteins that are either suppressed by two short hairpin RNAi (mir) or split in halves are reconstituted after FLP-mediated recombination (Figure 1.4 B and C).

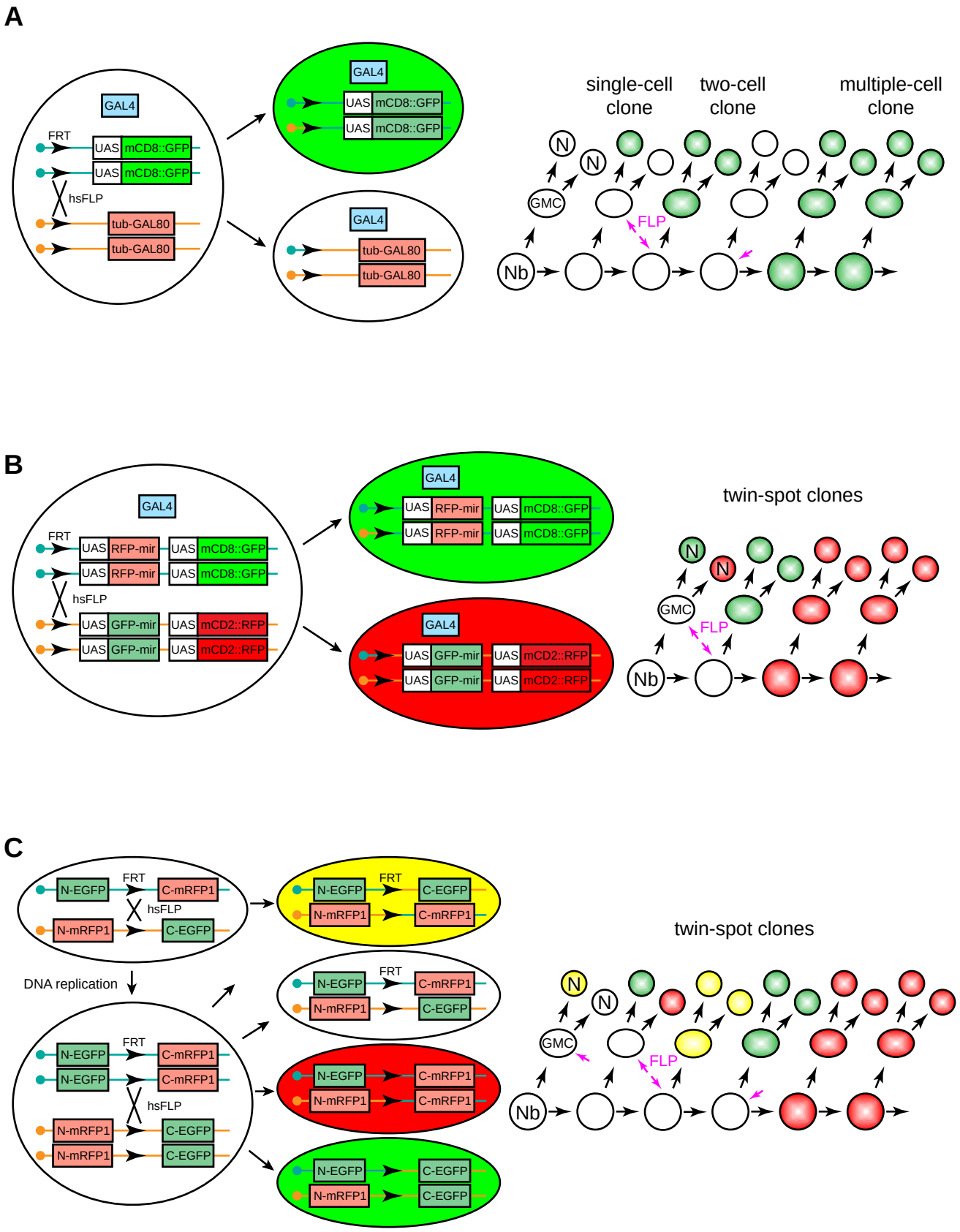

Figure 1.4 Mosaic analysis techniques to label neuronal clones

The FLP recombinase can also be used to induce intrachromosomal recombinations between FRT sites. Based on this, Flp-out methods have been developed to intersect two neuronal populations by driving FLP expression in one population and a UAS-FRT-Stop-FRT-reporter or effecters in the other (Horn and Handler, 2005).

1.1.4 VT library: a large collection of GAL4 lines and more

Due to aforementioned limitations of currently available enhancer-trap GAL4 drivers, a library of GAL4 lines has been generated in the lab using an enhancer-bashing strategy that has been previously described (Pfeiffer et al., 2008), with an aim of obtaining more restricted expression patterns.

The entire *Drosophila* genome was divided computationally into 63,000 tiles of 2kb fragments with an overlap of 200-400 bp that potentially contain enhancer elements, with consideration of avoiding tiles splitting genomic regions with high conservation scores (Stark, A. and Dickson B.J., unpublished). These tiles were named as Vienna Tiles (VT) and numbered as VTxxxxx starting from the far end of the X chromosome. The cloned constructs were injected and integrated into attp2 landing site by φC31-mediated recombination (Bidaye, 2012; Bischof et al., 2007; Groth et al., 2004). At present, the collection consists of about 8800 GAL4 lines (Christopher, M., Bidaye, S., Fellner, M., Wandl, S., Stark A. and Dickson B.J., unpublished).

In addition to the GAL4 lines, a smaller collection of LexA and split-GAL4 drivers were also cloned from GAL4 constructs and injected similarly (Pfeiffer et al., 2010). Most of the LexA drivers and the p65ADZp semi-drivers were injected into attp40 landing site, and ZpGAL4DBD semi-drivers into attp2, to facilitate combinatorial usages between LexA and GAL4 lines and between split halves (Fellner, M., Wandl, S. and Dickson B.J., unpublished).

1.1.5 Genetic toolkits to visualize, monitor or manipulate neuronal activity

To visualize GAL4-expressing neurons, the most commonly used reporter is the membrane-targeted UAS-mCD8::GFP, which fused mouse lymphocyte marker CD8 with the green fluorescent protein (Lee and Luo, 1999). The transmembrane CD8

domain allows cell surfaces and neuronal processes, including axons and dendrites, to be labeled together. For visualization of subcellular compartments, fluorescent markers are fused to different markers that target different compartments. UAS-nSyt::GFP (Zhang et al., 2002) is frequently used for labeling axons and UAS-DsCam17.1::GFP (Wang et al., 2004) and UAS-DenMark (Nicolai et al., 2010) for soma and dendrites. Various other fused proteins have also been developed and employed in flies, such as UAS-myr-GFP (Pfeiffer et al., 2010; Ritzenthaler et al., 2000), UAS-CD2-RFP (Yu et al., 2009b) and UAS-mCD8-Tomato (Toda et al., 2012). Photo-activatible GFP has also been developed and used in neuronal tracing (Datta et al., 2008).

To monitor neuronal activity, many genetically encoded calcium indicators have been developed to measure calcium dynamics as a proxy for neuronal activity (Yasuda et al., 2004), among which the UAS-GCaMP is the most highly developed. The original version of GCaMP was created as a fusion protein of the calmodulin-binding domain from the myosin light-chain kinase, circular permutated EGFP and the calmodulin, which increases its green fluorescence intensity upon binding to Ca^{+} ions (Nakai et al., 2001). A number of improved variants of GCaMP have since been engineered (Akerboom et al.; Muto et al., 2011; Ohkura et al., 2005; Tallini et al., 2006; Tian et al., 2009), among which GCaMP6 is the most current version with optimized performance in sensitivity and kinetics.

To manipulate neuronal activities, many tools have been developed. The most commonly used are UAS-dTrpA1 for activation, and UAS-shibire^{ts1}, UAS-TNT and UAS-Kir2.1 for silencing. The dTrpA1 channel is a non-selective catioin channel that can be opened by changes in temperatures and functions as thermal sensors in flies. Ectopic expression of the dTrpA1 in flies is able to activate neurons upon increasing the ambient temperature (Rosenzweig et al., 2008) and has been used to trigger singing behavior in *Drosophila* males upon thermal activation (von Philipsborn et al., 2011). UAS-shibire^{ts1} expresses a temperature-sensitive (>29°C) dominant negative allele of dynamin that allows acute (≈1min) and reversible silencin g of neuronal activities (Kitamoto, 2001; Koenig et al., 1983). UAS-TNT or UAS-TeTxLC encodes the light chain of tetanus toxin and effectively blocks vesicle fusion at synapse by cleaving neural synaptobrevin (Sweeney et al., 1995). UAS-Kir2.1 expresses a

vertebrate inwardly rectifying potassium channel, which hyperpolarizes neurons and prevents them from firing action potentials (Baines et al., 2001; Paradis et al., 2001). Both UAS-TNT and UAS-Kir2.1 function constitutively without temporal control and therefore may cause defects during developmental stage.

1.1.6 Strategies for neuronal circuitry mapping in *D. melanogaster*

With the availability of the aforementioned genetic toolkit, several strategies have been devised to identify neuronal circuitry under behaviors in *Drosophila*, including anatomical, physiological and behavioral approaches. For example, one can anatomically trace neuronal connection from sensory inputs to higher order center by using photoactivatible GFP (Datta et al., 2008) or link neurons to a certain behavior using functional imaging such as GCaMP (Kohatsu et al., 2011). The strategy we took in this study was to examine behavioral changes upon neuronal manipulation. The advantage of this strategy lies in its efficiency to screen a large number of neuronal subpopulations to identify functional relevant neurons.

Generally, for a screen-based strategy, one can use either silencing or activation approach to manipulate neuronal activities. Silencing approach allows identification of neurons necessary for a certain behavior, but is limited by the number and types of assays one can perform. Activation, on the other hand, might lead to ectopic behaviors in the absence of appropriate sensory stimuli and therefore not rely heavily on the behavioral assays. In this study, we adopted neuronal activation strategy and test activation-induced behavioral changes of both isolated and paired flies.

1.2 Results

1.2.1 Activation screen identified behavior-triggering GAL4 lines

In order to identify neuronal circuitry for certain behaviors, we combined the enhancer GAL4 library (VT lines) and the heat-sensitive cation channel dTrpA1 (Hamada et al., 2008) and performed an unbiased screen to search for GAL4 lines that would induce interesting ectopic behaviors upon acute thermal activation of the neurons being targeted. Such GAL4 lines through further analysis would ultimately lead us to

identify the neuronal components that are functionally relevant to a behavior, thereby providing an entry point into the circuit.

During the screen, test flies were raised at 22°C to prevent neuronal activation before testing and the tests of either single or paired flies from both sexes were recorded for 10 minutes under temperatures increasing from 25°C to 32°C for later manual annotation of various behavioral phenotypes (Figure 1.5A). In total, we screened 3470 GAL4 lines, 60% of which showed no apparent phenotypes. The rest of the GAL4 lines that showed some phenotype were categorized as either “weak phenotype” (inconsistent or ambiguous phenotypes across different flies, 12%) or “strong phenotype” (consistent and clear phenotypes, 28%) (Figure 1.5B). The majority of the threshold temperatures for the onset of the strong phenotypes were around 28-30°C, justifying our choice of the thermal window for observation (Figure 1.5C). The “strong phenotype” GAL4 lines showed a variety of behaviors (Figure 1.5D; Table 1.1).

1.2.2 Confirmation of positive GAL4 lines for phenotypes of interest

Among the various phenotypic behaviors, we focused our interests to the female following phenotype serendipitously observed in the screen (Chapter 2) and the ovipositor extrusion (& egg laying) phenotype (Chapter 3) (Figure 1.6A). The female following phenotype was observed in 6 GAL4 lines, in which test female flies under thermal activation orient towards and follow other flies with occasional wing extension. The phenotype occurs with both male and female targets, the latter of which often responds by ovipositor extrusion. Ovipositor extrusion is also the second phenotype that we are interested in. It normally occurs when a sexually unreceptive female rejects a courting male by extruding her ovipositor, the egg laying organ. Ovipositor extrusion was induced upon thermal activation in 232 GAL4 lines in the absence of a courting male and was sometimes accompanied with egg laying phenotype (20%). As both phenotypes require the use of ovipositor, we combined them together for further analysis.

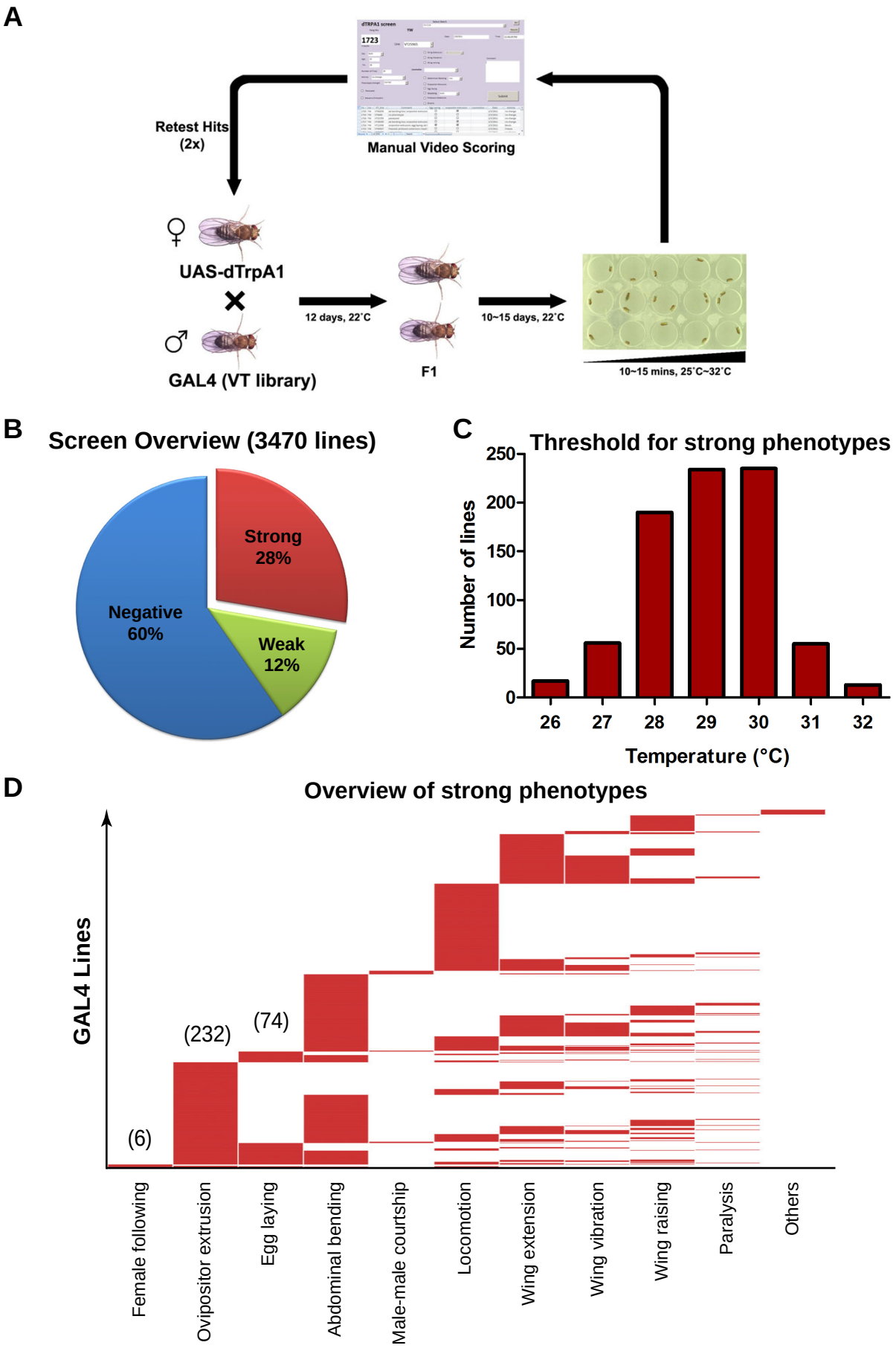

Figure 1.5 Scheme and overview of the neuronal activation screen

Phenotypes	Description
Female following	Female flies continuously orient and follow other flies (male or females) as they move about, with occasional tapping and wing extension, resembling aggression or male courtship.
Ovipositor extrusion	Female flies extrude their ovipositor (i.e., egg-laying organ) in the absence of a courting male to different extents, often accompanied with abdomen bending or egg laying.
Egg laying	Female flies lay eggs in the arena without food substrates. Eggs are sometimes stuck in the ovipositor.
Male-male courtship	Male flies vigorously follow and sing to other males, which is normally at very low level in wild-type controls.
Abdominal bending	Flies of either sex bend their abdomen, either upwards or downwards to different extents.
Locomotion	Flies of either sex display locomotion-related phenotypes, such as backward walking, turning, jumping, reduced or ceased activity, and defective walking.
Wing extension	Flies of either sex continuously or repeatedly extend either one or both of their wings with or without vibration.
Wing vibration	Flies of either sex vibrate one or both of their wings, either in a controlled manner as in singing or un-coordinately flapping.
Wing raising	Flies of either sex constantly raise their wings to an angel that is uncommon in wild-type flies.
Paralysis	Flies of either sex fail to maintain a normal stance posture and often fall onto their backs.
Others	Flies display some other rare phenotypes, such as escaping upon contacts, head movements, particularly strong grooming and feeding behavior.

Table 1.1 Observed phenotypes of the neuronal activation screen

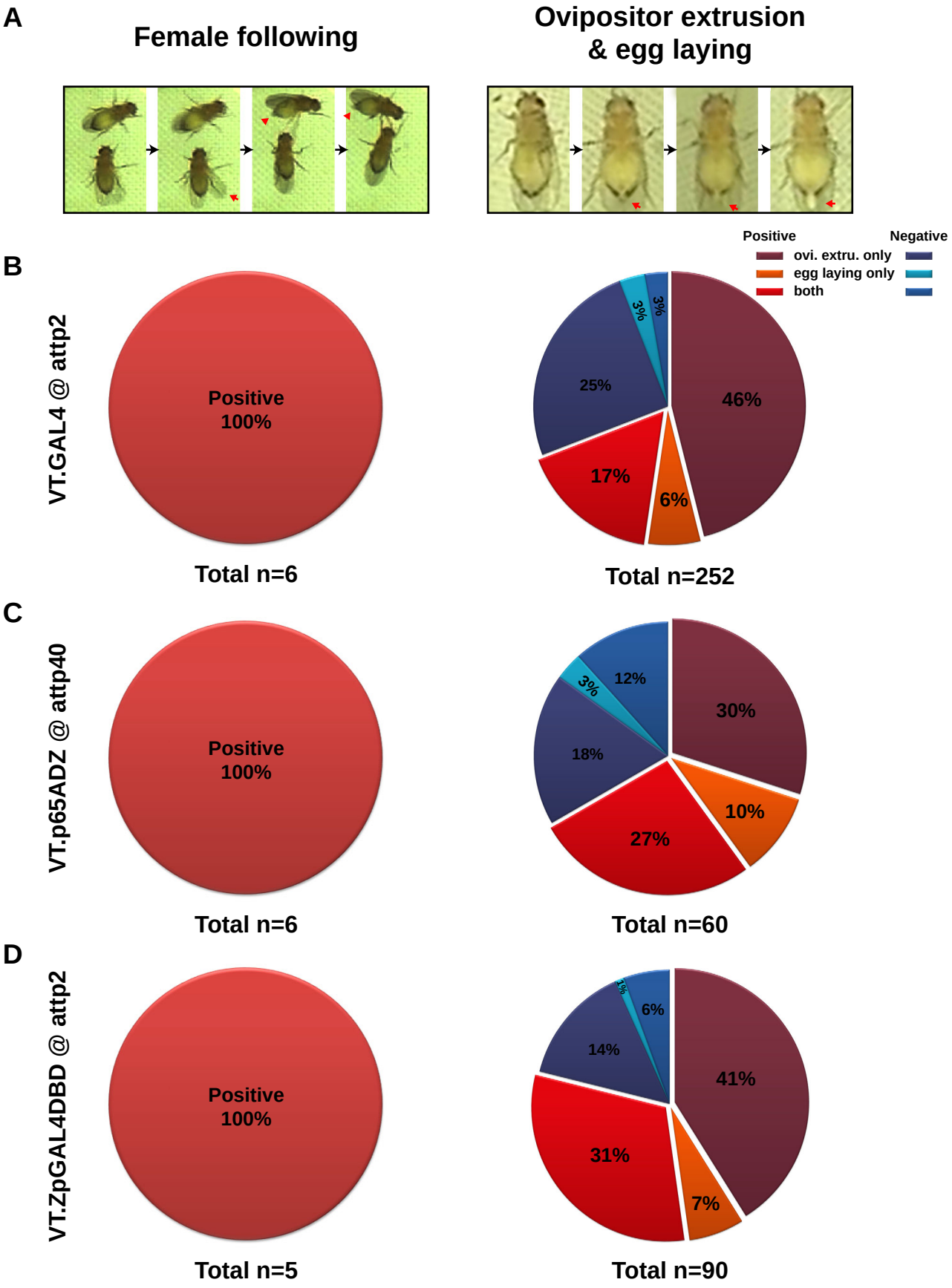

Figure 1.6 Confirmation of primary hits and derived split-GAL4 lines

The “strong phenotype” GAL4 lines from these annotated categories were further confirmed through retests, which were performed under similar conditions as in the primary tests for two times (n>30). For the following behavior, males or females were paired in each chamber. For ovipositor extrusion and egg laying, single females were place in each chamber. In summary, for female following behavior all of the 6 lines (100%) were confirmed as positive. For ovipositor extrusion and egg laying 118 (46%), 16 (6%) and 43 (17%) lines remained positive for showing each of the two phenotypes alone and both phenotypes respectively (Figure 1.6B).

1.2.3 Confirmation of split-GAL4 lines generated from the confirmed GAL4 lines of interest

A major challenge for neuronal mapping is that driver lines usually target too many cells. Although our enhancer bashing approach alleviates such issue compared with the traditional enhancer trap approach, it is still not a simple task to identify functionally relevant neurons directly from the driver lines. To further restrict the driver expression, we resorted to the intersectional power of the split-GAL4 system (Figure 1.3) by generating the split-GAL4 hemi-drivers (p65ADZp and ZpGAL4DBD) from the enhancer tiles of the confirmed GAL4 lines of interest. We tested these hemi-drivers under similar conditions as in the primary screen with complementary pan-neuronal hemi-drivers, elav-GAL4DBDZp and elav-p65ADZp. In summary, for female following all the available hemi-drivers were confirmed positive, while for ovipositor extrusion and egg laying an overall of 40 (67%) p65ADZp and 71 (79%) ZpGAL4DBD hemi-drivers were confirmed as positive (Figure 1.6C and D).

1.3 Discussion

Using *UAS-dTrpA1* which has been previously used in inducing male courtship in flies (von Philipsborn et al., 2011), we have screened more than 3000 enhancer GAL4 lines and identified those targeting neuronal populations that trigger various behavioral phenotypes upon neuronal activation. Interestingly, 60% of tested VT lines showed no apparent phenotypes in the screen. A parallel expression analysis of 2450 VT lines revealed that only 16% showed no neuronal expression and 24% showed sparse expression. This over-representation of behaviorally negative group

from the screen suggests that many neurons do not elicit any observable behavior upon activation and multiple types of neurons need to be stimulated simultaneously in order to trigger a behavioral output. It is also possible but unlikely due to sparse sampling of the VT library (40% coverage) that skewed our screen to target neurons that do not elicit behaviors upon activation. Nevertheless, similar to a gain-of-function genetic screen, there should be biologically non-relevant neurons whose activation induces certain phenotypes non-specifically or un-naturally, leading to false positive results in the screen. Therefore, the hit rate we observed might represent a combined result from these factors.

The “strong phenotypes” GAL4 lines start showing various behavioral phenotypes at different temperatures, but the onsets of the majority occur between 28°C to 30°C. The variation of thermal activation thresholds might be due to different levels of dTrpA1 expression. It might also be a result of various circuit dynamics, such as lateral inhibitions from routinely operating neuronal circuits. Some observed phenotypes are normally absent from wild-type flies presumably due to either lack of excitation or active suppression.

57% of these lines showed more than one phenotype. The different phenotypes displayed by one GAL4 usually started at different temperatures. A phenotype sometimes started at low temperature and disappeared at high temperature. This might be due to neuronal inactivation from synaptic fatigue or inhibitory feedback. It might also be due to the activation of a competing neuronal circuit, especially when another phenotype started to appear at the same time. Multiple phenotypes may also co-exist, suggesting lack of interference between the underlying neuronal circuits.

Among the 28% that showed robust and clear phenotypes, we decided to focus on those that showed female following and ovipositor extrusion (combined with egg laying). Female flies normally do not follow other flies and the fact that only 6 lines were identified from more than 3000 lines (0.2%) indicates that the functionally relevant neuronal cluster or combination of neuronal clusters is very specific. This seems not to be the case for ovipositor extrusion & egg laying as indicated by a much higher overall hit-rate from the primary screen (7.3%). For the two behavioral

categories, 100% and 69% of primary positive GAL4 lines were confirmed by retests respectively, suggesting that our neuronal activation screen was effective and robust.

The split-GAL4 hemi-drivers made from the confirmed GAL4 lines by using the same enhancer tiles were confirmed with a complementary pan-neuronal hemi-driver with a rate of 67% and 79% for p65ADZp and ZpGAL4DBD respectively. The lack of complete fidelity might be due to several factors: 1) landing-site effects, as original GAL4 were injected into app2 and p65ADZp hemi-drivers into attp40; 2) cloning errors; 3) insufficient expression to reconstitute function GAL4 proteins. It is also possible that the pan-neuronal hemi-drivers (elav-p65ADZp and elav-ZpGAL4DBD) used for testing are not truly pan-neuronal or do not coincide temporally with the hemi-drivers being tested.

There were a few limitations for our neuronal activation screen. 1) The pattern of action potentials elicited by TrpA1 thermal activation might be very artificial and never occur in normal behaving flies, thus generating phenotypes that are biologically irrelevant to the function of neurons activated. 2) Our screen was standardized to test flies aging from 10-15 days. If the expression of functionally relevant neurons in the GAL4 lines is either turned off too early or turned on too late, we would not be able to see an effect upon activation. 3) We used a varying temperature range for thermal activation. This benefits us in a way that we can explore a spectrum of activation conditions in one assay. However, certain phenotypes may be too transient for us to observe, if the thermal window for its manifestation is narrow. 4) Videos were manually annotated, leaving plenty of room for human error. In addition, subtle phenotypes that require quantitative measurements cannot be revealed. 5) It is not yet clear how much coverage of different neuronal types in the nervous system has been achieved by our activation screen which represents less than 40% of the whole current VT library (8779 lines). 6) The screen didn’t attempt to and cannot identify all neuronal components essential for a certain behavior. A complementary silencing screen would be helpful to identify other neural elements that are missed by the activation strategy.

Despite these limitations, our screen was effective and successful in identification of GAL4 lines that trigger behavioral changes. We have only pursued the GAL4 positive

lines of our interest, including female following, ovipositor extrusion and egg laying phenotypes in this study, and backward locomotion phenotypes in a parallel study (Bidaye, 2012). Other phenotypes might be also worth further investigation, such as male-male courtship, wing-related phenotypes and other locomotion phenotypes.

1.4 Figure legends

Figure 1.1 Organization of the nervous system of *D. melanogaster*

(A) The anterior brain. (B) The posterior brain. (C) The ventral VNC. (D) The dorsal VNC. A list of neuropils are marked with various colors and indicated by abbreviations. AL, antennal lobe; EB, ellipsoid body; MB, mushroom body; SOG, subesophageal ganglion; PI, pars interebralis; AMMC, antennal mechanosensory and motor center; PB, protocerebral bridge; NO, nodule; FB, fan-shaped body. Adapted from (Yu, 2009).

Figure 1.2 Generating GAL4 lines: enhancer trap vs. enhancer bashing

(A) The enhancer trap strategy: a modified P-element containing GAL4 sequence is mobilized by co-injected transposase and integrated randomly in the fly genome. (B) The enhancer bashing strategy: genomic sequences are divided into small enhancer-containing fragments, placed in front of GAL4 sequence and integrated to a specific genomic location containing attp sequence by φC31-mediated site-specific integration. Boxes with different colors indicate different genetic elements: red, enhancers; cyan, orange, and purple, exons from three different genes; green, genomic tiles containing potential enhancers; yellow, GAL4 sequence; blue, attB or attP sequence.

Figure 1.3 Intersectional genetics with Split GAL4 system

Principles of the split GAL4 system in restricting expression pattern. With normal GAL4 drivers creating by the enhancer bashing strategy, different neuronal sub-populations can be targeted, such as neuronal population A and B, targeted by drivers using Tile 1 and 2 respectively. In split GAL4 system, Tile 1 and 2 are used to drive expression of only half of the GAL4 protein linked to a zinc-finger domain (Zp), either the activation domain (p65ADZp) or the GAL4 DNA binding domain

(ZpGAL4DBD). GAL4 activity is reconstituted only in neurons where both halves are expressed, performing an “AND”-like operation.

Figure 1.4 Mosaic analysis techniques to label neuronal clones

(A) Conventional MARCM, mosaic analysis with a repressible cell marker, labels only one of the daughter cells after FLP/FRT-mediated mitotic recombination, leading to single-color labeling of single-cell, two-cell or multiple-cell clones. (B) Twin-spot MARCM uses two repressors and labels both of the daughter cells after mitotic recombination, leading to two-color labeling of clones with various sizes. (C) Twin-spot generator uses split half reporter sequences flanking a FRT site. Non-mitotic recombination leads to co-expression of both GFP and RFP reporters, generating yellow color. Mitotic recombination is able to produce three colors, RFP alone, GFP alone and both RFP and GFP. Different number of cells can be labeled in all three colors. Oval shapes represent cells and color fills represent labeling with different reporters. Scenarios with type-I neuroblast lineage is shown: Nb, neuroblast; GMC, ganglion mother cell; N, neuron; FLP, flippase activity. Purple arrows indicate expression of FLP activity and occurrence of mitotic recombination. Adapted from (Lee and Luo, 2001; Venken et al., 2011).

Figure 1.5 Scheme and overview of the neuronal activation screen

(A) A flowchart of the screen. Flies carrying UAS-dTrpA1 were crossed to each of the VT lines tested. Progenies were collected and aged under 22°C for 10-15 days before testing. Assays were performed in 10mm chambers with single or paired flies from both sexes for 10-15 min under a thermal gradient from 25°C to 32°C. Positives lines of interest were retested 2 times. (B) Overview of the screen. A total 3470 lines were tested. Bar graph shows the percentages for each category: strong, robust and clear phenotypes; weak, variable and not obvious phenotypes; negative, no obvious phenotypes. (C) Plot showing the distribution of temperatures required for observing strong phenotypes. (D) Overview of the GAL4 lines showing the strong phenotypes. Phenotypes of each GAL4 (Y axis) are indicated for each of the 11 annotative categories (X axis). Each red horizontal bar represents the presence of a phenotype under the corresponding category.

Figure 1.6 Confirmation of primary hits and derived split-GAL4 lines

(A) Female following (left) and ovipositor extrusion phenotypes (right). During the following behavior, the following female oriented and followed other flies with occasional wing extension (red arrow). A wild-type Canton S female often responded with ovipositor extrusion (red arrowheads) as if towards a courting male. Ovipositor extrusion was seen to be performed to different extents and sometimes accompanied with eggs (red arrows). (B) Retest overview of the GAL4 hits from the screen showing female following or ovipositor extrusion and egg laying phenotypes. (C) Test overview of the p65ADZp and (D) the ZpGAL4DBD hemi-drivers generated confirmed GAL4 tiles. Bar graphs represent percentages of lines being positive or negative for each category. Ovipositor extrusion and egg laying lines are divided into three sub-groups, ovipositor extrusion alone, egg laying alone, and both.

Table 1.1 Observed phenotypes of the neuronal activation screen

Eleven phenotypic categories that were manually annotated are described with more details and explanation.

1.5 Material and methods

Fly stocks

All enhancer GAL4 lines were from the VT library as described in the introduction. The neuronal activator strain *UAS-TrpA1* was generated as described in (von Philipsborn et al., 2011). The split-GAL4 hemi-drivers were generated by replacing the original GAL4 sequences of the VT constructs with the sequences of p65ADZp and ZpGAL4DBD and injecting them into attp40 and attp2 landing sites respectively. The constructs were cloned as described in (Pfeiffer et al., 2010).

Neuronal activation screen by thermal activation

Each of the VT lines tested was crossed to flies carrying *UAS-TrpA1*. Progenies from the crosses were collected shortly after eclosion and reared in groups of 10-20 flies at 22°C to prevent neuronal activation before testing. During the tests, 10 males and 10 females per genotype were transferred into a plate with 15 units of 10mm-diameter circular chambers in a format of 5 single males, 5 single females, 2 male-

male pairs, 2 female-female pairs and 1 male-female pair. The plate was then placed onto an aluminum sheet with a heating pad glued underneath. Videos of about 10 minutes were recorded while the temperatures inside the chambers were monitored and varied from 25°C to 32°C. Thorough annotation of the videos was performed manually.

Retesting of GAL4 and split GAL4 lines of interest

The retesting assays were performed under the same conditions as the primary screen. For the following phenotypes only pairs of male or female flies were tested. For ovipositor extrusion and egg laying, test females were mated by rearing together with males.

Chapter 2. Neuronal circuitry for female following

2.1 Background

2.1.1 Sexual dimorphisms as a result of evolution

In nature, males and females from the same species are commonly observed with phenotypic differences in morphology, size, ornamentation and behavior. The evolutionary forces that drive the selection of such dimorphic traits have been theorized to mainly come from natural selection and sexual selection.

In some species, such as the vesper bat *Myotis nigricans*, females are much larger than males. This has been proposed to be caused by natural selection due to fecundity advantages of larger females in producing more viable offspring or providing parental care (Bornholdt et al., 2008; Hayssen and Kunz, 1996). However, natural selection functions as a negative selector for dimorphic traits that have been evolved through sexual selection, such as increased ornamentation. Increased sexual dimorphism in coloration of males presumably makes them more conspicuous and thus more vulnerable to predation. It has been shown that there is a increase vulnerability of bird species with increased sexual dimorphism to predation by European sparrowhawks in Denmark (Moller and Nielsen, 2006).

Sexual dimorphic traits under the pressure of sexual selection are usually evolved through mate choice and intrasexual competition (Andersson, 1994). The direction and intensity of sexual selection are mainly defined by the ratio of males to sexually receptive females in a population at any given time (Emlen and Oring, 1977). In most animals, this ratio is biased towards males due to females' higher energy and time investment in gamete production and parental care (Trivers, 1972). The resultant intense male-male competition for mates gives females the freedom to "choose" among males whom to mate with (i.e. conventional sex role). Once a female preference towards certain male trait starts to be established, it has been theorized that both the female preference and the male trait will undergo rapid and divergent co-evolution as a result of an explosive positive feedback loop and proceed even

beyond the optimal level of survival until balanced by the counteracting natural selection (Fisher, 1930). This has been considered to result in sexual dimorphisms in ornamentation, such as peacock's large and colorful plumage, which Darwin described as "ornaments" (Darwin, 1859). Alternatively, the intensified male intrasexual competition may evolve on its own, leading to male dimorphic traits in aggression and weaponry, such as the antlers of male deer, which Darwin decribed as "weapons" (Darwin, 1871). In some species, the ratio of males to ready-to-mate females is biased towards females and females become the main competitors for mates, leading to a reversal of the sex role and the direction of sexual selection (Berglund et al., 1989; Oring and Lank, 1986; Sogabe and Yanagisawa, 2007).

2.1.2 Sexual determination pathway in *D. melanogaster*

In *Drosophila melanogaster*, males and females take conventional sex roles which dictate high levels of male competition and female mate choice, leading to sexual dimorphisms in courtship and aggression behaviors (Hall, 1994; Nilsen et al., 2004). These behavioral dimorphisms between sexes are specified through the genetic cascade of the sex determination pathway.

In fruit flies, sex is determined by the ratio of X chromosomes (X) to autosomes (A) in a cell autonomous manner. The ratio ranges from 0.5 to 1, with 0.5 being male, 1 being female, and in between intersex. Two copies of X chromosomes are sufficient to accumulate enough X-linked transcription factors to activate *in trans* the expression of the master control gene, *sex lethal* (*sxl*) (Cline, 1993). The Sxl protein subsequently functions as a splice factor and triggers the expression of *transformer* (*tra*) (Inoue et al., 1990). Together with the sex common *transformer-2* (*tra-2*), *tra* controls the alternative splicing of *doublesex* (*dsx*) and *fruitless* (*fru*) pre-mRNA, leading to the generation of male-specific Dsx^M and Fru^M proteins and female-specific Dsx^F proteins (Heinrichs et al., 1998; Hoshijima et al., 1991; Nagoshi et al., 1988; Ryner et al., 1996). Dsx and Fru are transcription factors of the zinc-finger family and the BTB-zinc-finger family respectively. Dsx proteins control sexual development in most somatic tissues with sexually dimorphic features, including sex comb on the foreleg, cuticle, oenocytes, fat body, gonads and genitalia (Camara et al., 2008; Ferveur et al., 1997; Keisman et al., 2001; Rideout et al., 2010; Robinett et al., 2010).

Dsx also regulates sexually dimorphic neuronal development in collaboration with Fru^M proteins in the central nervous system (Demir and Dickson, 2005; Rideout et al., 2010).

2.1.3 Sexual dimorphisms of following behavior in *D. melanogaster*

In *Drosphila*, following behavior directed towards conspecific individuals has always been treated as an integral component of more complex social behaviors, such as courtship and aggression (Hall, 1994; Nilsen et al., 2004), and therefore has not been studied independently as an isolated behavior so far. To appreciate the sexual dimorphisms of following behavior, it is necessary to examine the sexual dimorphism of courtship and aggression behaviors as a whole.

As the most obvious example for behavioral dimorphisms between sexes, courtship behavior consists of mainly male actions towards female flies and seemingly only passive participation of females (Spieth, 1974). During courtship, a male fly performs a stereotypic sequence of steps starting with orienting towards the female and tapping her abdomen with forelegs. The male then follows the female as she walks, during which the male keeps tapping her and in the meantime extends and vibrates his wings unilaterally to generate a “courtship song” consisting of either oscillatory “sine song” or trains of “pulse song” (Shorey, 1962). The pulse song consists of series of 35ms spaced pulses which is species-specific (Ewing and Bennet-Clark, 1968) and critical for both eliciting female receptivity and species recognition (Bennet-Clark and Ewing, 1969; Kyriacou and Hall, 1982). In the process of following, the male also extends his proboscis to lick the female’s genitalia and starts copulation attempts. However, the female spends most of her time wandering around and lacks any actions directed towards the male, except for some subtle acceptance and rejection response, such as vagina-plate opening, kicking, wing flicking and ovipositor extrusion (Hall, 1994).

There have been a small number of stand-alone studies reporting on more active roles of females during mating. Cook reported on observation of female following or chasing behavior towards either males or females in *Drosophila melanogaster* in both balancer (i.e. choromosomes carrying multiple nested inversions that are able to

suppress homologous recombination) flies (Cook, 1975) and wild-type flies (Cook, 1981). However, these studies remain to be validated by independent follow-up studies. In *Drosophila virilis* species, females have been reported to sing during courtship, performing a duet with males (Donegan and Ewing, 1980; Satokangas et al., 1994).

Aggression is another behavior known be sexually dimorphic in *Drosphila melanogaster*. It involves a set of stereotyped actions with an intention of attack and threat in competition for food, territory or mates, and establishes dominance hierarchies among individuals (Chen et al., 2002; Dow and Schilcher, 1975; Hoffmann, 1987; Jacobs, 1960; Nilsen et al., 2004). Under proper conditions, fights between pairs of males or females can be robustly observed, but with distinctive features, behavioral components and intensities. In a male fight, the male that wins the first encounter will win almost all following encounters, while such dominance relationship is absent in female fights. Some low intensity components of aggressive behaviors are shared by both male and female fights, such as approach, fencing, retreats and wing threats. Other components, especially those of higher intensity, are nonetheless sexually dimorphic or specific. For example, lunging, boxing, tussling, hold, and chasing (or following) are typical for male fights, whereas shoving (similar to lunging), high-posture fencing (similar to boxing) and head-butting are common in female fights (Nilsen et al., 2004). The overall intensity and robustness of aggression is much higher in male fights than female fights (Chen et al., 2002).

For both courtship and aggression to occur, it is essential for the courter or attacker to be close enough to direct their actions towards the receiver and maintain this proximity and directionality as the receiver moves away. This continuous process is subserved by the following (or chasing) behavior, which is employed heavily in male courtship and aggression but is absent or rare in females. Approach can be considered as a lesser form (in duration and intensity) or the initial stage of following. It seems to be present in both males and females in aggression nevertheless still with much lower frequency in females than males. Approach might also be involved in social aggregation, in which individual flies of both sexes aggregate in patches potentially facilitating cooperative food searches and colonization (Lof et al., 2009; Tinette et al., 2004).

2.1.4 Neural substrates of following behavior in *D. melanogaster*

The challenge that a fly faces during a following session under proper behavioral contexts is the need to visually detect the location and motion of the target fly and adjust its movement to keep it in the center of the visual field and in close proximity. Therefore, the underlying neural circuitry of following behavior in the central nervous system should be composed of three main sub-circuits: 1) higher order command circuits that evaluate sensory information and trigger following behavior appropriately; 2) visual circuits that compute target information and feed it onwards; 3) locomotion control circuits that generate directed walking pattern of following behavior upon reception of a command. A thorough understanding of how following directed to other flies is implemented neuronally would require an understanding of each of the sub-circuits and the interfaces between them. Following occurs mostly during male courtship and aggression, where the underlying neural mechanisms can most likely be revealed.

Courtship and aggression

Genetic access to neuronal populations underlying courtship and aggression is mainly provided by studies of *fruitless* and *doublesex* genes. The establishment of male-specific isoform of *fruitless* (Fru^M) as the genetic switch for male courtship behavior (Demir and Dickson, 2005; Manoli et al., 2005) and aggression behavior (Vrontou et al., 2006) has allowed the generation of fru-GAL4 using homologous recombination to access the Fru^M neuronal populations that give rises to courtship behavior (Stockinger et al., 2005) and control sexual dimorphic patterns of aggression (Chan and Kravitz, 2007). Similarly, dsx-GAL4 was generated to target Dsx^M and Dsx^F neurons which are required for male courtship and female sexual behaviors (Rideout et al., 2010). There are about 2000, 900 and 700 neurons for for Fru^M, Dsx^M and Dsx^F populations, respectively. Using MARCM or a FLP-in method, Fru^M expressing neurons (*fru*+ neurons) in the central nervous system have been

anatomically classified into about 100 neuronal clusters (Cachero et al., 2010; Yu et al., 2010), some of which have been functionally characterized. On the contrary, few of Dsx^M and Dsx^F neuronal populations have been studied.

The *fru*+ Or67d olfactory receptor neurons (ORNs) have been shown to respond to the male-specific volatile pheromone 11-cis-vaccenyl acetate (cVA) and mediate cVA-dependent courtship suppression towards males and mated females and aggression stimulation (Ejima et al., 2007; Kurtovic et al., 2007; Wang and Anderson, 2010). Or67d ORNs converge onto the DA1 glomerulus in the antennal lobe (Couto et al., 2005; Fishilevich and Vosshall, 2005), which is innervated by *fru*+ DA1 projection neurons that terminate sexual dimorphically in the lateral horn (Datta et al., 2008). Along this line of investigation, DA1 projection neurons have been further mapped to connect to *fru*+ DC1 neurons (aSP5 and aSP8) in the lateral horn which in turn connect to DN1 descending neuron (Ruta et al., 2010). The DA1 glomerulus is one of three *fru*+ glomeruli that are larger in male than females. (Manoli et al., 2005; Stockinger et al., 2005). The other two are VA1v and VL2a. VA1v is innervated by Or47b ORNs which respond to extracts from both male and female (Root et al., 2008) and are required for increased male-male courtship in males with cuticular hydrocarbons depleted (Wang et al., 2011). VL2a is innervated by Ir84a ORNs that respond to food-derived odors (Grosjean et al., 2011). Perturbation of either pathway reduces courtship. LAN1, a cluster of *ppk23*+ *fru*+ foreleg afferent neurons, has been shown to respond to two female enriched non-volatile pheromones, 7,11-HD and 7,11-ND, and mediate their courtship promoting effect (Thistle et al., 2012; Toda et al., 2012). The gustatory receptor Gr32a mediates the effects of (z)-7-tricosene (7T) in maintaining normal levels of aggression and suppression of male-male courtship, and also is required for cVA's aggression-promoting effect (Wang et al., 2011).

In the higher-order brain center, analysis with sexually mosaic animals has restricted the necessary and sufficient area for male courtship to the dorsal brain region (Hall, 1977). Using similar strategy with refined genetic tools, it was possible to restrict the region to a single male-specific neuronal cluster named P1, whose existence in females through sex change enables them to perform male-like courtship (Kimura et al., 2008). It has been shown that P1 neurons exist specifically in males and are programmed for cell death in females (Kimura et al., 2008). P1 can be activated by a

single touch on female's abdomen and induced activation of P1 with TrpA1 can trigger the whole series of courtship ritual, including proper courtship song, in the absence of a courting target (Kohatsu et al., 2011; von Philipsborn et al., 2011). Activation of P1 in the presence of a male target induces ectopic male-male courtship and blocking of P1 activity reduces courtship (Liu, 2012). Due to its functional relevance and anatomically extensive arborization and male-specific characteristics, P1 has been proposed to be an integration neuron for male courtship (Kohatsu et al., 2011).

Motion and position detection

Two visual responses of flies have studied extensively: optomotor response and fixation response (Figure 2.1A). Optomotor response is the turning reaction towards the rotating direction of large-field grating stimuli, as demonstrated in tethered flies inside a rotating drum with stripes (Blondeau and Heisenberg, 1982; Buchner, 1976; Gotz, 1964); while fixation response refers to flies' ability to keep a visual target (e.g. a black bar) in front of them for prolonged period of time, as shown in tethered flies which were allowed to control the position of the visual target through a feedback loop (Reichardt and Wenking, 1969). These two responses are thought to represent outputs of two different visual processing systems due to their different spatial sensitivity and dynamics (Bahl et al., 2013).

Based on behavioral data of optomotor response from beetles and tethered houseflies, the "Reichardt detector", a mathematical model of motion detection was developed to describe the signal processing from photoreceptor inputs to direction-selective outputs (Reichardt, 1987) (Figure 2.1B). This model describes the optomotor response in terms of stimulus parameters with surprising accuracy and details (Haag et al., 1999) and has been used to explain motion detection in many species (Borst and Egelhaaf, 1989). Only some of the processing stages proposed by the model have been mapped to specific neural substrates. It has been shown that the main inputs to the motion detection system are provided by the lamina neurons L1 and L2 which segregate visual inputs from photoreceptors R1-6 in retina into an ON and an OFF pathway (Eichner et al., 2011; Joesch et al., 2010) and then converge via T4 and T5 neurons onto the dendritic area of the main output neurons,

the motion sensitive (HS and VS) lobula plate tangential cells (LPTC) (Bausenwein et al., 1992; Bausenwein and Fischbach, 1992; Schnell et al., 2012) (Figure 2.1C and D). Block of L1/L2 and T4/T5 completely abolishes motion response in LPTCs and renders flies motion blind (Bahl et al., 2013; Joesch et al., 2010).

While the optomotor response is exclusively supported by the motion detection circuit, the fixation response is controlled by both the motion detection circuit and a parallel position circuit. The position system has only been revealed recently with motion blind (T4/T5 blocked) flies that still show fixation response (Bahl et al., 2013). The LPTC output neurons of the position system seems to be different from those of the motion detection system (VS and HS) (Bahl et al., 2013), consistent from finding from larger fly species (Liang et al., 2012).

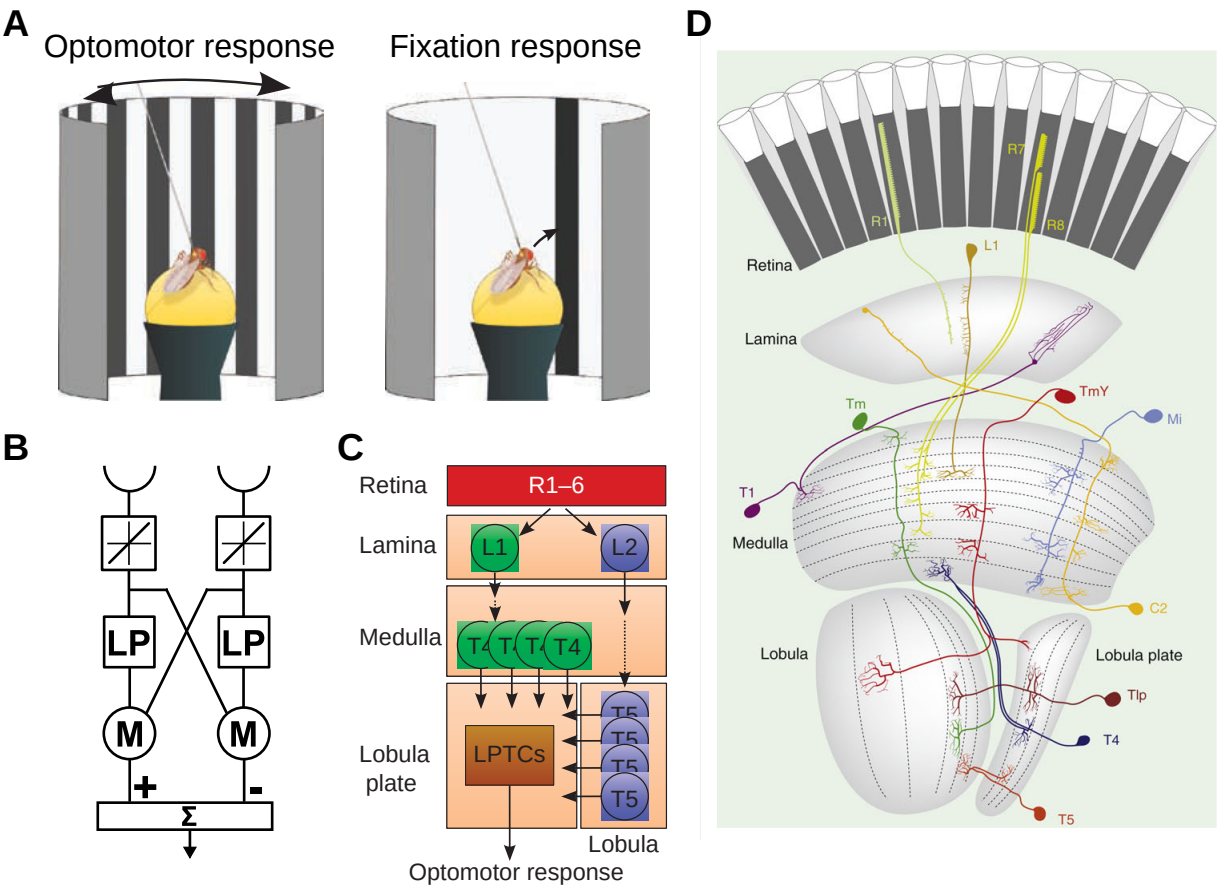

Figure 2.1 Optomotor response and fixation response

Control of directed locomotion

During the process of following, a fly needs to maneuver its own movement based on visual inputs to move forward or turn towards the target, by adjusting its step size or leg direction. Through genetic lesion experiments with mutagenesis and mosaic techniques in *Drosophila melanogster*, the brain areas that perform such control functions have been suggested to reside in specific brain structures, called the central complex (Strauss, 2002b). The central complex consists of a topographically organized set of neuropils in the center of insects' brain (Figure 1.1)., which are interconnected by columnar interneurons with many regular projection patterns (Hanesch et al., 1989). It receives inputs from multiple sensory pathways, such as e-vector of polarized light (Heinze and Homberg, 2007), tactile (Ritzmann et al., 2008) and visual inputs (Neuser et al., 2008; Poeck et al., 2008), and is considered to be a center of information processing and integration (Strauss, 2002a). Based on functional and anatomical studies, a theoretical model has been proposed to explain mechanisms of orientation (or following) towards a target (Triphan et al., 2010). The model proposes: 1) the the protocerebrum bridge (PB) forms a topographic map containing information about the direction and azimuth position of the visual target; 2) asymmetrical representation of the target increases step size on the contralateral side, which causes turning towards the target (Figure 2.2A); 3) symmetrical representation of the target increases step size on both sides, leading to forward locomotion (Figure 2.2B). Nevertheless, the neuronal identities for higher order neurons controlling directed walking remain largely unknown. The only one that has been identified is a cluster of descending command neurons that are both necessary and sufficient for backward locomotion (Bidaye, 2012).

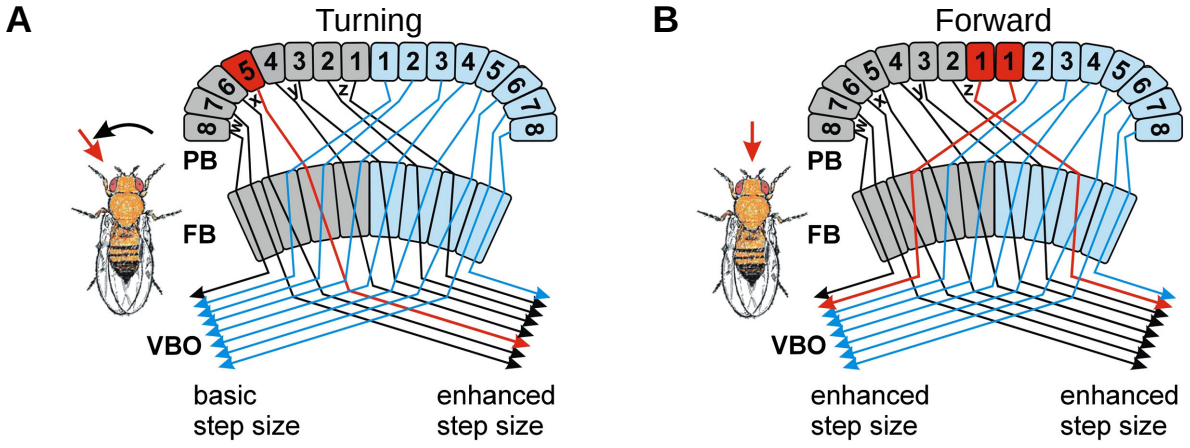

Figure 2.2 Models of central complex in target directed locomotion

2.2 Results

2.2.1 Identification of female-specific neuronal cluster implicated in female following behavior

In order to identify the neuronal cluster(s) that trigger the following behavior in females, we first examined the expression pattern of the six positive GAL4 lines which were crossed to a fly stock carrying a *UAS-mCD8::GFP* transgene and stained with antibodies against GFP and neuropil (nc82). Expression of these GAL4 drivers varies in terms of sparseness and spatial pattern (Figure 2.3A and B). Some are relatively sparse (*VT2064*, *VT25602*, and *VT25965*) while the others are quite broad. But all of them label multiple types of neurons and it was not possible to straightforwardly identify and make conclusions about the functionally relevant neurons from these drivers. Therefore, we decided to analyze these images more carefully with a hope that we might notice some neurons that are: 1) common to all six positive GAL4 drivers and 2) sexually dimorphic or specific to females, as males don't show the same ectopic following behavior towards inappropriate target, such as another male. It would not allow us to draw conclusions but would provide likely neuronal candidates to further tested.

Indeed, detailed image analysis by comparing among the six lines and between male and female within each line revealed a single neuronal cluster that is apparently common to all 6 positive lines and is specifically labeled in females (Figure 2.3A). The cell bodies of this neuronal type are located in the posterior of the brain below the protocerebral bridge (PB). Its projection curves dorsal-anteriorly crossing the PB and arborizes extensively around the mushroom calyx and possibly on the contralateral side as well. Due to these characteristics, it was possible to reliably identify this neuronal class from staining of different drivers. Although this neuronal cluster was the only one that we could anatomically identify, it doesn't exclude the possibility that there are other neurons that are also jointly labeled by the GAL4 lines but less obvious to be noticed. Nevertheless, this female specific cluster serves as a very likely candidate for us to test.

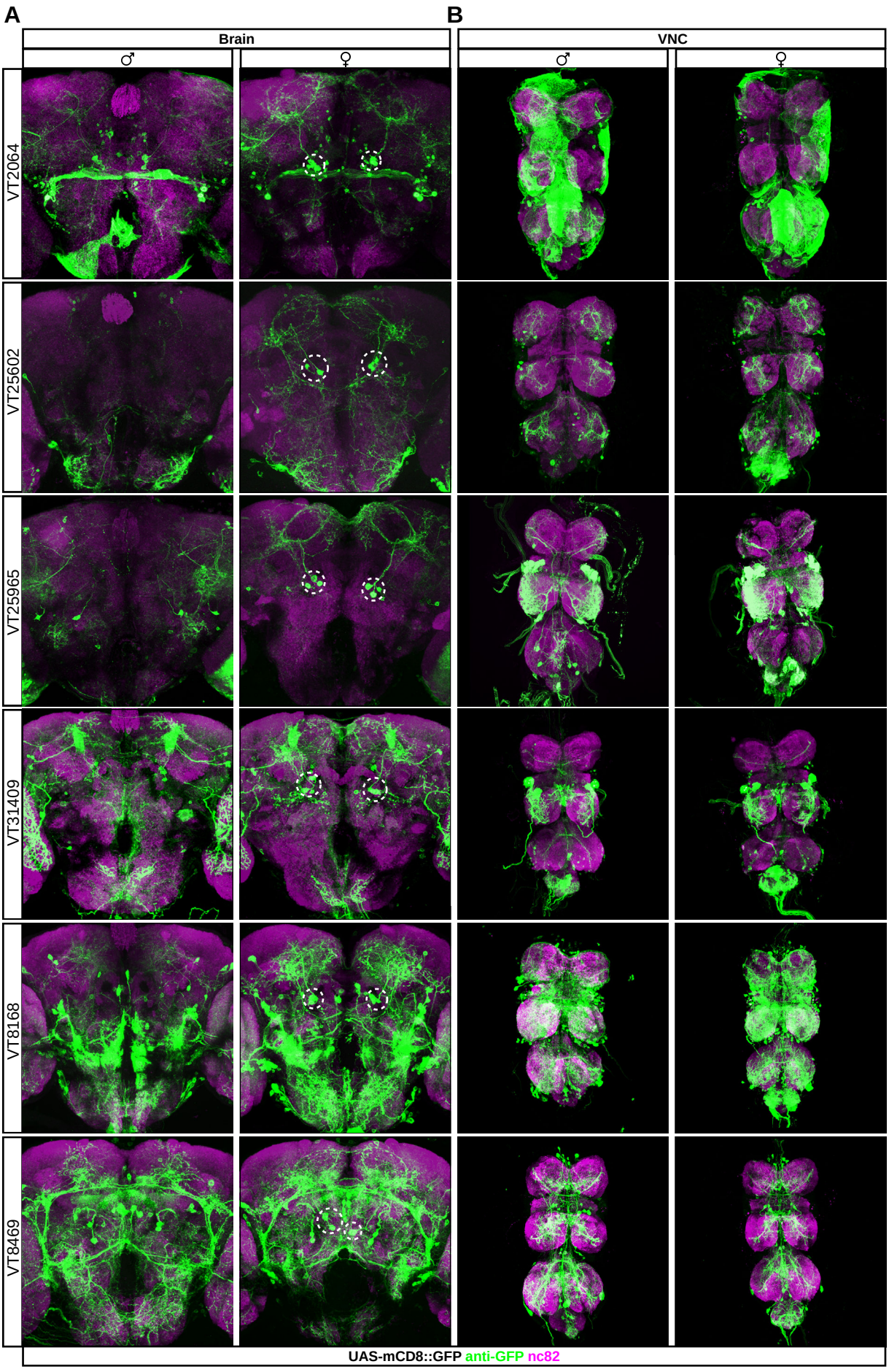

Figure 2.3 Expression analysis identified one female-specific neuronal cluster as a likely candidate for female following behavior

2.2.2 MARCM correlated two neuronal types with female following

Although image analysis revealed a female-specific neuronal cluster as a likely candidate for the following behavior in females, it does not provide sufficient evidence to make a strong conclusion due to the non-restrictive nature of the positive GAL4 expressions. In order to specifically target individual neuronal types and stimulate their activity, one approach is to use stochastic labeling techniques to label and activate neurons randomly and observe corresponding behavior upon thermal activation. In our study, we employed the mosaic analysis with a repressible cell marker (MARCM) which utilizes hs-FLP/FRT-mediated mitotic recombination to create GAL80-free homozygous daughter cell(s) where both GFP and TrpA1 are expressed in an otherwise heterozygous animal in which GAL4 activity is actively suppressed by GAL80 (Lee and Luo, 1999) (Figure 2.4A). Based on stained images, *VT2064* was selected due to its relatively sparse expression in comparison with other positive GAL4 lines (glial cells were labeled in the VNC) (Figure 2.4B). To generate GAL80-free neuronal clones, progenies of interest were subjected to a one-time heat-shock at different developmental stages, which determined whether clones of multiple cells, two cells or one cell will be targeted (Lee and Luo, 2001) (Figure 1.4A). Subsequently, female flies with proper genotypes were first tested for presence or absence of following behavior upon thermal activation and then dissected and stained for expression which was later exhaustively analyzed for different neuronal types.

In total, we tested more than 2000 flies and identified 37 flies that showed following behavior upon activation. These 37 following flies were stained together with 37 control flies that showed no following behavior upon activation (3 controls were abandoned later for lack of expression). Image analysis of stainings obtained from these flies identified about 57 types of neurons (37 in the brain and 20 in the VNC); however, many of these were labeled infrequently. An average of 6 to 8 types neurons were labeled per fly in both following and non-following groups, indicating that the induced neuronal labeling was relatively un-biased (Figure 2.4I). The most frequently labeled 20 types of neuronal classes were segmented from sparse labeling images (Neuron 10 not shown) (Figure 2.4C; see Figure S1-4 for description and image of each neuronal type). Scoring of the images from individual flies according to

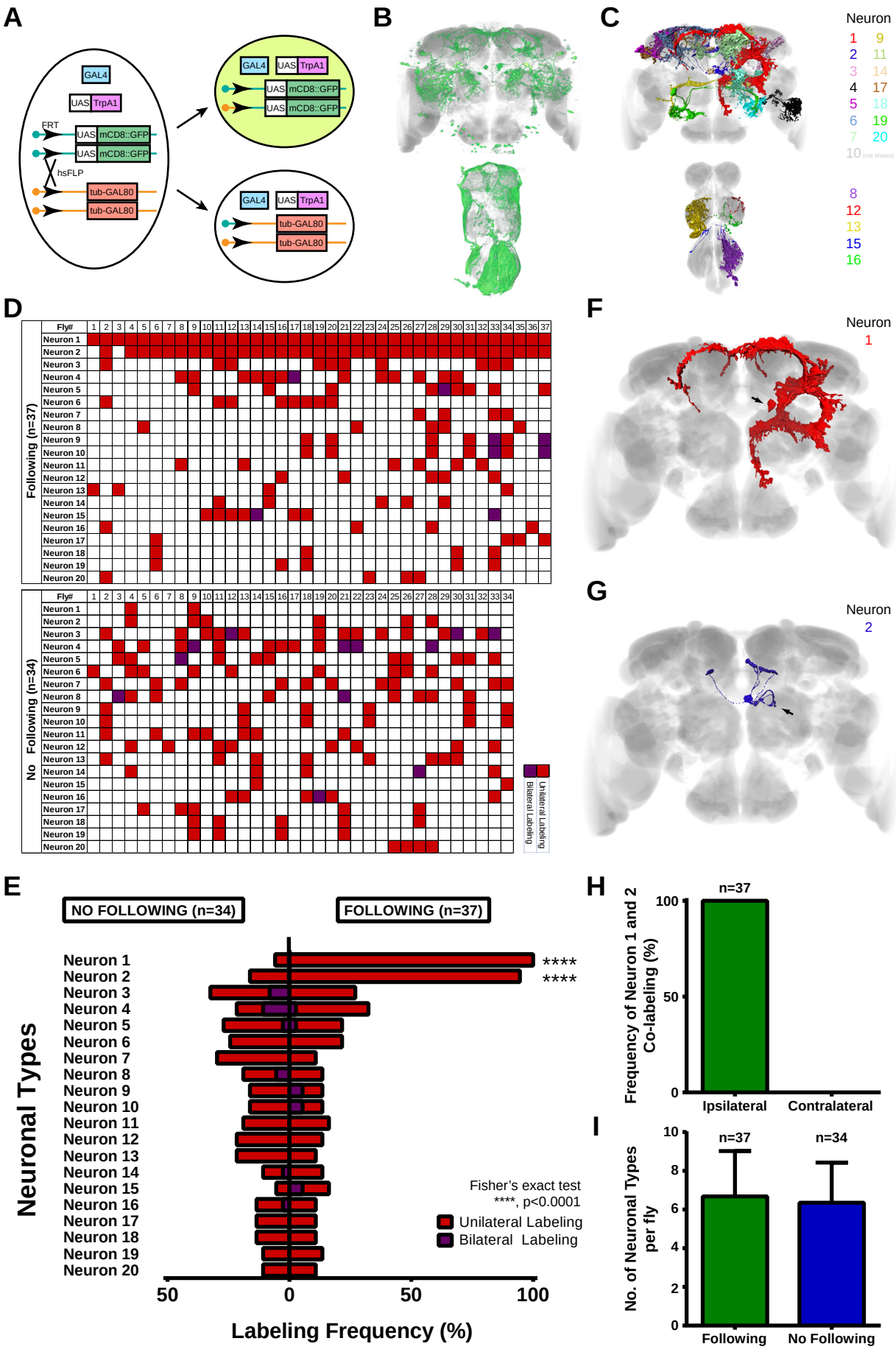

Figure 2.4 MARCM correlates two neuronal types with female following

these neuronal types revealed a significant enrichment of Neuron 1 and Neuron 2 in the following group (100% and 95%) versus the no following group (6% and 16%) (Figure 2.4D and E).

Interestingly, Neuron 1 was the female-specific candidate neuron that we identified initially from direct comparison of positive GAL4 expressions (Figure 2.4B). Like we observed earlier, the cell bodies of Neuron 1 are generally large in size and are located in the posterior of the brain below the protocerebral bridge (PB). Its projection curves dorsal-anteriorly passing through PB and bifurcates near the mushroom body calyx. One branch arborizes extensively in the ipsilateral hemisphere forming a ring-like structure and the other crosses to the contralateral hemisphere with arborization near the pars intercerebralis (PI) region.

The cell bodies of Neuron 2 are much smaller and are located in close proximity to those of Neuron 1. Unlike Neuron 1, its projection travels only anteriorly and arborizes in the fan-shaped body (Figure 2.4G). Coincidentally, in all occasions that Neuron 1 and Neuron 2 were co-labeled (n=37), they were all labeled in the same hemisphere (Figure 2.4H), suggesting that they might be generated from the same lineage within a small time window and therefore inseparable in our MARCM experiment due to the temporal imprecision of heat-shock treatments (on the scale of days).

2.2.3 Neuron 1 was confirmed by split-GAL4 and Hap1 systems

Although MARCM helped us to shorten our list of candidates to only two types of neurons, we were still unable to conclusively prove that either one or both of them are essential for trigger following behavior in females upon activation. Therefore, we sought to take advantage of the split-GAL4 system and alternative expression system to search for restricted driver lines which should reliable target the functionally relevant neurons. Such drivers, once identified, would allow us not only to make conclusions about the identity of functionally relevant neurons, but also precisely access them in further behavioral analysis and neuronal characterization.

We designed a matrix with the confirmed split-GAL4 hemi-drivers that were confirmed as positive for following behavior with complementary pan-neuronal hemi-

drivers (Figure 1.6B and C) and selectively tested 11 combinations (Figure S5). All the split combinations that were tested showed female following behavior upon activation, while expression analysis identified only two reciprocal combinations that specifically label only one cluster of brain neurons throughout the central nervous system (Figure 2.5A; Figure S5). The only neuronal cluster labeled in these split-GAL4 combinations was Neuron 1, consisting of about 4 strongly labeled cells and 2 very weakly labeled ones. We chose one of the two splits, *VT25602.p65AD;VT2064.GAL4DBD*, for behavior analysis. Female test flies with both dTrpA1 and the split GAL4 driver or controls with either one of them were paired with Canton S males and tested under different temperatures. The elicited following behavior was then measured as a fraction of time that flies spend in following in a 10-min assay (following index). While at 25°C neither control nor test flies showed any following behavior, both 28°C and 31°C were sufficient to stimulate significantly increased level of following behavior in the test flies but not the control flies which showed similar amount of movement (Figure 2.5B). Therefore, activation of Neuron 1 alone is sufficient to trigger following in females.

Furthermore, we also tested if the gender of the target or the mating status of the test females affects the following behavior. As a result, we didn't see any difference in following indexes between male and female targets at 28°C (Figure S6A) and between virgin test flies and mated test flies at 28°C and 31°C (Figure S6B).

In parallel, we used the enhancer tiles from the positive GAL4 lines to generate driver lines with independent expression systems. The *VT8469.Hap1* driver showed female following behavior when tested with *HBS-TrpA1* and labels only two neuronal clusters in the brain including Neuron 1 (Figure S7A). There are also 4 cells of Neuron 1 labeled by the *VT8469.Hap1*. The other type of brain neurons consists of two cells and is located anteriorly in the brain with arborization spatially separated from Neuron 1 (Figure 2.5C). In the VNC, this driver labels only 2 cells in the medial metathoracic ganglion which endogenously activate HBS sequence without a Hap1 driver (Figure S7B). Similarly, thermal activation of Neuron 1 using *VT8469.Hap1* and *HBS-TrpA1* under elevated temperatures induces female following to a level compared to split GAL4 driver. Control flies showed no following behavior at all temperatures (Figure 2.5D).

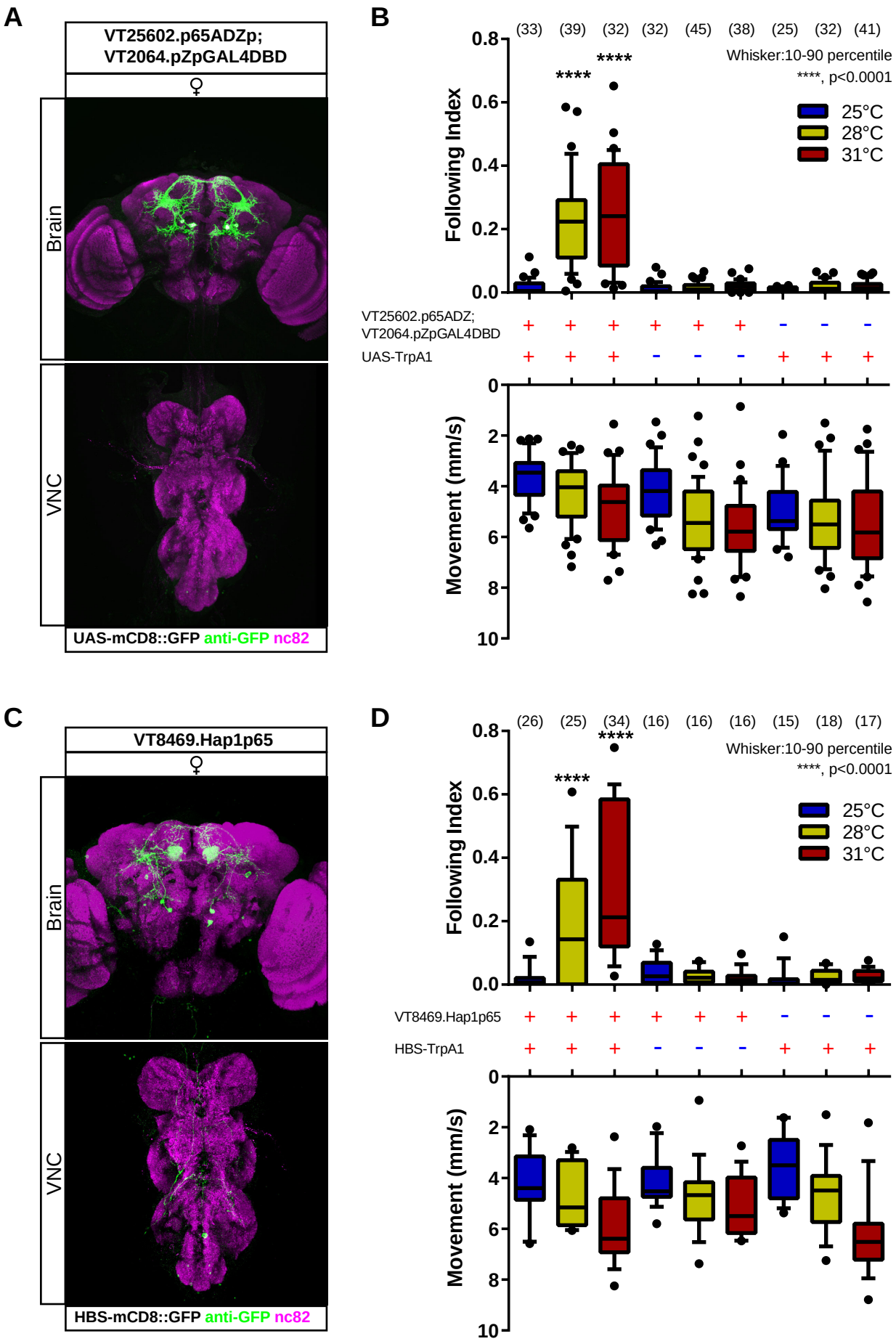

Figure 2.5 Restricted split-GAL4 and Hap1 drivers induce female following

Both the split GAL4 and the Hap1 drivers label Neuron 1 strongly and induce female following upon thermal activation robustly, although the Hap1 driver seems somewhat weaker than the spilt GAL4 driver in expression level (Figure 2.5A and C) and behavioral strength (mainly at 28°C, Figure 2.5B and D). Taken together, with the help of these newly identified driver lines, we were able to conclude that Neuron 1, named as pMP8 hereafter, induces female following when being activated. The pMP8 neurons can be thus defined behaviorally by its effect in triggering female following and genetically by the *VT25602.p65AD;VT2064.GAL4DBD* split GAL4 (named also as *pMP8.split* hereafter) and the *VT8469.Hap1* drivers.

2.2.4 pMP8 is co-labeled by all female-following inducible driver lines

The pMP8 neurons are located in the posterior of the brain below the protocerebral bridge (PB) and project characteristically crossing the PB and bifurcates to arborize extensively in the ipsilateral hemisphere and sparsely in the contralateral hemisphere, as we previously observed (Fig. 2.6A).

To confirm that the pMP8 neurons are commonly labeled by all the drivers that trigger female following upon activation, including the split GAL4, Hap1, and previously identified positive GAL4 drivers, we labeled pMP8 with *VT8469.Hap1* and independently with various (split) GAL4 lines and checked for overlaps in expression pattern. As a result, we found that *VT8469.Hap1* shares about 4 pMP8 cells with *pMP8.split* driver which labels about 6 cells (5.64±0.63, n=14, counted with nuclear marker) (Figure 2.6B). These 4 shared cells from pMP8 are much stronger than the two uncommon cells in expression intensity (indicated by arrows in Figure 2.6B) and are also present in all the six positive GAL4 lines identified from the screen (showing only three in Fig. 2.6C). In addition, we were also able to confirm this anatomical commonality behaviorally using *VT8469.Hap1* and *HBS-GAL80* to suppress GAL4 activities in pMP8 from the six positive GAL4 hits (i.e. the split GAL4 cannot be suppressed due to its p65 activation domain) (Figure 2.6D). Expression of *UAS-TrpA1* in the pMP8-excluded neuronal populations targeted by these GAL4 drivers failed to elicit female following upon thermal activation, but leaves other phenotypes

intact, suggesting pMP8 is indeed the functionally relevant neurons for female following targeted by these GAL4 drivers (data not shown).

In summary, the pMP8 clusters consist of 4 strongly labeled neurons that shared among all the positive drivers for female following and possibly another two weakly labeled neurons that seems to be present only in some drivers. Since the minimal 4 shared neurons are sufficient (MARCM data indicate that one cell is sufficient) for inducing female following and strongly labeled by our split GAL4 driver, we decided focus our further analysis on these 4 cells.

2.2.5 pMP8 belongs to *fru*+ and *dsx*+ circuits and its development is regulated by *dsx*

Since *fruitless* and *doublesex* regulate most neuronal dimorphisms between sexes, we first checked if the pMP8 cluster belongs to *fruitless*+ or *doublesex*+ neuronal population. To test this, we labeled pMP8 with *VT25602.GAL4* and *VT8469.Hap1* and checked if pMP8 is also labeled by *fru-LexA* and *dsx-GAL4* respectively. As a result, we observed all 4 pMP8 cells are co-labeled by *fru-LexA* and *dsx-GAL4* (Figure 2.7A and B), suggesting that pMP8 is part of the *fru*+ and *dsx*+ neuronal circuits which are known to be required for sexually dimorphic behaviors.

We moved on to test if the female specificity of pMP8 is regulated by *fru* or *dsx* by labeling pMP8 in *fru* or *dsx* mutants. We tested this in dominant negative mutants of *fru* and *dsx* respectively. In fru^{M}/+ females which display male-like courtship, pMP8 is still present and is morphologically intact, while in wild-type females expressing Dsx^{M} proteins which become intersex, the cell number of pMP8 is significantly reduced from about 4 (3.81±0.40, n=16) cells to about 2 cells (1.94±0.93, n=16) ($p<0.0001$) (Figure 2.7C). This suggests that the presence of pMP8 in females depends on the normal function of female-specific Dsx^{F}. What remains to be tested is whether pMP8 exists in fru^{F} and *dsx* homozygous mutants.

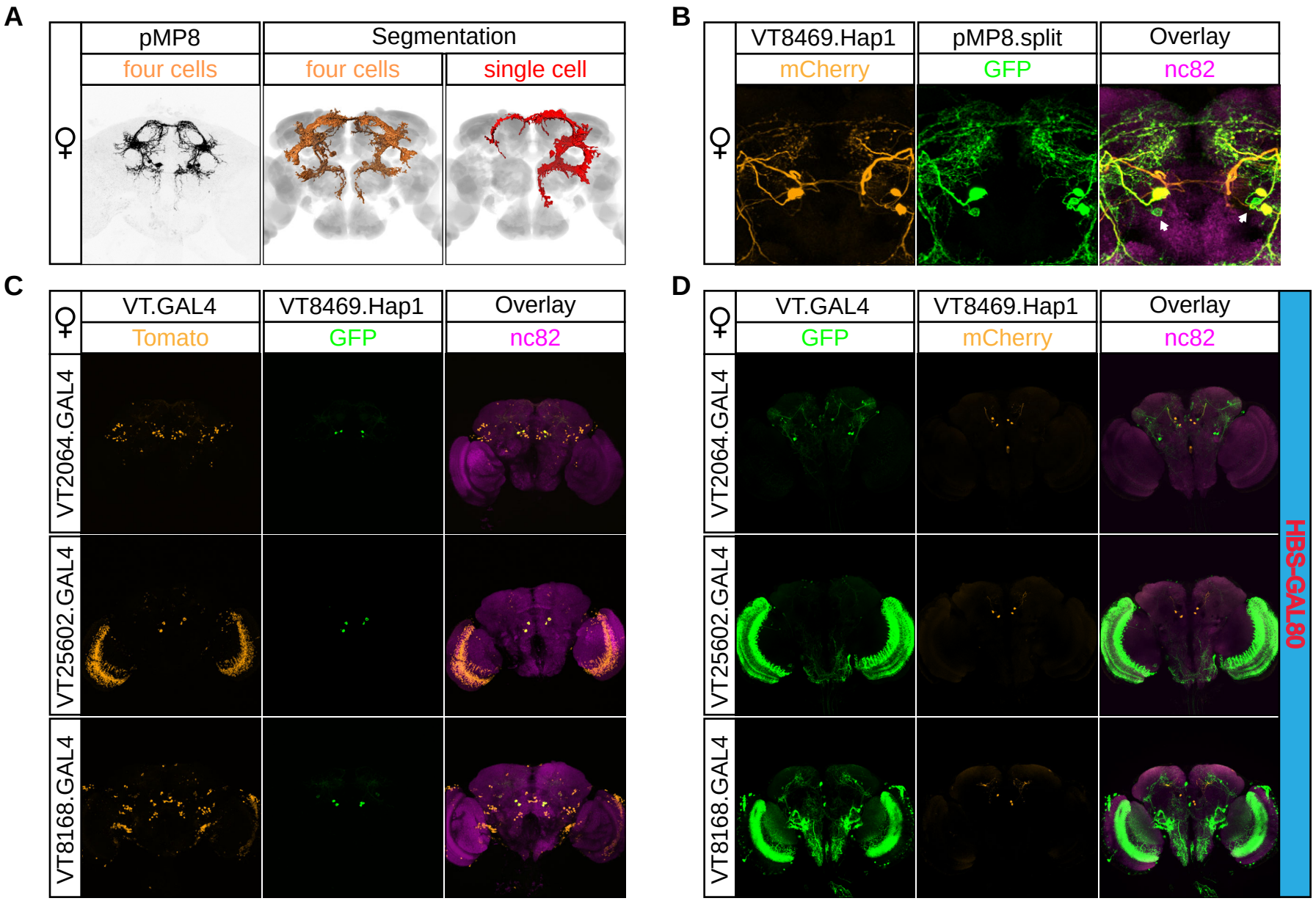

Figure 2.6 pMP8 is commonly targeted by all the positive lines

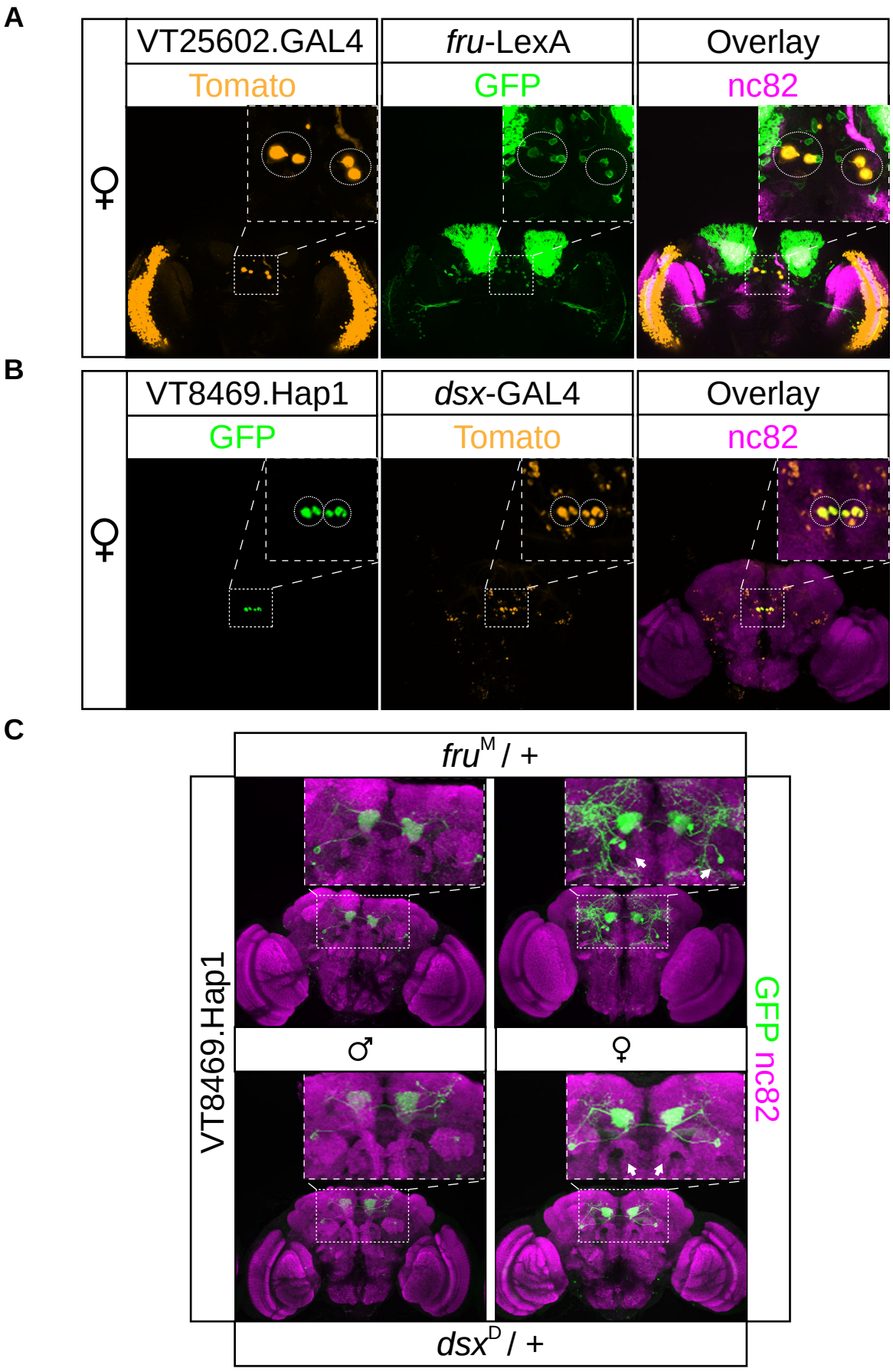

Figure 2.7 pMP8 is *fru*+, *dsx*+ and depends on dsx^{F}

2.2.6 pMP8 functions via acetylcholine to induce female following

The induction of female following by pMP8 activation must be mediated through downstream partners that receive inputs from pMP8. In order to characterize what neurotransmitters pMP8 uses to communicate to these neurons, we labeled pMP8 with pMP8.spilt driver and stained with antibodies against ChAT (choline acetyltransferase) and GABA. We found that pMP8 is positive for ChAT (Figure 2.8A) but not GABA (data not shown).

To further test if pMP8 uses acetylcholine to induce female following, we performed RNAi experiments against *ChAT* in pMP8 activated flies under elevated temperature and checked if female following is suppressed. We used two independent RNAi lines containing inverted repeat sequences (dsRNA), one of which was integrated using randomly insertion (#1, GD) and the other using site-specific integration (#2, TriP). A strain carrying UAS-GFP transgene with VALUIM10 vector backbone was used for background control of RNAi #2. As a result, we observed that RNAi #1 significantly suppresses but does not abolish female following, while RNAi #2 reduces it to almost zero similar to non-TrpA1 control (Figure 2.8B), suggesting that pMP8 indeed uses ACh to activate downstream neurons in triggering female following.

2.2.7 pMP8 is both anatomically and behaviorally asymmetrical

The arborization of pMP8 spans over extensive area and contains featured ring-like structure, which poses the question where pMP8 receives its inputs and sends its outputs. To address this, we expressed reporter genes that are localized to specific neuronal compartments. We used *UAS-DenMark* and *UAS-Synaptotagmin::GFP* to label postsynaptic and presynaptic regions respectively. To our surprise, we didn't see clear segregation between these two markers (Figure 2.9A). There are several possibilities: 1) the markers we used are not completely specific for labeling corresponding sub-cellular compartments, at least not in pMP8; 2) the markers are specific, indicating that pMP8 processes information locally with inputs closely located near outputs; 3) the two pMP8 cells on the same side might have complementary or different polarities, leading to overlap of both markers when

A

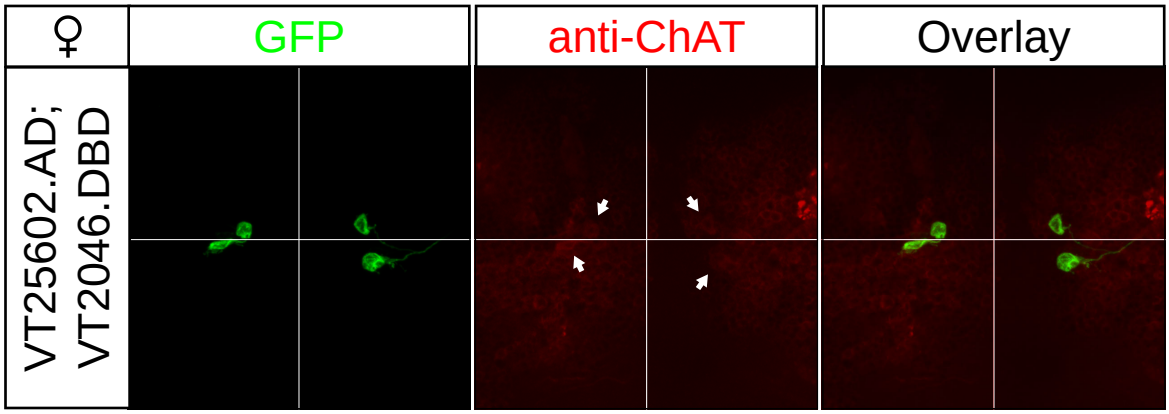

B

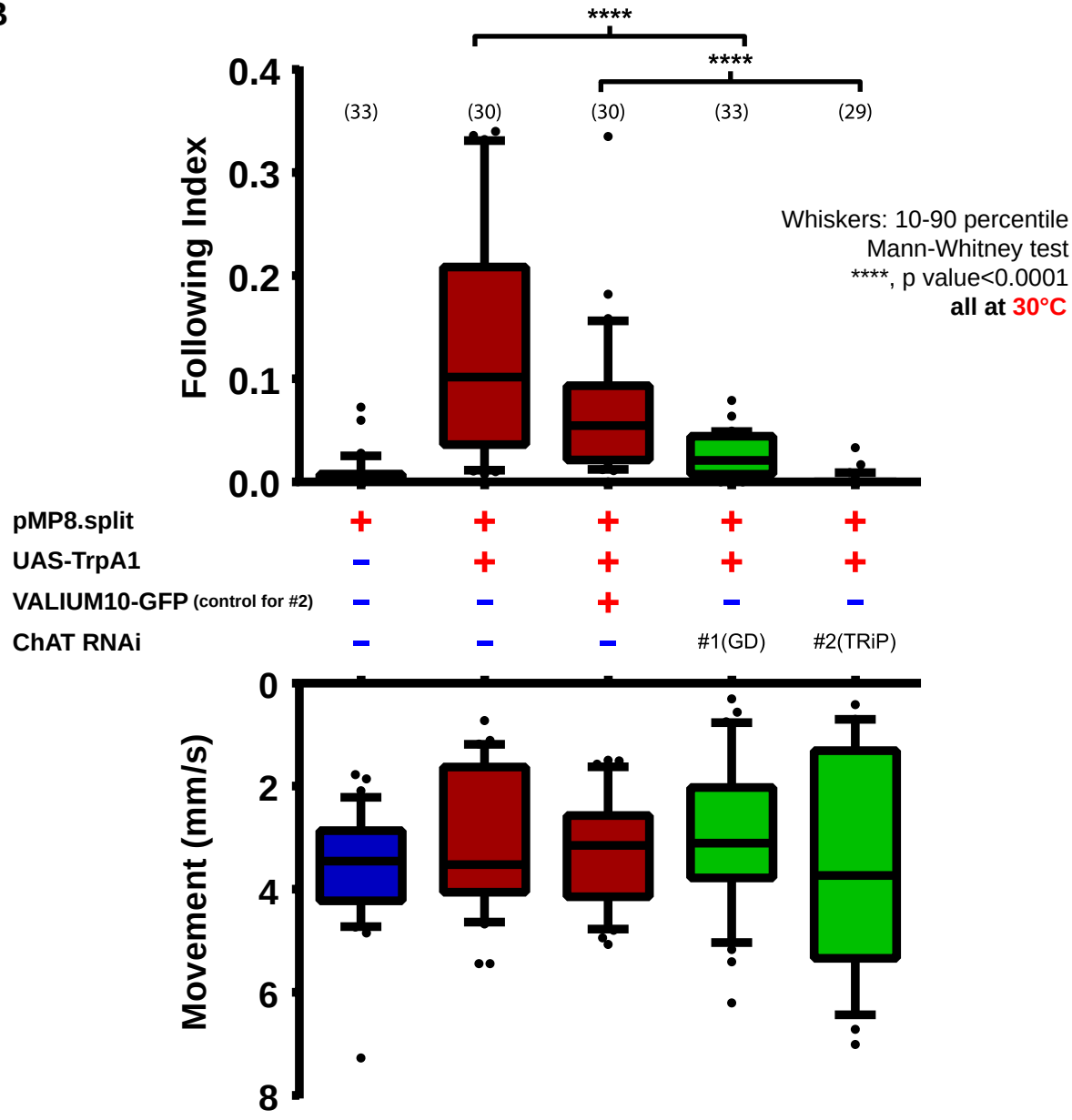

Figure 2.8 pMP8 triggers female following through acetylcholine

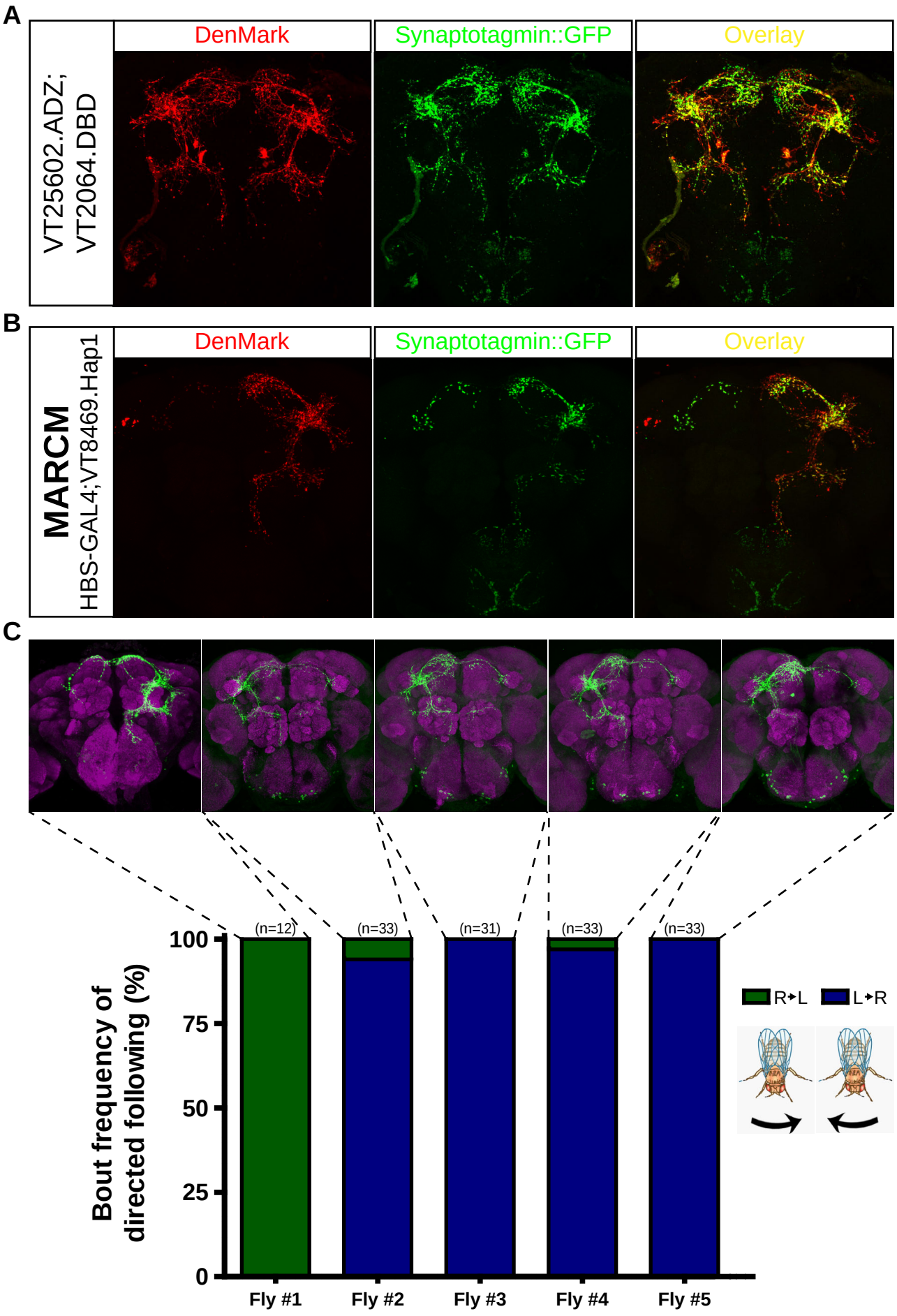

Figure 2.9 Anatomical and behavioral asymmetry of pMP8

observed together; 4) pMP8 might have different polarity for ipsi- and contra-lateral arborizations.

To exclude the last two possibilities, we need to be able to visualize sub-cellular compartments in a single pMP8 cell, for which we applied MARCM but with *UAS-DenMark* and *UAS-Synaptotagmin::GFP* instead of *UAS-mCD8::GFP*. We used the *VT8469.Hap1* in combination with *HBS-GAL4* to convert the driver from Hap1 system to GAL4 system to drive expression of the UAS reporters. This conversion and the use of the Hap1 driver instead of the *pMP8.split* is necessary because the split GAL4 driver cannot be suppressed by *tub-GAL80* due to its p65 activation domain and cannot be used for MARCM experiments. We were able to generate single-cell clones in a number of flies (n=8) and observed an asymmetry of labeling between ipsi- and contra-lateral hemispheres (Figure 2.9B). In the ipsilateral hemisphere, the dorsal region of the arborization of a single pMP8 was still intermingled with both pre- and post-synaptic markers; the ventral region contains predominantly postsynaptic DenMark signals. In the contralateral hemisphere, only synaptotagmin::GFP was strongly expressed at a similar level to the ipsilateral hemisphere, while DenMark proteins were barely visible. This suggests that pMP8 neurons receive inputs from the ventral region of ipsilateral arborizations, send outputs through contralateral arborizations, and may do both in the dorsal area of ipsilateral arborizations.

Interestingly, we observed a similar behavioral asymmetry in flies in which pMP8 neurons were singularly or unilaterally activated. We noticed, during the MARCM experiment of *VT2064* that narrowed down to two neuronal types, that unilateral labeling of pMP8 sometimes resulted in directional preference of target movements (Fly#1 in Figure 2.9), i.e. pMP8 unilaterally activated flies only respond to target moving in one direction but not the other (left-to-right or right-to-left). This was not observed in all the flies in which pMP8 was unilaterally activated, possibly due to the confounding contribution from other neurons labeled together. To confirm this behavioral asymmetry, we needed to generate flies with only unilateral pPM8 cells labeled, tested for behavioral asymmetry and correlated that with the laterality of the labeled pMP8 cells. However, it was not trivial to obtain clones of pMP8 without any other neurons labeled in the first MARCM experiments due to the driver's non-restricted expression pattern. Therefore, we again used *VT8469.Hap1* and *HBS-*

GAL4, together with *UAS-TrpA1* and *UAS-mCD8::GFP* in a MARCM system. So far we were able to obtain another 4 flies with unilateral pMP8 neuron labeled (Fly #2 to #5 in Figure 2.9C). From the preliminary data, we could observe a correlation that activation of pMP8 unilaterally tends to induce following behavior only towards flies moving from contralateral direction, e.g. flies with left-hemisphere pMP8 activated (e.g. Fly #1) will follow flies moving from right to left side.

2.2.8 pMP8 was most effectively silenced by shibire^{ts}

Female following behavior was only observed when pMP8 was artificially activated. However, it is not clear whether pMP8 is also involved in normal female following behaviors. In order to test this, we need to be able to silence pMP8 effectively. We co-expressed different silencers together with *UAS-Trpa1* in pMP8 and determined the effectiveness of these silencers in blocking TrpA1-mediated activation of pMP8. Although failure to block pMP8 activation by TrpA1 doesn't mean the silencers are not effective under normal condition, success to do so guarantees their performance in silencing pMP8.

We tested three silencers, *UAS-shibire^{ts1}*, *UAS-TNT* and *UAS-Kir2.1*. While both TNT and Kir2.1 function as silencers at normal temperature, shibire^{ts1} requires elevated temperatures around 30°C. Both TrpA1 and shibire^{ts1} depend on elevated temperature for their functions, but may have diverse kinetics. TrpA1 is able to induce following in pMP8 around 26.5°C which is well below the optimal working temperature of shibire^{ts1}. Therefore, as temperature rises from 25°C towards 30°C, one might expect a competition between the two effectors, which is indeed what we observed. We found that at 27°C there is a small but significant increase of following compared to the non-following controls and this increase is completely abolished at 30°C, suggesting that shibire^{ts1} effectively silenced pMP8 despite of the competition from TrpA1. On the contrary, at 27°C both TNT and Kir2.1 were able to block following completely. However, when temperature reaches 30°C, they start to lose their battle with TrpA1: the following index was significantly reduced at this temperature but remained substantially above zero. This indicates that TNT and Kir2.1 are less efficient and successful in blocking pMP8 activation than shibire^{ts1}.

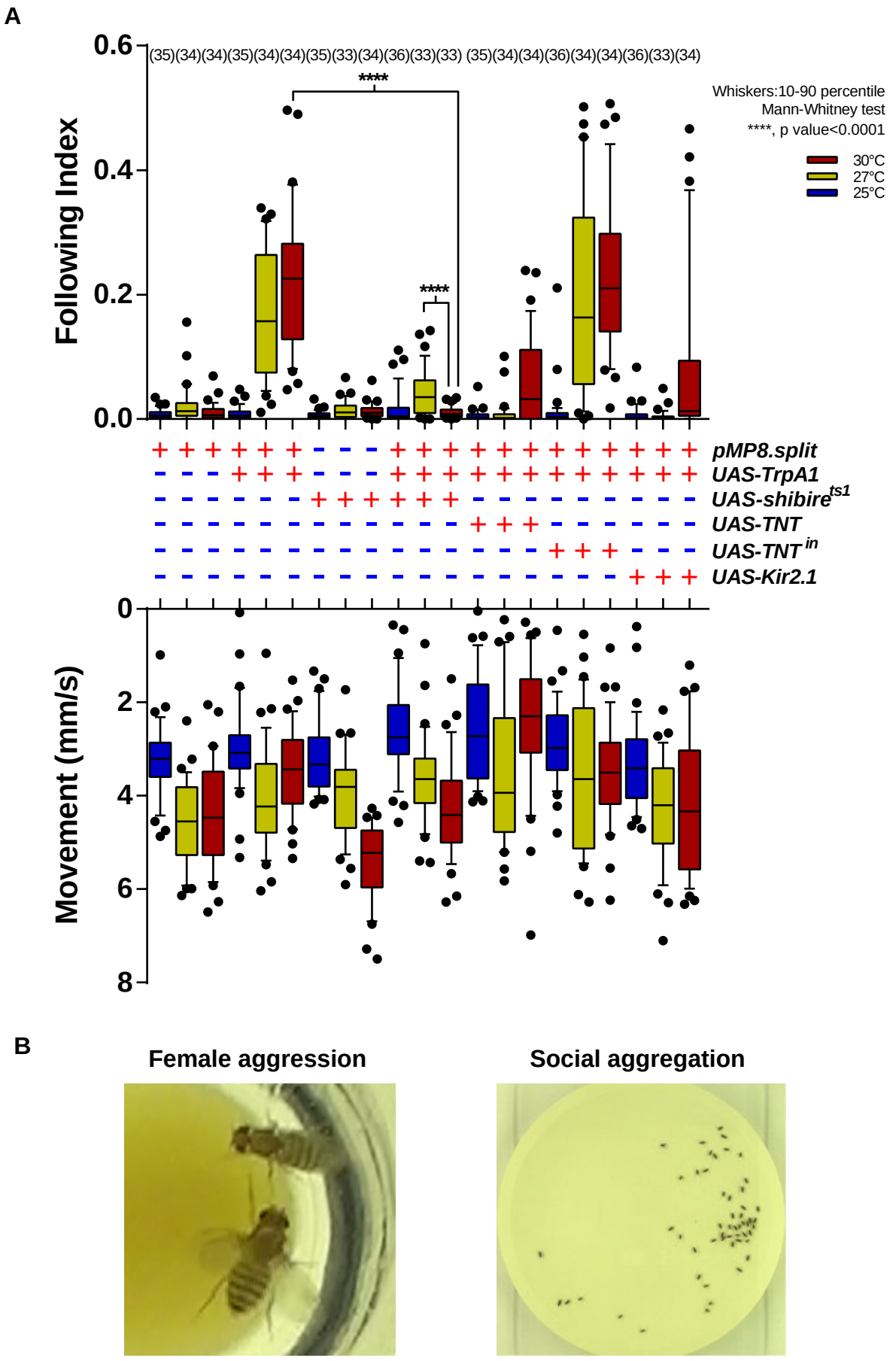

Figure 2.10 pMP8 is most effectively silenced with *shibire*^{ts}

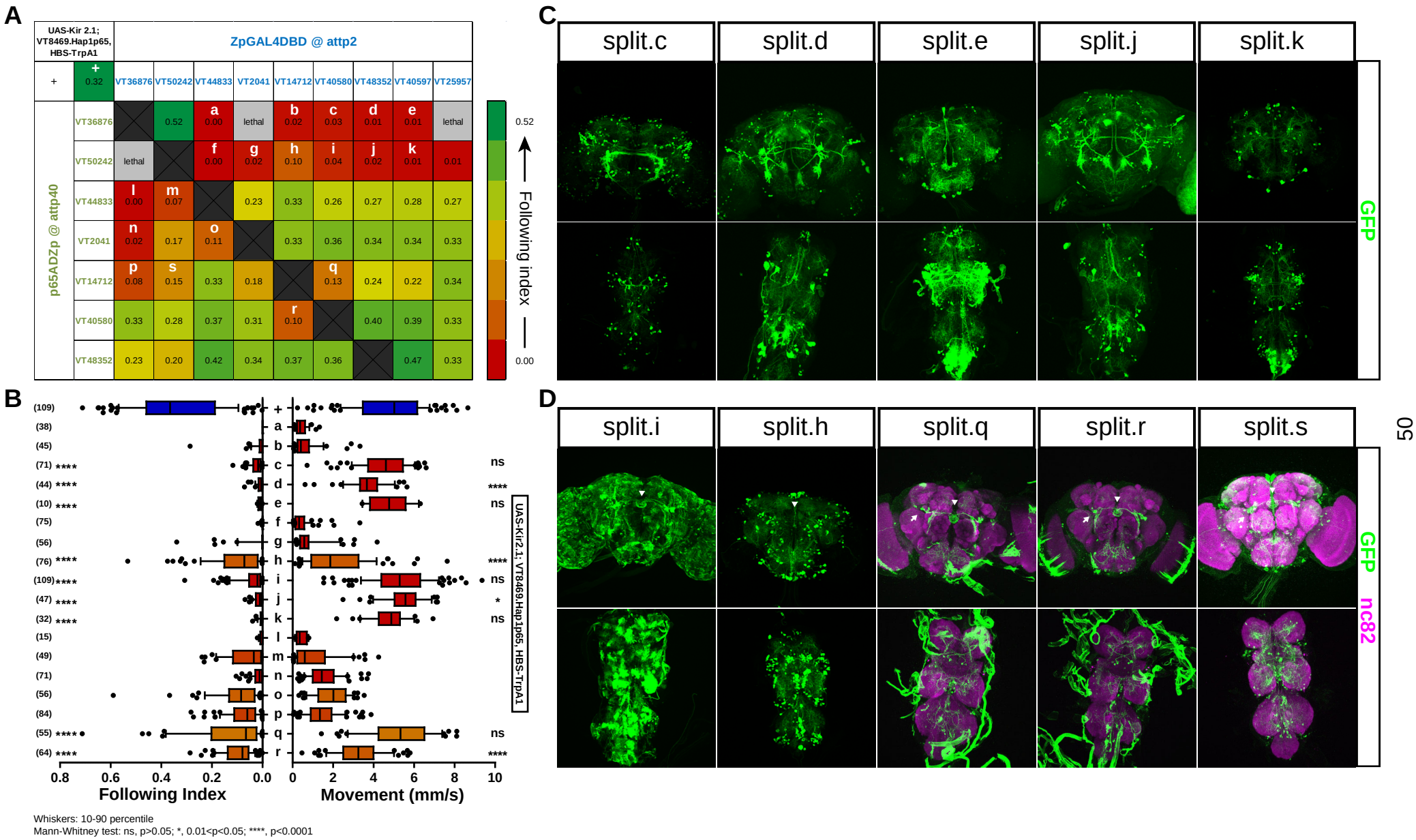

Figure 2.11 Epistasis screen with split GAL4 identified a potential circuit component

With this knowledge, we are confident in our ability to block pMP8's activities. As discussed in the introduction, the most well known cases when female flies display following-like behavior are aggression and social aggregation. However, we could observe these behaviors in a wild type strain but not in the *pMP8.split* driver and *UAS-shibire^{ts1}* strains. This might be due to the relatively fast selection of aggressive traits that have been described in a few studies (Dierick and Greenspan, 2006; Penn et al., 2010). Therefore, backcrossing to wild type strains that show robust aggression is under way. Nevertheless, we do have some preliminary data showing either prolonged silencing or ablation of pMP8 neurons leads to increased female following behavior (data not shown). The phenotypic similarity between activation and silencing experiments seems contradictory but can be potentially explained by complex circuit feedback or plasticity mechanisms. This suggests that the activities of pMP8 neurons are somehow required in maintaining normal female behaviors.

2.2.9 Epistasis screen identified potential circuit partners of pMP8

The identification of pMP8 provided us an entry point into the neuronal circuit for following behavior, but does not reveal enough insight in how it functions in relation to the whole circuit. In order to understand the mechanisms of pMP8 in instructing following behavior, it is essential to expand our knowledge and identify more components of the circuit partners. Therefore, we conceived an epistasis screen to look for neurons that upon silencing suppress following behavior in pMP8 activated females. We used *VT8469.Hap1* to activate pMP8 and in the meanwhile expressed *UAS-Kir2.1* or *LexAop-TNT* in 450 GAL4 or LexA drivers that were selected based on anatomical overlap with pMP8 and relevant behavioral data from silencing experiments. As a result, we identified 9 GAL4 lines and 3 LexA lines that were able to antagonize pMP8 activation, leading to abolished or significantly reduced female following. Consistent with general observation, these GAL4 or LexA lines are also broad in expression, necessitating further spatial restriction (data not shown).

From the 9 positive GAL4 lines, we made split hemi-drivers (both hemi-drivers for 7 lines, one hemi-driver for 2 lines) and then generated all 56 possible split combination drivers for behavioral tests as shown in the matrix (Figure 2.11A). Following indexes were quantified for lines with viable progenies when crossed to screening stock

(*UAS-Kir2.1;VT8469.Hap1,HBS-TrpA1*) and plotted with color-codes indicating strength of following suppression (with red as strongest). 18 split combinations showing strong or intermediate phenotypes were separately plotted with quantification of movement level (Figure 2.11B). Among these, 12 split combinations showed complete abolishment of pMP8-induced following and the rest 6 split combinations had their following index significantly reduced ($p<0.0001$). It is possible that some of these phenotypes may be attributed to general loss of activity. Indeed, movements measured by average speed were close to zero in 5 combinations and significantly reduced in another 6 combinations. Most of these showing impaired movements also have very broad expression. The expressions of the 6 combinations (split.c, d, e, I, j and k) which showed complete loss of following and normal movements range from intermediate to broad (Figure 2.11 C and D). Comparison between these lines did not reveal any neurons in common. However, we were able to identify a common type of neurons in those (split.h, q, r and s) showing relatively weaker phenotypes with normal or slightly reduced movements (Figure 2.11D). The cell bodies of this neuronal class are located above antennal lobe and the projection travels horizontally into ellipsoid body of the central complex. These neurons were also seen in one combination that showed strongest phenotype and normal movement (split.i, Figure 2.11D). The arborization of these neurons does not overlap with that of pMP8 neurons, suggesting that it might be required for following to occur but not directly connected to pMP8. Further experiments are needed to prove that this neuronal class is indispensable for following behavior or to identify other neurons from these split combinations.

2.2.10 pMP8 may originate from the same clonal lineage as P1

Since the following behavior of pMP8-activated females resembles male courtship, could pMP8 neurons also resemble the neurons that are involved in male courtship? Indeed, we found that pMP8 neurons share several similarities with the male specific P1 neurons (Figure 2.12A). Neurons of both pMP8 and P1 neurons have their cell bodies located at the posterior of the brain below the protocerebrum bridge (PB), send projections dorsally crossing the PB, arborize extensive at the clamp, belong to the *fru*+ and *dsx*+ population, exist only in one sex or the other and trigger courtship-like following or courtship behaviors upon activation. Clonally related neurons can

A

	Morphology	Molecular marker	Sexual dimorphism	Induced behavior
pMP8	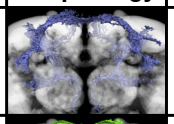	*fru+, dsx+*	female specific	following
P1	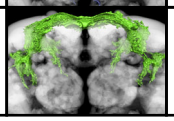	*fru+, dsx+*	male specific	courtship

B

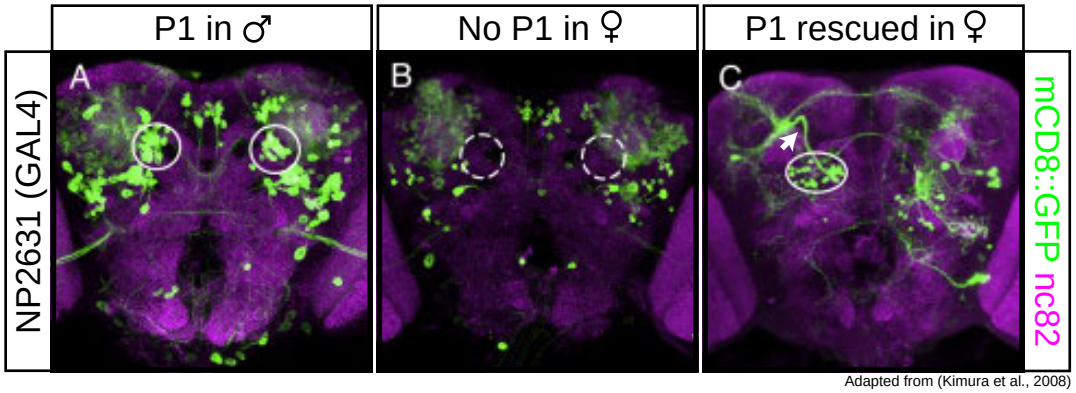

Adapted from (Kimura et al., 2008)

C

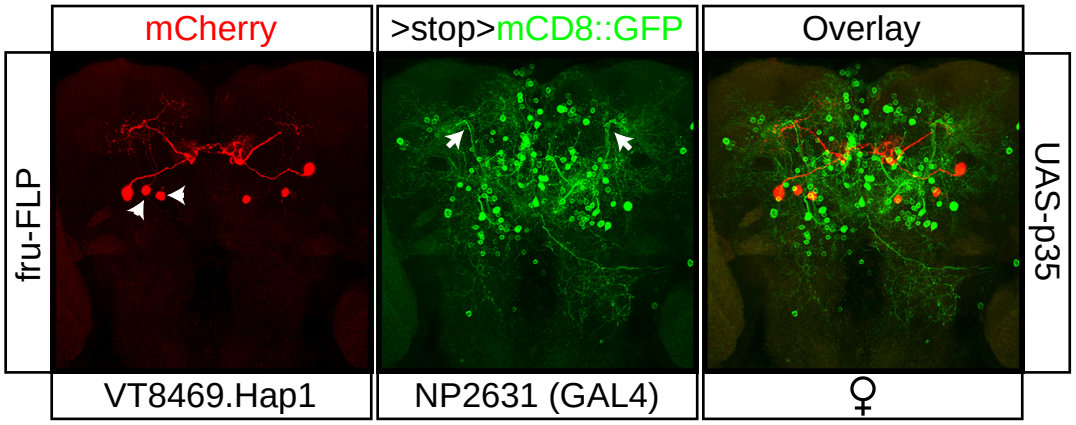

D

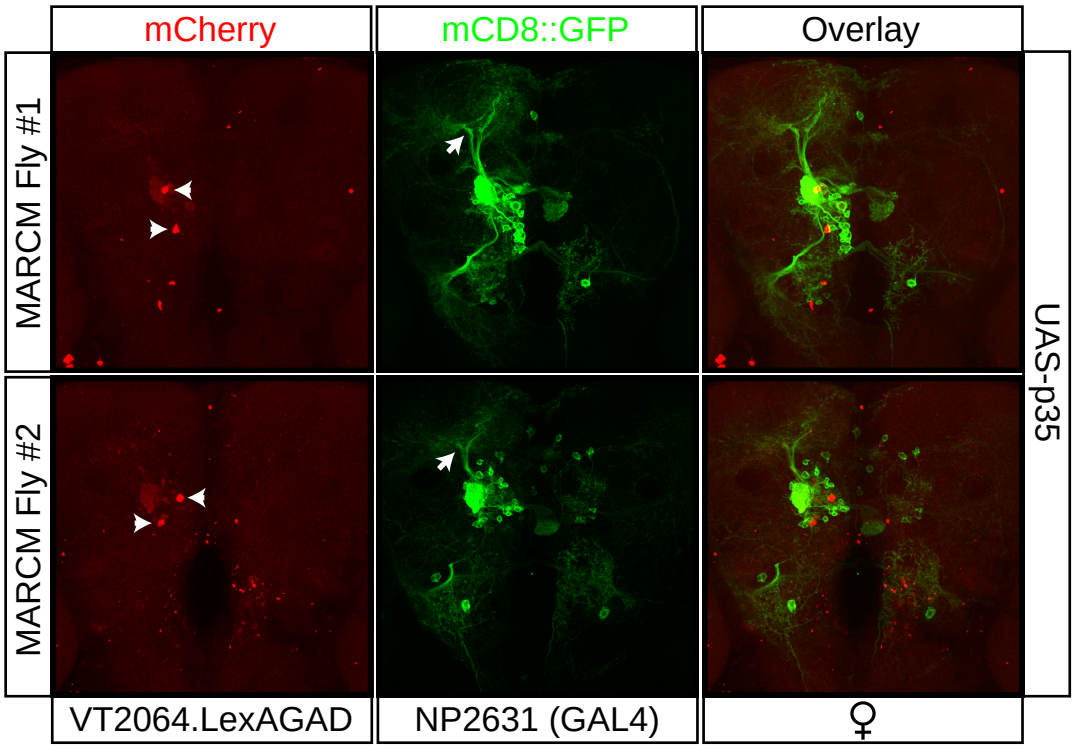

Figure 2.12 pMP8 may originate from the same neuroblast as P1

share similar cell body location, projection and arborization pattern (Ito et al., 2013; Yu et al., 2013), and function (Li et al., 2012; Ohtsuki et al., 2012). Could pMP8 and P1 originate from the same clonal lineage? An obstacle to answer this question is that in adult fly they don't exist in the same animal, due to their sex specificity. To overcome this problem, we need to create animals with both neurons present. It has been shown that P1 undergoes programmed cell death in females during development and can be rescued in females by knocking down three apoptosis genes at once (Kimura et al., 2008) (Figure 2.12B). Similarly, using *UAS-p35*, we were able to block apoptosis in P1 neurons and rescue a number of them in females, as identified by their featured projection pattern (indicated by arrows in Figure 2.12C). We could confirm that pMP8 and P1 neurons are not the same neurons labeled genetically by different drivers as co-labeled pMP8 do not overlap with rescued P1 neurons (Figure 2.12C). To test if pMP8 and P1 share the same clonal lineage, we generated clones labeling the whole cluster of either pMP8 or P1 neurons, by performing early heat-shock with MARCM. From about 100 samples, we were able to obtain two flies with either pMP8 or P1 labeled. In these two flies, both pMP8 (2 neurons) and P1 (unknown) neurons are labeled in the same hemisphere. This preliminary data suggests that pMP8 and P1 may indeed share the same lineage and co-exist during development before each undergoes programmed cell death in either males or females.

2.3 Discussion

Female-specific neurons enabling male-like behaviors

Evolution has accumulated an array of behaviors essential for each animal's survival and reproduction, some of which have been shaped sexual-dimorphically through sexual selection. In *Drosophila*, courtship and aggression are two such behaviors. A distinct feature between males and females during these behavior is that males heavily perform following or chasing while females don't. It has been unclear whether this distinction represents an absence of neuronal elements that enable females to perform male-like behaviors or a dimorphic employment of such neural substrates. Previous studies have identified a male-specific neuronal class (P1) which enables male courtship (Kimura et al., 2008), suggesting that the lack of male courtship

behaviors in females might be due to lack of P1 neurons. However, our serendipitous observation of the courtship- or aggression-like following phenotype in females when a subpopulation of neurons were artificially activated, suggests that females possess the necessary neuronal elements and the ability to behave like males. Using the genetic toolkits of *D. melanogaster*, we were able to reveal the identity of these neuronal elements in females to be the pMP8 neuronal cluster. pMP8 neurons are female specific, because 6 independent GAL4 drivers all targeted this cluster only in females and expression of Dsx^{M} in females reduced their cell number. Therefore, our data suggest that evolution might have separately generated in female flies the pMP8 neurons sufficiently for powering male-like behaviors but have naturally adapted them in a female-specific manner.

Sex-specific neuronal elements regulate sex-common circuits?

Detailed characterization of pMP8 neurons showed that many aspects of them were similar to that of the male-specific P1 neurons, including cell body location, arborization pattern, molecular marker (*fru*+ and *dsx*+), sex specificity and ability to trigger male-like following behavior. They share functional and molecular similarities, but they are not the same neurons, as P1 neurons are programmed to undergo cell death in females (Kimura et al., 2008) and rescued P1 neurons in females don't coincide with pMP8 cells (Figure 2.12C). Furthermore, our preliminary lineage analysis of pMP8 and rescued P1 neurons in females supports a model in which pMP8 and P1 might be generated by the same neuroblast and co-exist at early developmental stage but soon afterwards each undergoes sex-specific cell death in males and females respectively. Although the pMP8 and P1 clusters are sexually dimorphic, they might be wired into a sexually common neuronal circuit as both are able to trigger similar behavioral outputs and females with rescued P1 behave like males (Vera, unpublished data).

From an evo-devo perspective, one might speculate how pMP8 and P1 have evolved. In one scenario, both female and male flies might initially share a common ancestral neuronal cluster and behave similarly during courtship or aggression. Under the pressure of sexual selection, this cluster of neurons might be subsequently divided into two sub-types, pMP8 and P1, which undergo sexual dimorphic

modification and ultimately only survive in one sex or the other. Alternatively, the putative ancestral neurons could differentiate into an equal number of ancestral pMP8 neurons in females and P1 neurons in males, which then undergo sex-specific programmed cell death and result in reduced but non-overlapping sub-sets of pMP8 and P1 neurons. Regardless of the processes, the initial properties of the ancestral neurons (resembling pMP8 or P1 or something intermediate) might determine the direction of selection and the initial behavioral roles each sex take. This neuronal evolution of sexual dimorphisms in key components in an otherwise sexually common neuronal circuit might create a sexually regulated switch in the circuit that subserves the corresponding evolution of behavioral sexual dimorphisms, leading to the formation of conventional sex roles in flies.

Possible biological and evolutionary functions of pMP8

An important question un-addressed in this study is what functions pMP8 neurons normally have. Assuming pMP8 neurons indeed play a role in female behavior, it is most likely to find such a role in aggression or social aggregation behaviors, where females normally display following or approach behavior. Given pMP8 neurons' extensive arborization and central location, it would not be surprising if it indeed plays a role in integrating sensory inputs from different modalities and determining when a bout of following behavior needs to be triggered. Alternatively, it is possible that pMP8 neurons are behaviorally non-functional in females, although their functions seem to be required at least for normal female behavior as suggested by our observation that prolonged silencing or ablation of pMP8 leads to ectopic following (data not shown). The activities of pMP8 neurons might be needed for maintaining the integrity of the underlying neuronal circuitry or the balance with other antagonizing components in the circuit to permit normal female behaviors, but not used to trigger any behavioral outputs. This might be a result of pMP8 being residual neurons from evolution. If this is indeed the case, such neurons that are non-functional but required for normal functions might potentially serve as backup substrates for future evolution to work on. In the event of males being the restrictive factor for reproduction, such as reduced number or fertility due to environmental change, the existence and the adaptation of such neuronal substrates would allow females to evolve to actively seek and secure a mate and would be advantageous

and beneficial for the survival of the species. The existence of neurons like pMP8 in females might be the underlying neuronal mechanisms for species in which sex role reversals have been shown, such as in monogamous pipefish (Berglund et al., 1989; Sogabe and Yanagisawa, 2007), polyandry spotted sandpipers (Oring and Lank, 1986), female-dominant butterfly *Acraea encedon* whose males are mostly killed by infection of male-killing *Wolbachia* (Jiggins et al., 1998), and possibly also in species that females take more active role, such as *Drosophila virilis* species whose females perform duet with males during courtship (Donegan and Ewing, 1980; Satokangas et al., 1994).

Probable mechanistic models of pMP8-mediated following

The pMP8 and P1 neurons are similar in morphology and in their ability to induce following behaviors. It's natural to assume that there's a causal link between their morphology and function. How does their arborization pattern give rise to their function in triggering following behavior?

To implement the following behavior, a minimum of three components is necessary, 1) command system to decide when it should happen; 2) visual system to provide spatial information of targets; 3) locomotion system to adjust walking pattern in repose to target movement. Given their extensive arborization, central location, and no apparent link to sensory or locomotion pathways, pMP8 is more likely to be involved in the command system and seems to be supported by our experimental observation as well. Directional and positional visual information of a target is continuously generated from the motion detection and the position system and sent to higher brain centers through projections neurons. Under normal conditions, this visual information is sufficient to cause female flies to follow a moving bar, as in optomotor or fixation response, but not a small object such as a walking fly. However, when pMP8 neurons are activated, following behavior towards a fly can also be triggered. This suggests that the visual circuits are connected to the locomotion circuits, but the point of connection is gated by activities of pMP8 neurons when the target is a fly. The gating function of pMP8 neurons is further supported and extended by the observation that unilateral activation of pMP8 neurons leads to selective following response towards targets moving from contralateral direction

(Figure 2.9C). Because visual systems compute target information regardless of its moving direction, the asymmetrical following response further suggests that pMP8 neurons gate the communication between visual and locomotion circuits asymmetrically (ipsilateral vs. contralateral).

How and where does this asymmetrical gating occur? Single-cell labeling of pMP8 neurons with polarity markers suggest that pMP8 neurons send outputs bilaterally but receive inputs only unilaterally from the ipsilateral hemisphere. The asymmetry of pMP8 gating function could arise from two sources: spatial asymmetry of output sites or connection asymmetry to neurons with directional responses. It is possible that pMP8's outputs to ipsi- and contra-lateral hemispheres are different and the asymmetrical gating could occur in either one of them. Our data are not sufficient to distinguish these two possibilities. Alternatively, the outputs of pMP8 in both hemispheres may be the same, but the asymmetrical gating may happen on both sides due to connections with neurons sensitive to movements from one direction only. For example, right-hemisphere pMP8 neurons may only gate connections between left-to-right motion sensitive LPTCs and left-to-right turning neurons. This would require the connections between the visual and the locomotion systems topographically organized. Although this is unclear, such topographical organization is well known within each system. It would not be surprising if the connections between them are also organized in a similar manner.

Once the gating from pMP8 neurons is permissive, the locomotion circuit would respond to inputs from the visual system carried by different lobula plate tangential cells (LPTC), such as the motion sensitive LPTCs (Bausenwein et al., 1992; Bausenwein and Fischbach, 1992; Schnell et al., 2012). Specific body movement, such as turning, may be triggered depending on the visual inputs. The central complex is likely to underlie the locomotion circuit. The ellipsoid body neuron that was shared by several split GAL4 combinations from the epistasis screen might be part of this circuit. Although a neuronal component of circuit that controls backward walking has been identified (Bidaye, 2012), much remains to be identified.

Other components of the following circuitry

Identification of pMP8 alone provides an important entry point into the following behavior and the underlying neuronal circuitry, but is not enough to explain how the following behavior is orchestrated. For this purpose, more components of the circuit need to be identified and characterized. These components should include neurons from the three systems aforementioned. The more important ones, however, are those that directly interface with pMP8, because these interfaces are where neuronal interactions happen, such as the gating function of pMP8, and thus would reveal much insight of the underlying mechanisms.

To map the outputs of pMP8, we have performed an epistasis screen to identify neurons whose activities are required for following behavior. We have found driver lines with relatively sparse expression, but have not determined which neurons are functionally relevant. We could try to further restrict the expression through anatomical or behavioral assays. This would require screening more driver lines and is not an easy task, especially without knowing the number and identity of the neurons that we are looking for. A better and probably more efficient approach is to perform physiological studies, such as calcium imaging with GCaMP. If a downstream neuron connects directly to pMP8, we would expect to see a calcium response in this neuron upon pMP8 activation. We would start test with the drivers we currently identified but may also screen other VT lines. For finding the inputs to pMP8, a similar imaging approach can be taken by imaging pMP8 and looking for neurons whose activation is able to induce a calcium response.

2.4 Figure legends

Figure 2.1 Optomotor response and fixation response

(A) Optomotor response, as observed in an assay in which a tethered fly turns towards the direction of rotating stripes. (B) Fixation response. When the tethered fly is given control of a bar stimulus, it tends to fixate the bar right in front of it. (C) Original “Reichardt detector” mathematical model for explaining motion detection. (D) Simplified scheme of optic lobe illustrating the identified organization of the motion detection system. (D) Illustration of diverse neuronal types observed in the optic lobe. Adapted from (Bahl et al., 2013; Borst, 2009).

Figure 2.2 Models of central complex in target directed locomotion

(A and B) Hypothetic models of the central complex in controlling object-oriented turning (A) and forward walking with increased speed (B). The protocerebral bridge (PB) is considered to contain a topographical representation of a target's azimuth position and its activity is hypothesized to increase the contralateral step size. If the target is sideways to the fly, asymmetrical activation of the PB would increase step size more on the contralateral side, resulting in turning (A). If the target is in the front, symmetrical activation of PB would result in speeding up. Adapted from (Triphan et al., 2010).

Figure 2.3 Expression analysis identified one female-specific neuronal cluster as a likely candidate for female following behavior

(A) Brain and (B) VNC expression of six GAL4 lines that induce following behavior in females upon thermal activation. Both males and females with *VT.GAL4*s and *UAS-mCD8::GFP* were stained with anti-GFP (green) and mAb nc82 (magenta) and visualized from posterior (A) and ventral (B) perspectives. A female-specific neuron in the posterior brain (dashed circles) was identified as common to all six lines and serves a likely candidate for the female following behavior.

Figure 2.4 MARCM correlates two neuronal types with female following

(A) Adaptation of MACRM (a mosaic analysis with a repressible cell marker) with the additional use of *UAS-TrpA1*. Adapted from (Lee and Luo, 2001). (B) Expression of *VT2064.GAL4* with *UAS-mCD8::GFP* registered onto a standard brain and VNC. Glial expression was observed in the VNC. (C) Segmentations of 20 most frequently observed neuronal types from MARCM of *VT2064.GAL4* (neuron 10 is not shown) represented in various colors. (D) Expression of GFP in each of the 20 types of neurons in 37 following and 34 non-following females. Each column represents one fly; each row, one neuronal type. Color-coding indicates whether a neuronal type is labeled unilaterally (red) or bilaterally (purple). Blank indicates no labeling. (E) The labeling frequency of each of the 20 neuronal types in either no-following group or following group, ****, $p<0.0001$, Fisher's exact test. Color-coded bars represent frequency of either unilateral (red) or bilateral (purple) labeling. (F and G) Segmentation of a single cell of Neuron 1 (F) and multiple cells of Neuron 2 (G) registered onto a standard brain template. Cell bodies are indicated by arrows. (H)

Frequency of Neuron 1 and Neuron2 co-labeled ipsilaterally or contralaterally. (I) Number of neuronal types labeled in each fly in the following and no following groups, p=0.4522, Mann-Whitney test.

Figure 2.5 Restricted split-GAL4 and Hap1 drivers induce female following

(A) Brain and VNC of a *VT25602.p65ADZ, VT2064.pZpGAL4DBD, UAS-mCD8::GFP* female stained with anti-GFP (green) and mAb nc82 (magenta). (B) Following behavior of *VT25602.p65ADZ, VT2064.pZpGAL4DBD, UAS-TrpA1* females and control females with either the driver or the effecter alone were automatically tracked using a tracking software developed by Machacek, C. (Matebook). Following index was quantified as percentage of time spent in following within 10min at three different temperatures. Average speed (mm/s) was used as a measure of general movements. Box charts were plotted with whiskers representing 10-90 percentile. Numbers on top of each bar represent the number of flies tested. Test flies showed significantly increased following index at both 28°C and 30°C comparing to controls (****, p<0.0001, Mann-Whitney Test). (C) Brain and VNC expression of a *VT8469.Hap1p65, HBS-mCD8::GFP* female, stained similarly as in (A). (D) Following behavior of *VT8469.Hap1p65, HBS-TrpA1* females and controls were quantified similarly as in (B).

Figure 2.6 pMP8 is commonly targeted by all the positive lines

(A) An inverted staining image of 4 pMP8 neurons from a *VT25602.p65ADZp, VT2064.ZpGAL4DBD, UAS-mCD8::GFP* female fly stained with anti-GFP (black) and segmentations of 4 pMP8 cells (orange) and 1 pMP8 cell (red) in standard brains. (B) Brain staining of a *VT8469.Hap1, HBS-mCherry,VT25602.p65ADZp, VT2064.ZpGAL4DBD, UAS-mCD8::GFP* female. The 4 pMP8 cells were co-labeled by both drivers. 2 additional weaker neurons were only labeled by the split GAL4 driver. (C) Brain stainings of females carrying *VT8469.Hap1, HBS-mCD8::GFP, UAS-mCD8::Tomato* and one of the three VT GAL4 lines *VT2064, VT25602, VT8168*. The 4 pMP8 neurons labeled by the *VT8469.Hap1* driver were also targeted by all three GAL4 lines. (D) Brain stainings of females carrying *VT8469.Hap1, HBS-mCD8::mCherry, HBS-GAL80, UAS-mCD8::GFP* and one of the three VT GAL4 lines *VT2064, VT25602, VT8168*. GAL4-driven GFP signals in pMP8 were suppressed by

expression of GAL80 with *VT8469.Hap1*. (B, C, and D) Flies brains were stained with anti-DsRed (orange), anti-GFP (green) and nc82 (magenta).

Figure 2.7 pMP8 is fru+, dsx+ and depends on dsxF

(A) Brain staining of a *VT25602.GAL4, UAS-mCD8::Tomato, fru-LexA, LexAop-mCD2::GFP* female with similar antibodies as in (A). The 4 pMP8 cells labeled by the *VT25602.GAL4* were also labeled by *fru-LexA*. (B) Brain staining of *VT8469.Hap1, HBS-mCD8::GFP, dsx-GAL4, UAS-mCD8::Tomato* female using similar antibodies as in (A). The 4 pMP8 neurons were co-labeled by both drivers. (C) Visualization of pMP8 neurons in both male and female flies with genotypes of fru^{M}/+ and dsx^{D}/+ using the *VT8469.Hap1* driver stained with anti-GFP (green) and mAb nc82 (magenta). pMP8 neurons were unaffected by fru^{M} but were lost or reduced in dsx^{D}/+ flies in which Dsx^{M} proteins antagonized Dsx^{F}. Boxed regions are enlarged in the insets.

Figure 2.8 pMP8 triggers female following through acetylcholine

(A) Brain of a *pMP8.split, UAS-mCD8::GFP* female stained with anti-GFP (green) and anti-ChAT (red). All 4 pMP8 cells were labeled by anti-ChAT staining. (B) Two RNAi lines against ChAT suppressed pMP8-mediated female following by TrpA1activation at 30°C. Flies carrying VALIUM10-GFP was used for background control of RNAi#2. Bar colors indicate different groups: control without TrpA1 (blue), control with TrpA1 (red), and test groups with RNAi (green). P values were calculated using Mann-Whitney test (****, $p<0.0001$).

Figure 2.9 Anatomical and behavioral asymmetry of pMP8

(A) Brain staining of a *pMP8.split, UAS-DenMark, UAS-Synaptotagmin::GFP* female fly, labeling 4 pMP8 cells. Pre- (green) and post-synaptic (red) markers intermingled in most areas. (B) A MARCM clone that expressed the two polarity markers in a single pMP8 cell. Presynaptic sites (green) predominate in the contralateral arborization and postsynaptic sites (red) predominate in the ventral area of the ipsilateral arborization. (A and B) Brains were stained with anti-DsRed (red) and anti-GFP (green). (C) Selective following behavior of 5 MARCM flies with pMP8 unilaterally labeled towards targets moving in a specific direction. Frequency of following bouts towards targets moving from right to left (green) and left to right (blue)

(from the test fly's perspective) was plotted as percentages of all observed events for each fly. Numbers on top of each bar represents the total number of following bouts for each fly. Brain images of each fly are shown on top, stained with anti-GFP (green) and nc82 (magenta). Fly #1 is significantly different from the other flies (Fisher's exact test, $p<0.0001$). Fly#2 to #5 are not significantly different from each other (Fisher's exact test, $p=0.3018$).

Figure 2.10 pMP8 is most effectively silenced with shibire^{ts}

(A) Following indexes of female flies co-expressing *UAS-TrpA1* and one of the three silencers, *UAS-shibire^{ts}, UAS-TNT* and *UAS-Kir2.1*, and respective control flies. The "+" (red) and "-" (blue) symbols indicate the presence and absence of each transgenic elements respectively. Bar colors indicate test temperatures at 25°C (blue), 27°C (yellow) and 30°C (red). Higher temperature seemed to be associated with stronger TrpA1-mediated activation. Both *UAS-TNT* and *UAS-Kir2.1* were able to abolish following behavior induced by pMP8 activation at 27°C but only significantly reduced it at 30°C. *UAS-shibire^{ts}* was able to abolish stronger TrpA1 activation at 30°C, suggesting that it is a more effective silencer than the other two. (B) Possible behaviors to test the biological functions of pMP8, showing two female flies during aggression (left) and a group of males and females during social aggregation (right). Canton S flies were used in these assays.

Figure 2.11 Epistasis screen with split GAL4 identified potential circuit components

(A) Split GAL4 matrix of epistasis screen to suppress pMP8-induced following behavior, showing following indexes of each split GAL4 combinations expressing *UAS-Kir2.1* with a background of *VT8469.Hap1, HBS-TrpA1*. Hemi-drivers of p65ADZp and ZpGAL4DBD halves are shown on the left and the top of the matrix respectively. Color-coding indicates the level of following indexes, from the strongest suppression (red) to no suppression (green). Letters (white) in the cells that showed strongest suppression of following behaviors (red) are used to represent the identities of split GAL4 combinations. Control fly with no split GAL4 combinations is shown in the top-left corner (+). (B) Box plot showing following indexes (left) and movements (right) of split combinations with abolished or reduced following and the control. Each split combination is represented by a corresponding letter as shown in the matrix (A).

Split combinations that showed abolished or reduced following and normal or slightly reduced movements were selected for further studies (Mann-Whitney test: ns, $p>0.05$; *, $0.01<p<0.05$; ****, $p<0.0001$). (C) Brain and VNC expressions of those that abolished following behavior and showed normal movements (also split.i in (D)), imaged after fixation without antibody staining (GFP, green). (D) Brain and VNC expression of 5 split combinations that seemed to label a common neuron, stained with no antibodies in split.i and h (GFP, green), and with anti-GFP (green) and nc82 (magenta) in split.q, r, and s. Arrows indicate the location of cell bodies and arrowheads indicate the arborizations in the ellipsoid body.

Figure 2.12 pMP8 may originate from the same neuroblast as P1

(A) Similarities between pMP8 and P1 neurons. (B) Male-specific P1 neurons could be rescued in a females using *H99* deficiency (with deletions of three cell death genes *hid, grim* and *rpr*) (White et al., 1994) in a MARCM clone. Arrow indicates the characteristic projection pattern of P1 neurons. Images were adapted from (Kimura et al., 2008). (C) Brain of a *VT8469.Hap1, HBS-mCherry, NP2631(GAL4), UAS-p35, UAS-fruFLP, UAS>stop>mCD8::GFP* female. In this female fly, P1 neurons were rescued in females using *UAS-p35* and visualized by *fruFLP* and a reporter with a stop cassette. P1 neurons seemed to be different cells from the pMP8 neurons (arrowheads). (D) Brain expressions of two MARCM flies carrying trangenes of *VT2064.LexAGAD, LexAop-mCherry, NP2631(GAL4), UAS-p35, UAS-mCD8::GFP*. In both samples, pMP8 neurons (arrowheads) were found together with P1 neurons in the same hemispheres, suggesting that they are clonally related. (C and D) Brain samples were stained with anti-DsRed (red) and anti-GFP (green). Arrows indicate the projections of P1 neurons and arrowheads indicate the cell bodies of pMP8 neurons.

2.5 Material and methods

Fly stocks

MARCM stocks: 1) *hs-FLP*; FRT^{G13}, *tub-GAL80*; 2) FRT^{G13}, *UAS-mCD8-GFP*; 3) $neoFRT^{19A}$; 4) *hsFLP*, *tub-GAL80*, $neoFRT^{19A}$ and *UAS-mCD8::GFP, UAS-DenMark,*

UAS-synaptotagmin::GFP, *dsx*^{D} were obtained from Bloomington *Drosophila* Stock Center. RNAi lines against ChAT were requested from VDRC stock center (GD20183) and Bloomington (TRiP.JF01877). *NP2631* was obtained from the *Drosophila* Genetics Resource Center, Japan. *UAS-TrpA1* was provided by Garrity, P. (Hamada et al., 2008) and *UAS-TrpA1* (VIE-260b) was described in (von Philipsborn et al., 2011). *LexAop-mCherry* was requested from Landgraf, M.'s lab. *HBS-GAL80* and *HBS-GAL4* were generated by Feng, K. in VIE-260b. *fru*^{M} was described in (Demir and Dickson, 2005). Other stocks that were used include *UAS-TNTin* and *UAS-TNT* (Sweeney et al., 1995), *UAS-Kir2.1* (Baines et al., 2001), *UAS-mCD8::Tomato* (Toda et al., 2012), *UAS-shibire*^{ts1} and *LexAop-myr::mCherry* (Pfeiffer et al., 2012), *fru*^{FLP} and *UAS>stop>mCD8::GFP* (Yu et al., 2010).

Immunohistochemistry and image registration

Flies were reared at 25°C and aged for 4-6 days after eclosion before dissection and staining as described in (Yu et al., 2010). Antibodies used were rabbit anti-GFP (Torrey Pines Biolabs, 1:6000), chicken anti-GFP (Abcam, 1:6000), rabbit polyconal anti-dsRed (Clontech, Living Color®, 1:1000), mouse mAb anti-ChAT (DSHB, 1:100), mouse mouse mAb nc82 (DSHB, 1:20) and secondary Alexa 488, 568, and 647 antibodies (Invitrogen, 1:1000). Obtained stainings were registered onto a standard brain or VNC template as described in (Yu et al., 2010).

Behavioral assay and quantification

Test female flies were paired with *white-* wild type males and assayed for female following behavior in 10mm courtship chamber for 10min under different temperatures. Ambient temperatures were adjusted to maintain constant using a heating glass on top of the courtship chamber and a power supply with a feedback controller. Male flies were used as targets to improve automatic tracking. For quantification of pMP8 mediated following behavior, test females were reared with males to prevent copulation during the assay which may disrupt female following. Automatic quantification was performed using a tracking software developed by Machacek, C. (Matebook). Percentage of time spent in following within a 10min assay, the following index (FI), was used as a measure of following behavior. Average speed was used as a control for fly movements.

MARCM (mosaic analysis with a repressible cell marker)

Flies carrying appropriated transgenes were crossed and progenies from the crosses were heat shocked at late embryo and early larvae stage for 1hr to 1.5hr. Several MARCM experiments were conducted in this study: 1) For MARCM with *VT2064.GAL4*, flies carrying *FRT^{G13}, UAS-mCD8-GFP; UAS-TrpA1* and *hs-FLP; FRT^{G13}, tub-GAL80; VT2064.GAL4* were crossed. 2) For MARCM with polarity markers, *neoFRT^{19A}; HBS-GAL4; VT8469.Hap1p65* and *hsFLP, tub-GAL80, neoFRT19A; UAS-DenMark, UAS-synaptotagmin::GFP; UAS-DenMark, UAS-synaptotagmin::GFP* were used. 3) For MARCM addressing directional preference of unilaterally activated pMP8, *neoFRT^{19A}; HBS-GAL4; VT8469.Hap1p65* flies were crossed to *hsFLP, tub-GAL80, neoFRT^{19A}; UAS-mCD8::GFP; UAS-TrpA1*. 4) For MARCM on rescued P1 and pMP8, *neoFRT^{19A}; UAS-p35, NP2631; VT2064.LexAGAD* and *hsFLP, tub-GAL80, neoFRT^{19A}; UAS-mCD8::GFP; LexAop-myr::mCherry* were used.

Epistasis screen

Two stocks were used in the epistasis screen: 1) *UAS-Kir2.1; VT8469.Hap1, HBS-TrpA1*; 2) *Lexop-TNT; VT8469.Hap1, HBS-TrpA1*. Screening was done by crossing these two stocks to respective GAL4 or LexA driver lines selected based on anatomical overlap with pMP8 arborization or functional studies. Suppression of following was measured by reduced following indexes and movement was used to control for locomotion defects.

Chapter 3. Neuronal circuitry for female rejection response

3.1 Background

3.1.1 Female mating decision in *D. melanogaster*

In *Drosophila*, like most other species with conventional sex role, males compete for mates and females choose their mates. During courtship, a female fly actively evaluates the quality of the courting male through multiple sensory cues and responds with a mating decision based on the male's quality and her own physiological states (Dickson, 2008). If the female decides to accept the male for copulation, she slows down and opens her vaginal plate. Otherwise, she rejects the male by extruding her ovipositor towards him or runs away. The major factors that regulate a female's sexual receptivity are the pheromonal and acoustic cues from males and her own sexual maturity and mating status.

Pheromones

Two pheromones that stimulate female receptivity have been identified, the volatile 11-cis-vaccenyl acetate (cVA) and the non-volatile pheromone (z)-7-tricosene (7T). cVA is specifically synthesized in male ejaculatory bulb (Butterworth, 1969) and induces females receptivity through Or67d olfactory receptor neurons (Kurtovic et al., 2007). 7T is a male-specific cuticular hydrocarbon and at higher levels reduces latency to copulation (Grillet et al., 2006).

Courtship song

The most important signal from males is the courtship song they play during courtship. Males that don't sing or sing poorly have little success in mating (Sturtevant, 1915; von Schilcher, 1976). Playback of a prerecorded high-quality song is able to rescue the mating failure of mute males (Bennet-Clark and Ewing, 1967). The male courtship song consists of a mixture of "pulse song" and "sine song", which

are trains of regularly spaced monocyclic pulses and sinusoidal hums (~160Hz) respectively. A critical parameter of the courtship song is the time interval between pulses, the interpulse interval (IPI). The IPI is species-specific (Ewing and Bennet-Clark, 1968) and has been implicated in species recognition (Bennet-Clark and Ewing, 1969; Kyriacou and Hall, 1982).

The courtship song is then detected through rotational movements of the antenna which are induced by sound-invoked air particle vibration (Gopfert and Robert, 2002). These movements are picked up by the stretch-receptor neurons in the Johnston's organ, the fly's "ear" (Albert and Gopfert, 2006). The Johnston's organ neurons (JON) are the primary auditory neurons and can be subdivided into five subgroups based on the distinct regions they innervate in the antennal mechanosensory and motor center (AMMC) in the brain (Kamikouchi et al., 2006). JONs are topographically organized: each JON typically innervates only one region of the AMMC and JONs innervating each region are clustered in the JO (Kamikouchi et al., 2006). JONs innervating region A and B have been shown to respond to sound (Kamikouchi et al., 2009).

Sexual maturity

Newborn females do not mate within approximately the first 24hrs and gradually become fully receptive (Manning, 1967). The genetic and neural basis of this transition has remained largely unknown, except for the implication of Juvenile hormone by a few observations. 1) The activities of juvenile hormone stimulates oocyte development (Wyatt and Davey, 1996) and correlate temporally with the development of sexual receptivity (Ringo, 1996). 2) Topical application of juvenile hormone and implanting of tissues active secreting juvenile hormone both accelerated the onset of receptivity (Manning, 1966). 3) Mutant females with defective juvenile hormone synthesis have very low receptivity (Ringo et al., 1991).

Mating status

Drosophila virgin females become unreceptive to courting males up to 10 days after mating, accompanied with significant increase of egg laying rate and various other changes, known as the "post-mating switch" (Kubli, 2003; Manning, 1962). Two

mechanisms have been suggested for the cause of this switch: “copulation effect” and “sperm effect” (Manning, 1967). The “copulation effect” lasts for 4 to 8 hr and could be due to mating plugs formed by male seminal fluid (Lung and Wolfner, 2001; Manning, 1967). On the other hand, the “sperm effect” can last 8 to 10 days after mating until sperm is depleted from storage (Manning, 1967). The initial phase of this sperm effect has been associated with several peptides from the male seminal fluid, including the sex peptide (SP or Acp70A) (Aigaki et al., 1991; Chen et al., 1988), DUP99B (Saudan et al., 2002) and Acp26Aa (Chapman et al., 2001; Herndon and Wolfner, 1995), but only SP has been shown to be required for the “sperm effect” persistently (Chapman et al., 2003; Liu and Kubli, 2003). SP, synthesized from male accessory glands (Cirera and Aguade, 1997), binds to sperm tail with the N-terminus and starts to gradually cleave off its functional C-terminus after transferred to the female reproductive tract during copulation, underlying the persistent effect of post-mating switch (Peng et al., 2005; Schmidt et al., 1993).

On the female side, the receptor for sex peptide (SPR) has been uncovered in a recent pan-neuronal genome-wide RNAi screen for egg laying phenotype and shown to be required for post-mating switch of both receptivity and egg laying (Yapici et al., 2008). The primary sensory neurons where SPR mediates the post-mating switch in females have also been identified by screening different neuronal sub-populations with RNAi against *SPR* gene (Hasemeyer et al., 2009; Yang et al., 2009). These receptor neurons reside in the female reproductive tract, send projections to the abdominal ganglion region in the VNC and are molecularly defined to be *fru*+ and *ppk*+ (Hasemeyer et al., 2009). Secondary order neurons that connect these sensory neurons to the central brain have also been identified and were shown to mediate the post-mating switch (Feng, K., Palfreyman, M.T. and Dickson, B.J., unpublished).

3.1.2 Neuronal basis of female mating decision

Our knowledge about the underlying neuronal basis that control female mating decision remains limited and scattered among a few independently studied sensory pathways and classes of interneurons, such as the cVA pathway mediated by Or67d ORNs (Kurtovic et al., 2007) and DA1 PNs (Couto et al., 2005; Fishilevich and Vosshall, 2005), the sex peptide pathway mediated by female oviduct *fru*+ and *ppk*+

neurons (Hasemeyer et al., 2009; Yang et al., 2009) and secondary order neurons (Feng, K., Palfreyman, M.T. and Dickson, B.J., unpublished), SIFamide neurons (Terhzaz et al., 2007) and *spinster* expressing neurons (Sakurai et al., 2012). However, the higher brain centers that integrate these different pathway or neurons remain largely unknown.

3.1.3 Strategies to identify higher order neurons for female receptivity

Our ultimate goal is to identify the higher order neuronal circuitry that integrates different sensory pathways to make mating decisions in female flies. Traditionally, due to the relative ease of manipulation and observation, studies have been focused on mapping sensory input pathways that induce or suppress female receptivity, while the motor outputs that represent a female's mating decision have been rarely addressed. Efforts to identify the integration centers from sensory pathways beyond secondary order neurons have been difficult, due to increasing complexity of connections from multiple pathways. We hypothesized that the connections from putative integration centers to motor outputs might be more straightforward and easier to be mapped, as presumably little computation is needed for behavior execution once a mating decision is made. The main behavioral outputs of a female's mating decision are either acceptance by vaginal plate opening or rejection by ovipositor extrusion. Because the vaginal plate opening is too subtle to be observed, we decided to focus on the ovipositor extrusion behavior and perform a neuronal screen.

Generally, for a screen-based strategy, one can use either silencing or activation approach to manipulate activities of neuronal subpopulations and examine corresponding behavioral changes. For silencing approach, we may look for neurons that either reduce or increase female receptivity, which has led to the identification of the secondary order neurons that relay SP signals into the central brain (Feng, K., Palfreyman, M.T. and Dickson, B.J., unpublished), or ovipositor extrusions. Alternatively, one can also activate different subsets of neurons and look for similar phenotypes. We decided to start the screen with activation approach and then complement with silencing approach in secondary characterizations. Since females normally only perform ovipositor extrusion when courted by a male, we used isolated

females and therefore any ovipositor extrusion can be ascribed to our neuronal manipulation. We hoped to find neurons that control ovipositor extrusion close to the motor output end and then trace upward to the central brain.

3.2 Results

3.2.1 Screening with split GAL4 drivers to obtain restricted expression patterns that induce ovipositor extrusion

From our neuronal activation screen and retests, we have identified 252 GAL4 lines and confirmed 177 of them which showed either ovipositor extrusion or egg laying phenotypes upon TrpA1-mediated activation. We have then taken the tiles (i.e. genomic fragments used for driving GAL4 expression) from these confirmed GAL4 lines to generate split hemi-drivers, from which we have tested 60 p65ADZp and 90 ZpGAL4DBD and confirmed 40 and 71 respectively (see Chapter 1). We wanted to obtain split GAL4 combinations that give restricted expression so that we can link behaviors to specific neurons functionally and anatomically. Therefore, we created a 40x71 matrix of split GAL4 hemi-drivers and tested some of these combinations both behaviorally and anatomically (Figure 3.1A and B). So far, we have tested 261 split GAL4 combinations and identified 156 combinations that are positive for ovipositor extrusion. The positive GAL4 combinations that have restricted expression patterns facilitated linking behaviors to specific neurons. We compared these expression patterns and identified three types of neurons that occurred frequently and all the sparse combinations obtained seemed to label at least one of them.

3.2.2 vMtAb: an ascending neuron in the VNC that elicits ovipositor extrusion

The first type of neurons was seen in the expression of many split GAL4 combinations (Figure 3.2A). It consists of two cells that are located medially at the ventral region between the abdominal ganglion and the metathoracic ganglion, therefore named as vMtAb (Figure 3.2B). These neurons project through dorsal VNC and arborize in the SOG and posterior brain regions (Figure 3.2B). Stainings with polarity markers, *UAS-DenMark* and *UAS-synaptotagmin::GFP* confirmed vMtAb

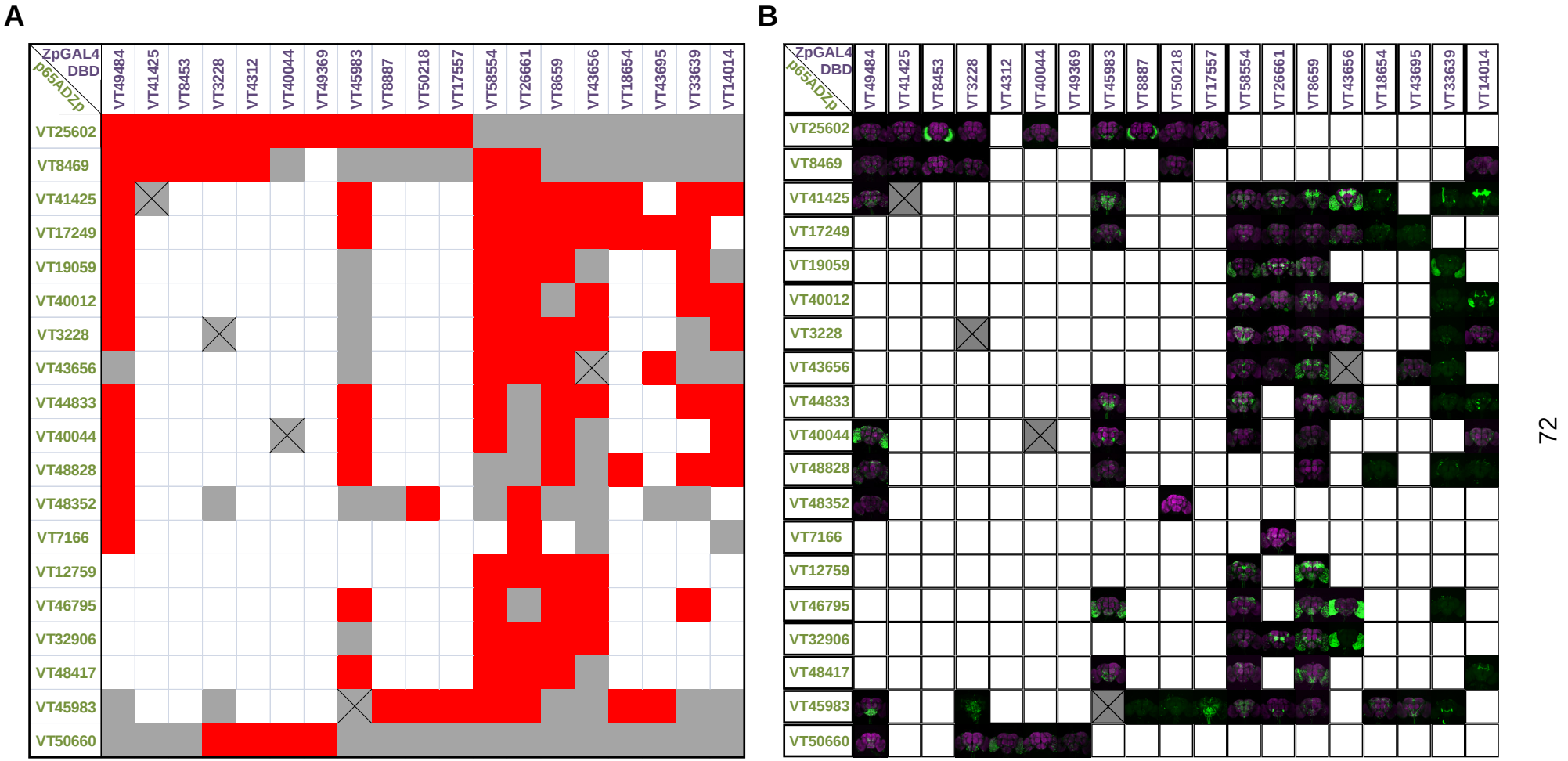

Figure 3.1 Screening with split GAL4 combinations for ovipositor extrusion

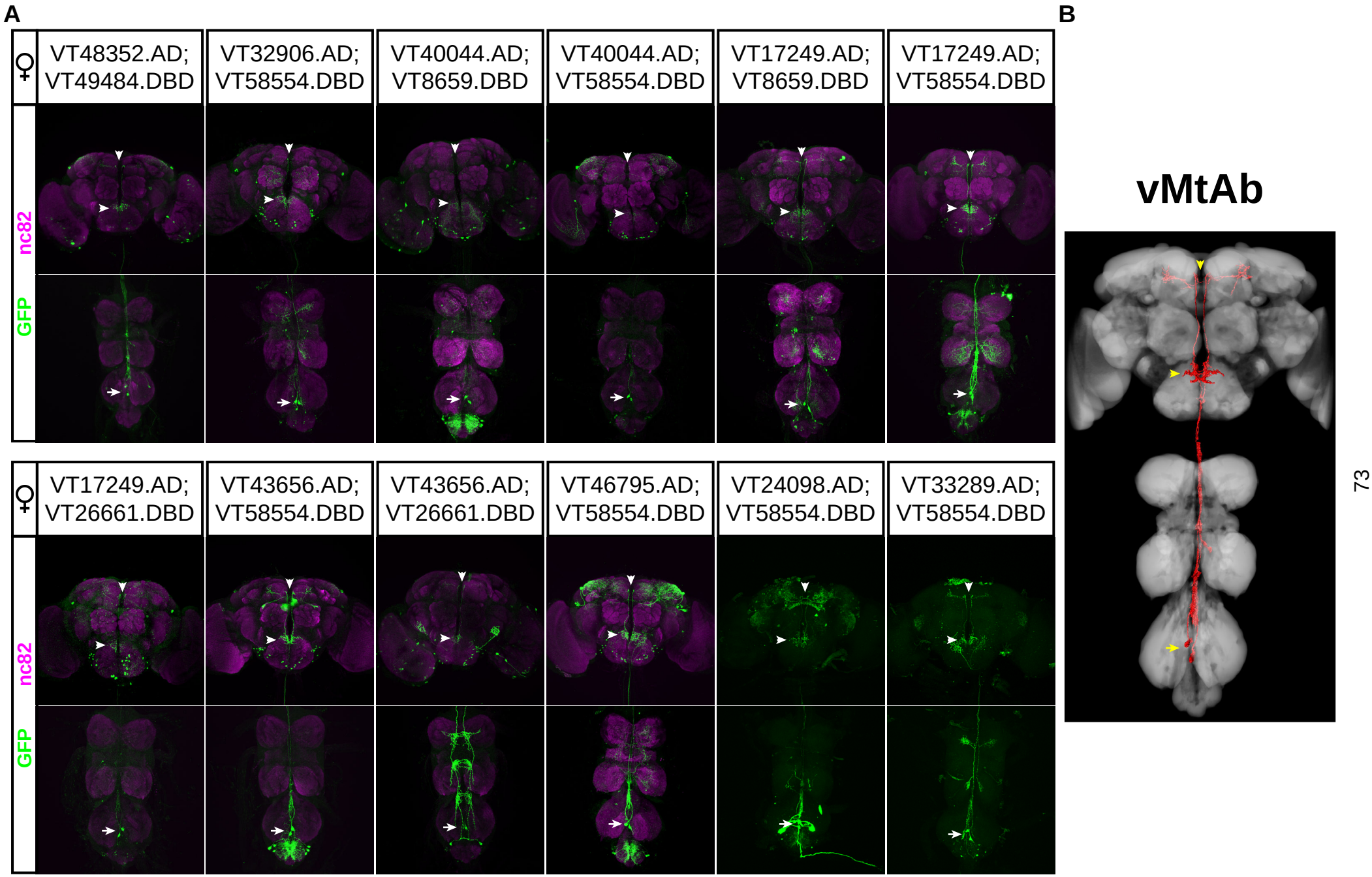

Figure 3.2 vMtAb: an ascending neuron in the VNC that elicits ovipositor extrusion

neurons as ascending neurons (Figure 3.3A). They receive inputs in the VNC and send outputs to both the SOG and posterior brain regions (Figure 3.3A). Acute silencing of vMtAb neurons with *UAS-shibire*^{ts} in females at 30°C significantly reduced the copulation rate, suggesting that vMtAb may be involved in regulating female receptivity.

3.2.3 Ab1 and Ab2: abdominal ganglion neurons that evoke ovipositor extrusion

Apart from vMtAb neurons, we found two additional types of neurons, Ab1 and Ab2, which appeared frequently in the split GAL4 combinations that induced ovipositor extrusion upon activation (Figure 3.4A and Figure 3.5A). These two neurons were sometimes co-labeled with vMtAb, which seemed to evoke stronger extrusion. However, this might be due to different levels of expressions and need to be tested more rigorously.

Ab1 is cluster of local interneurons in the abdominal ganglion (Figure 3.4B). Its cell bodies are usually located laterally in the abdominal ganglion and the arborizations are confined to the anterior region leaving the distal part un-innervated. Ab1 has no apparent projections. Ab2 seems to be a group of motor neurons with projections travelling down to the abdomen (Figure 3.5B). Its arborizations in the abdominal ganglion are mainly in the central area. Functions of both Ab1 and Ab2 in female sexual behaviors remain to be tested.

3.3 Discussion

Using the split-GAL4 system, we were able to further restrict the expression patterns of many originally broad GAL4 lines and maintain their ability in evoking the ovipositor extrusion phenotype. By examination of the sparse split-GAL4 combinations and comparison of the expression patterns among them, we were able to identify three neuronal clusters that trigger female ovipositor extrusion upon activation: vMtAb, Ab1 and Ab2.

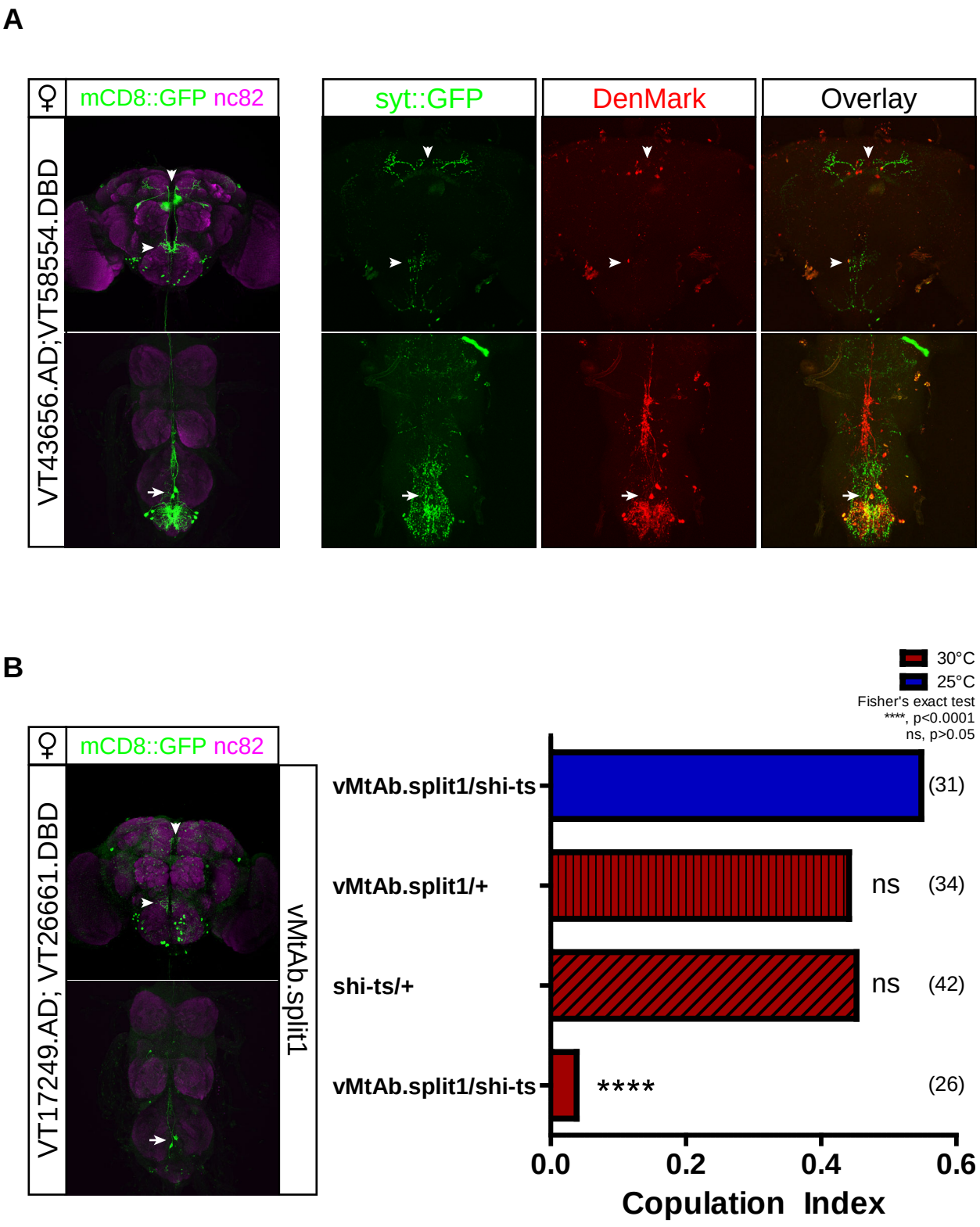

Figure 3.3 vMtAb ascending neurons are involved in female receptivity

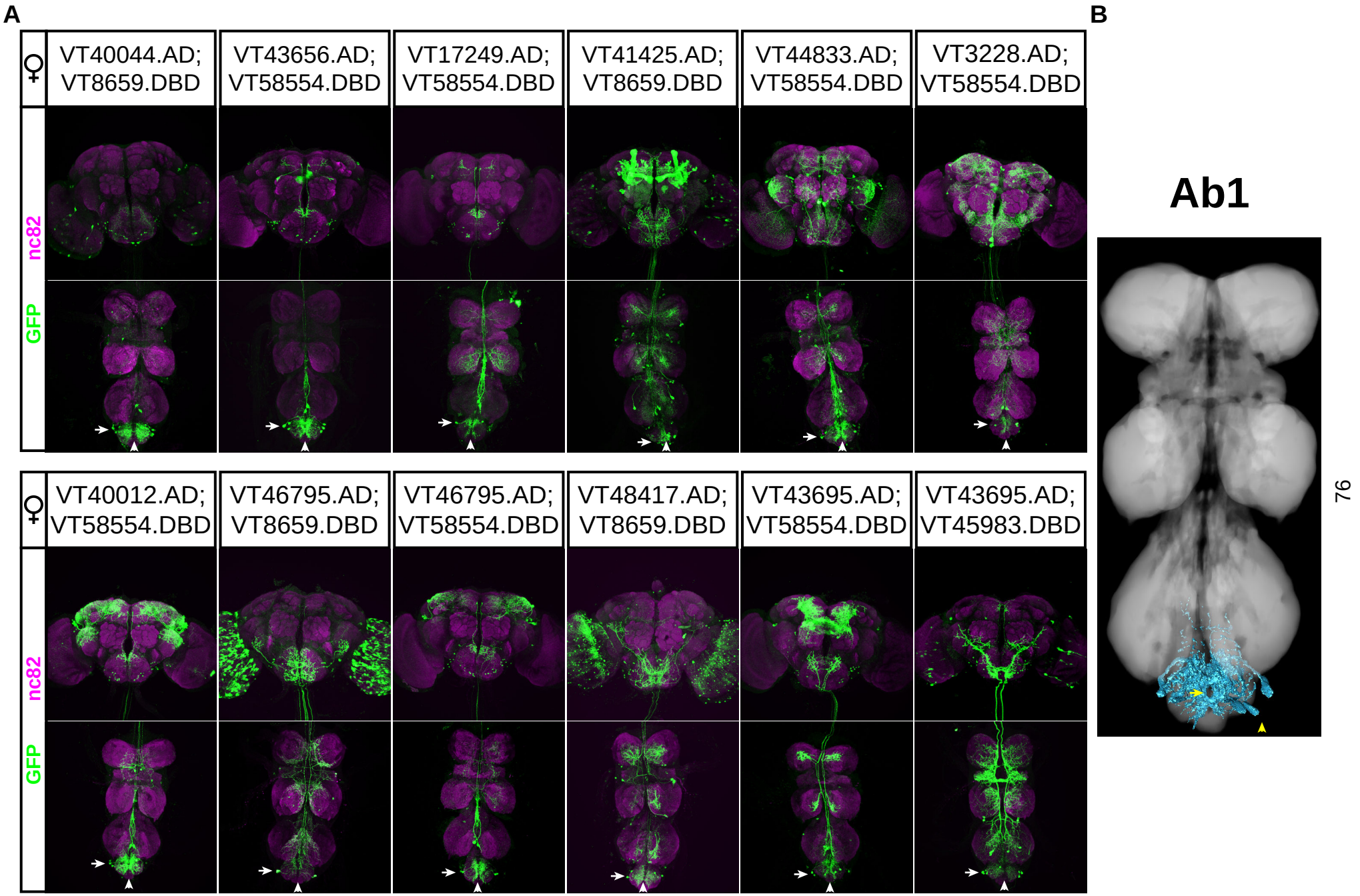

Figure 3.4 Ab1: an abdominal ganglion interneuron that elicits ovipositor extrusion

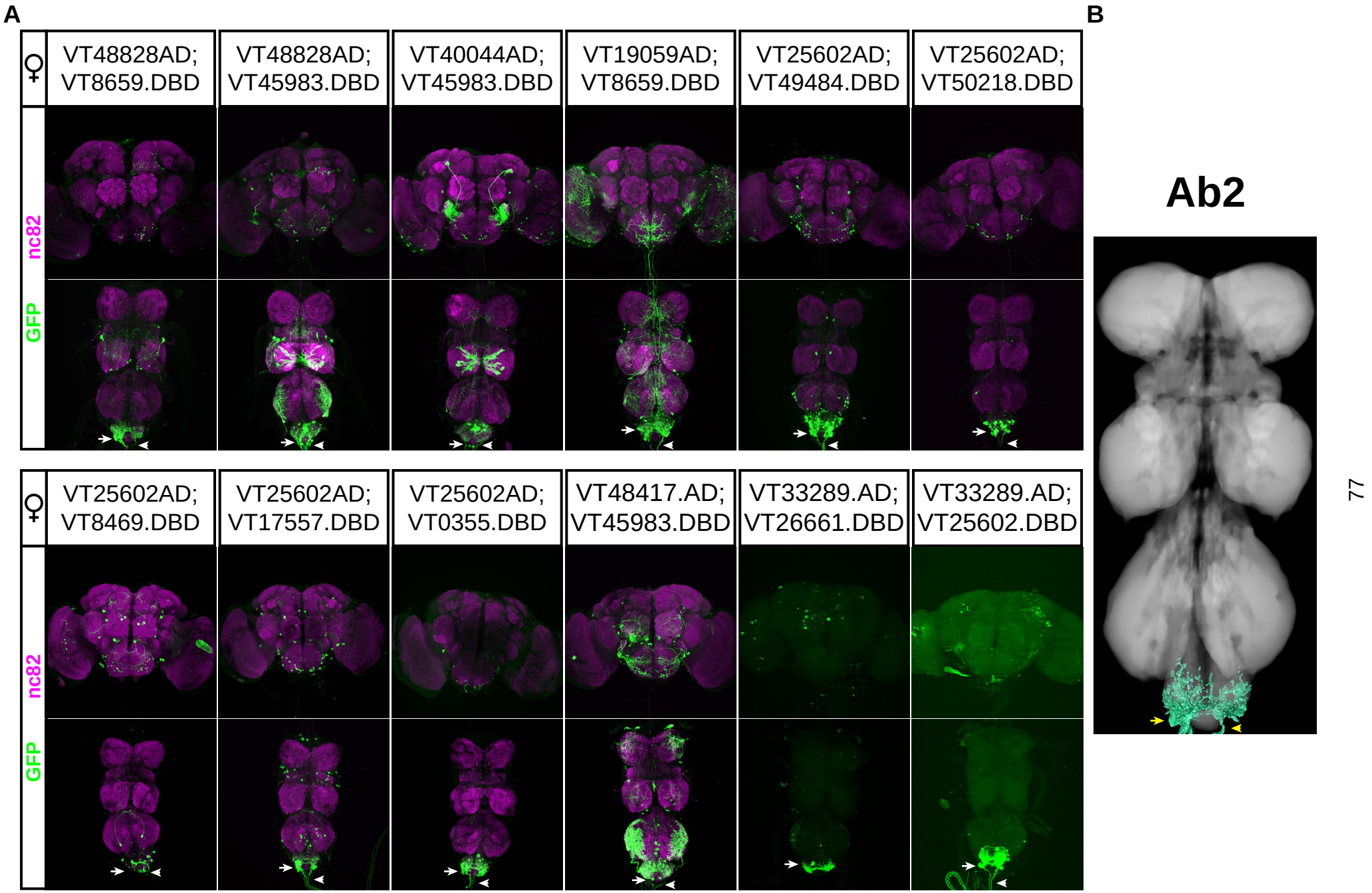

Figure 3.5 Ab2: an abdominal ganglion motor neuron that elicits ovipositor extrusion

Activating of vMtAb alone in split-GAL4 combinations that label neither Ab1 nor Ab2 only triggers ovipositor extrusions weakly. This may be due to weaker expression of these drivers in vMtAb, but it is also possible that vMtAb may indeed evoke only weak ovipositor extrusion. The weak extrusion could underlie the vaginal plate opening required for copulation (Dickson, 2008) or the partial ovipositor extrusion that has been proposed to stimulate male courtship (Lasbleiz et al., 2006). This is consistent with the observation that blocking vMtAb activities reduced female receptivity significantly. vMtAb might function in relaying certain sensory information about the presence of a male or the proprioceptive information of the female's readiness for copulation. These hypotheses remain to be tested.

Ab1 and Ab2 neurons seem to trigger stronger phenotypes upon activation. Ab1 may be involved in some local processing. Ab2 may be the motor neurons innervating ovipositor extrusion muscles, which can be tested by staining the oviducts and examining the site of innervations.

These three neuronal classes cover almost all of the sparse GAL4 combinations we tested, suggesting that our strategies were effective in mapping these neurons. The neurons we identified seem to be either close to motor outputs pathways (Ab1 and Ab2) as we expected or sensory pathways (vMtAb). It is known that descending signals from brain is required for either acceptance for copulation or rejection with ovipositor extrusion, because decapitated females show neither of these behaviors (not shown). However, we didn't uncover any brain interneurons or descending neurons in our screen. This might be due to several reasons. 1) We have only screened a small subset of the 41x71 matrix. Novel types of neurons may be uncovered by screening more of the split GAL4 combinations. 2) Our neuronal activation strategy is only sensitive to neurons whose activation leads to ovipositor extrusion phenotype. If a brain neuron needs to be silenced to trigger ovipositor extrusion, we may not identify it in the activation screen. 3) The descending brain signal may represent permission for ovipositor extrusion through neuronal modulation of corresponding motor circuits, rather than a direct command. This suggests that additional sensory integration must happen in the VNC to control the timing of ovipositor extrusion. This is also consistent with behavioral observations that mated females only display the rejection response when a male is courting.

To advance our study, we need to: 1) characterize the three identified neuronal classes in more details; 2) screen more split GAL4 combinations and focus on those that target none of the aforementioned neuronal classes; 3) design new assays to increase the sensitivity of our screen, such as testing virgin or mated females paired with a wild-type male for increased or decreased ovipositor extrusion, and similar silencing assays. With the identification of more circuit components, especially the ones in the higher order center, we may start to understand holistically the neural basis of female mating decisions.

3.4 Figure legends

Figure 3.1 Screening with split GAL4 combinations for ovipositor extrusion

(A) A 19x19 split GAL4 matrix of hemi-drivers showing ovipositor extrusion or egg laying phenotypes upon activation. The color of the cells indicates different status for each split combinations: blank, not tested; grey, negative; red, positive. (B) Brain expression of the split GAL4 combinations showing ovipositor extrusion.

Figure 3.2 vMtAb: an ascending neuron in the VNC that elicits ovipositor extrusion

(A) Expressions of split GAL4 combinations that showed ovipositor extrusion upon activation and label a common VNC neuron (vMtAb). (B) Segmented representation of vMtAb. The two cell bodies of vMtAb (arrows) are located at the ventral region between metathoracic ganglion and abdominal ganglion. Their projections travel upwards into central brain and arborize at the anterior SOG and posterior protocerebrum regions (arrowheads).

Figure 3.3 vMtAb ascending neurons are involved in female receptivity

(A) Expressions of female flies with *UAS-mCD8::GFP* and *UAS-sytnaptogamin::GFP*, *UAS-DenMark* driven by *VT43656.p65ADZp; VT58554.ZpGAL4DBD*. The former was stained with anti-GFP (green) and mAb nc82 (magenta); the latter was stained with anti-GFP (green) and anti-DsRed (red). (B) Expression of *VT17249.p65ADZp; VT26661.ZpGAL4DBD* is shown on the left (green, GFP; magenta, nc82). Blocking of

vMtAb neurons with this split GAL4 driver using *UAS-shibire^{ts}* significantly reduces copulation rate at 30°C as shown on the right (Fisher's exact test, ****, p<0.0001).

Figure 3.4 Ab1: an abdominal ganglion interneuron that elicits ovipositor extrusion

(A) Expressions of split GAL4 combinations that showed ovipositor extrusion upon activation and label a common abdominal ganglion local neuron (Ab1). (B) Segmented representation of Ab1. The cell bodies of Ab1 (arrows) are located at lateral or medial abdominal ganglion. Ab1 neurons arborize locally in the abdominal ganglion except the distal region (arrowheads).

Figure 3.5 Ab2: an abdominal ganglion motor neuron that elicits ovipositor extrusion

(A) Expressions of split GAL4 combinations that showed ovipositor extrusion upon activation and label a common abdominal ganglion motor neuron (Ab2). (B) Segmented representation of Ab2. The cell bodies of Ab2 (arrows) are located at lateral or medial abdominal ganglion. Ab2 neurons arborize locally in the abdominal ganglion except the distal region and also project to downwards into the abdomen (arrowheads), possibly innervating muscles in the oviduct.

3.5 Material and methods

Fly stocks, immunohistochemistry and image registration

These are the same as described in Chapter 2.

Behavior assays

For ovipositor extrusion, assays were performed under similar conditions as the primary screen (Chapter 1). Isolated mated or virgin females were tested under elevated temperatures. For female receptivity assays, virgin females were reared at 25°C for 3-5 days after eclosion before tests. Each female was then paired with a *w+* Canton S male for 30min in a 10mm courtship chamber. Percentage of copulation was used as a measure of female receptivity.

Supplemental figures

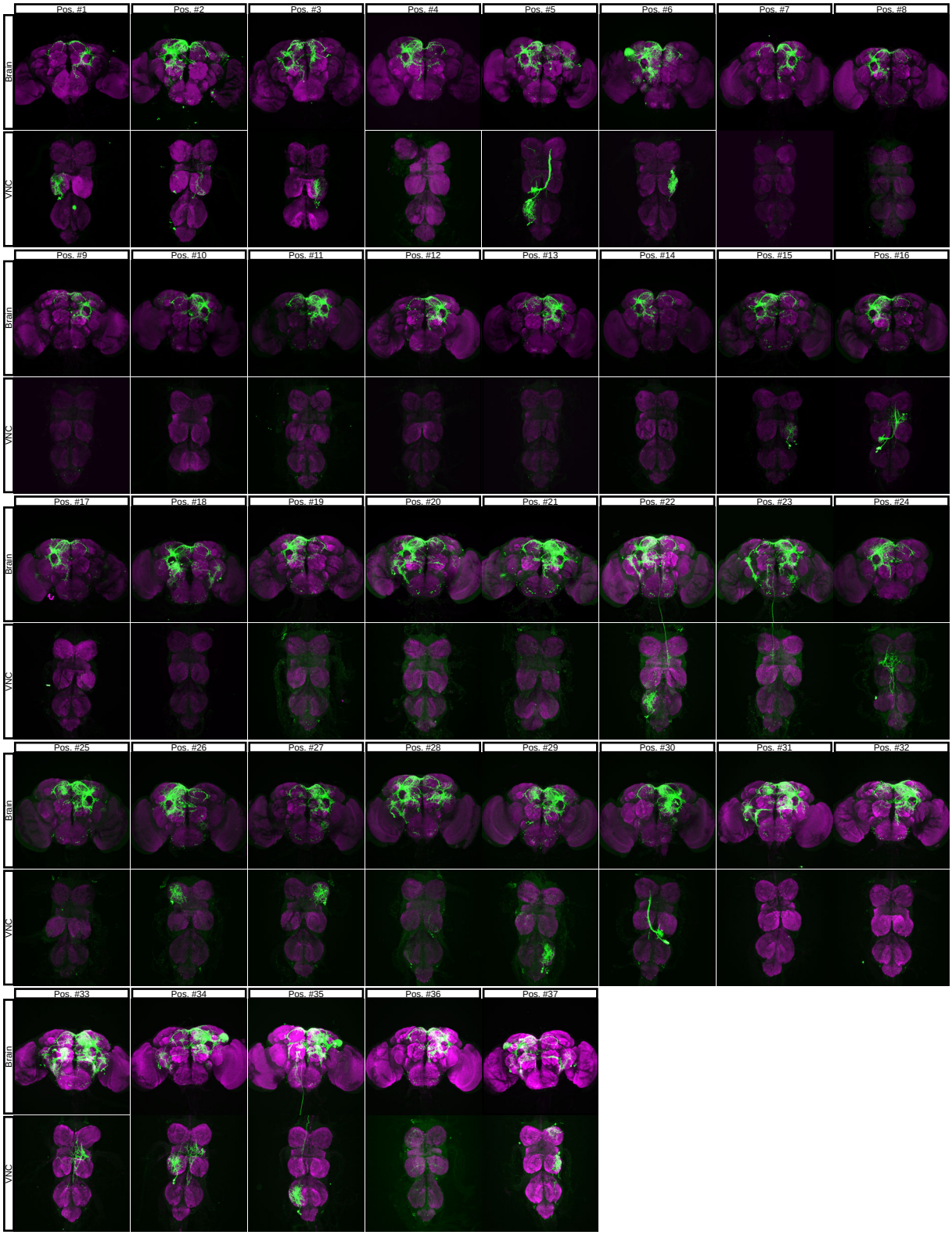

Figure S1 MARCM expression of female flies showing following

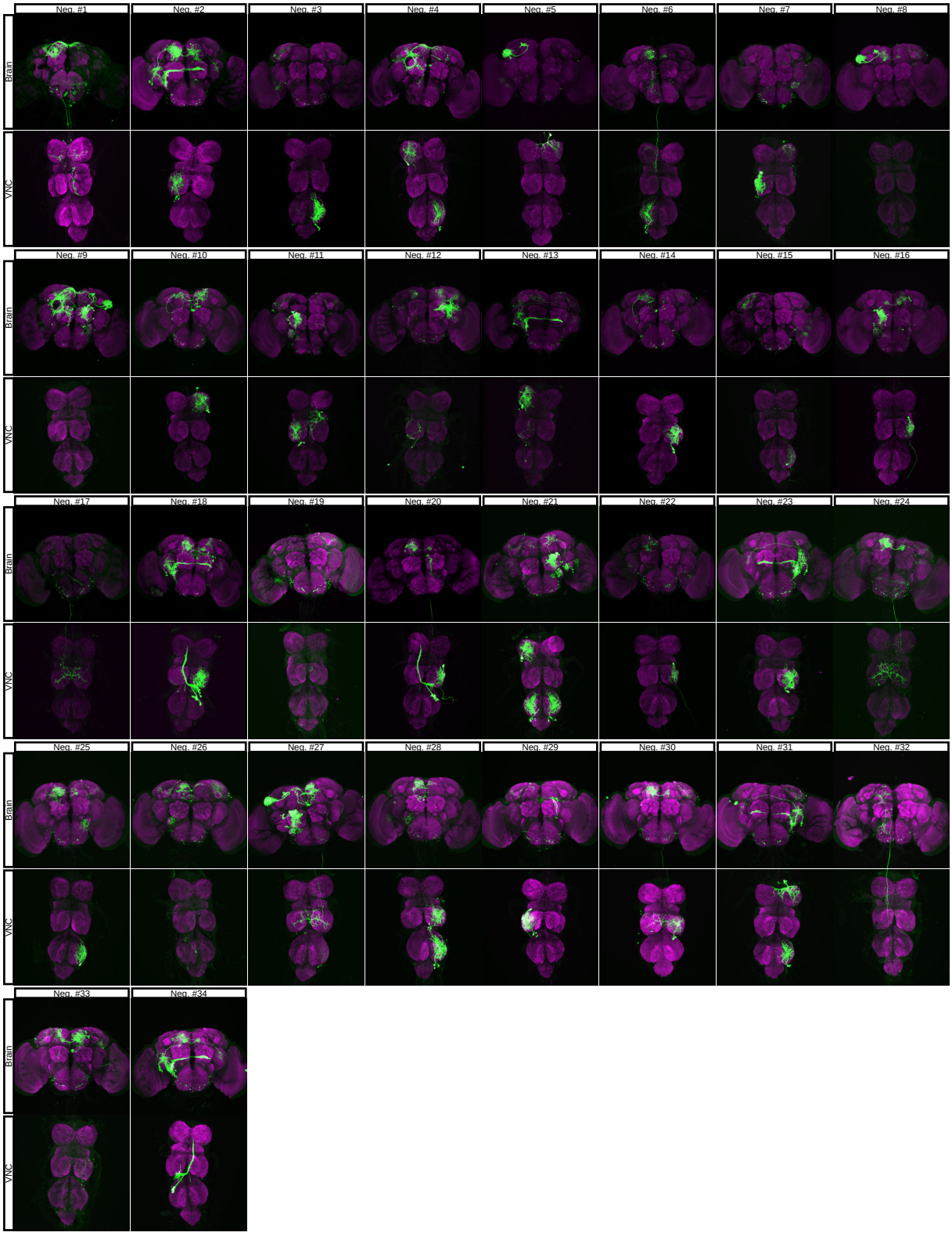

Figure S2 MARCM expression of female flies showing no following

Neuronal type	Description	Anatomy
Neuron 1	Cell bodies located ventral to the protocerebral bridge (PB). Projection curves and crosses the PB laterally and dorsally to the mushroom body (MB) calyx and bifurcates, with one branch arborises in the ipsilateral medial protocerebrum (Pr) and the other arborizes in the contralateral medial Pr.	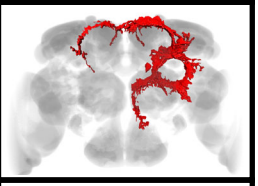
Neuron 2	Cell bodies located ventral to the protocerebral bridge. Projection travels anteriorly and aroborizes in the fan-shaped body (FB).	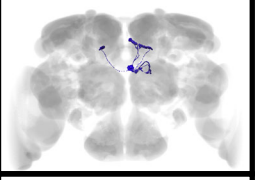
Neuron 3	Cell bodies located above MB calyx. Projection curves ventrally and travels anteriorly to arborize in medial protocerebrum.	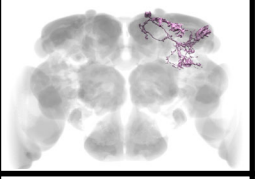
Neuron 4	Cell bodies located near the optic lobe. Projection travels laterally into the lobula and arborizes locally.	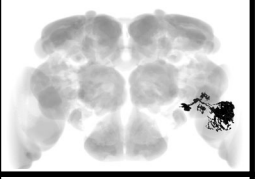
Neuron 5	Cell bodies located anterior to lateral horn (LH). Projection curves medially and arborizes locally in the superior Pr.	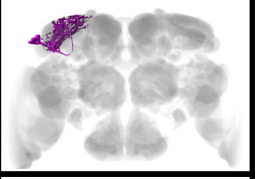
Neuron 6	Cell bodies located ventral to the protocerebral bridge. Projection curves and crosses the PB laterally and dorsally to the MB calyx. Arborization mainly confined to the superior region in both lateral and medial Pr in ipilateral hemishpere and medial Pr in the contralateral hemisphere.	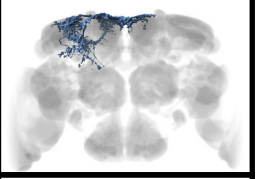
Neuron 7	Cell bodies located in the dorsal pars intercerebralis (PI). Projection travels laterally and bifurcates with one branch arborizing locally in the dorsal superior Pr and the other contralaterally arborizing in the medial Pr.	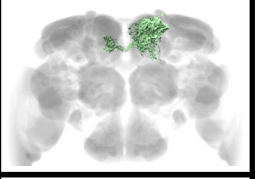
Neuron 8	Cell bodies located in the ventral region between the metathoracic (Mt) and the abdominal neuromeres (Abd). Projection enters Mt and arborizes locally in the ipilateral Mt.	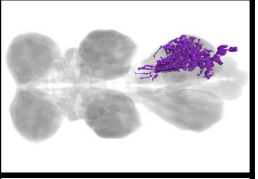
Neuron 9	Cell bodies located posterior to the subesophageal ganglion (SOG). Projection travels anteriorly and bifurcates with one branch arborizing ventrally and the other forming a dense fiber that projects to the contralateral hemisphere.	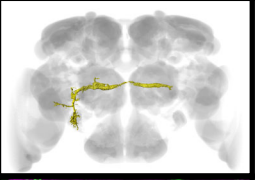
Neuron 10	Cell bodies located laterally to the ventral lateral Pr. Projection curves dorsal-medially and arborize locally in the ventral lateral Pr. Always co-appear with Neuron 9.	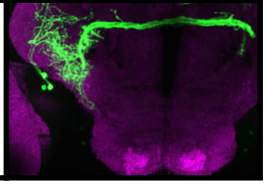

Figure S3 Neuronal types annotated in MARCM (Neuron 1-10)

Neuronal type	Description	Anatomy
Neuron 11	Cell bodies located at posterior lateral Pr. Projection bifurcates dorsally towards the superiora anterior Pr, with lateral branch arborizing locally in the ipilateral superior Pr and the medial branch arborizing both ip- and contra-lateral medial Pr.	
Neuron 12	Cell bodies located ventral-laterally between the prothoracic (Prt) and mesothoracic neuromeres (Ms). Neurites project to the iplateral Ms and arborize locally.	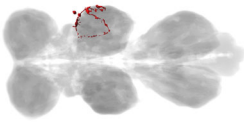
Neuron 13	Cell bodies located ventral-laterally between the Ms and Mt neuromeres. Neurites project to the ipilateral Ms and arborize locally.	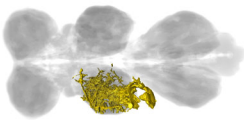
Neuron 14	Cell bodies located above the PB. Projection crosses the PB and curves ventral-anteriorly to arborize in the FB.	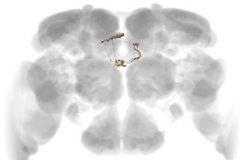
Neuron 15	Cell bodies located in the ventral-lateral region between Ms and Mt. Projection travles anterior-medially and arborize in the medial Mt in the iplateral side.	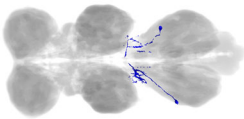
Neuron 16	Cell bodies located in the ventral-medial region between Ms and Abd. Neurites project and arborize the lateral medial area of the ipilateral Ms. Possible arborization in the medial area of contralateral Ms.	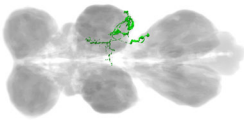
Neuron 17	Cell body located posterior to the LH. Projection travels laterally first and then bifurcate to form arborization in both the LH and the superior Pr.	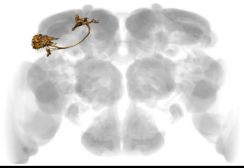
Neuron 18	Cell bodies located above the antenna lobe (AL). Neurites project to AL and arborize locally.	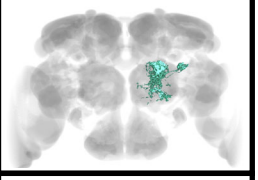
Neuron 19	Cell bodies located anterior lateral to AL. Projection curves ventral-medially and bifurcates. One branch arborizes locally in the antennal mechanosensory and motor center (AMMC) and the other projects dorsal-medially to arborize the AMMC in the contralateral hemisphere.	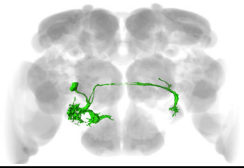
Neuron 20	Cell bodies located at the posterior lateral Pr. Projection curves ventral-anteriorly to arborize in the lateral posterior Pr.	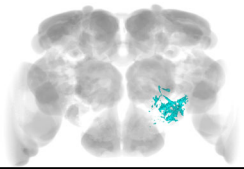

Figure S4 Neuronal types annotated in MARCM (Neuron 11-20)

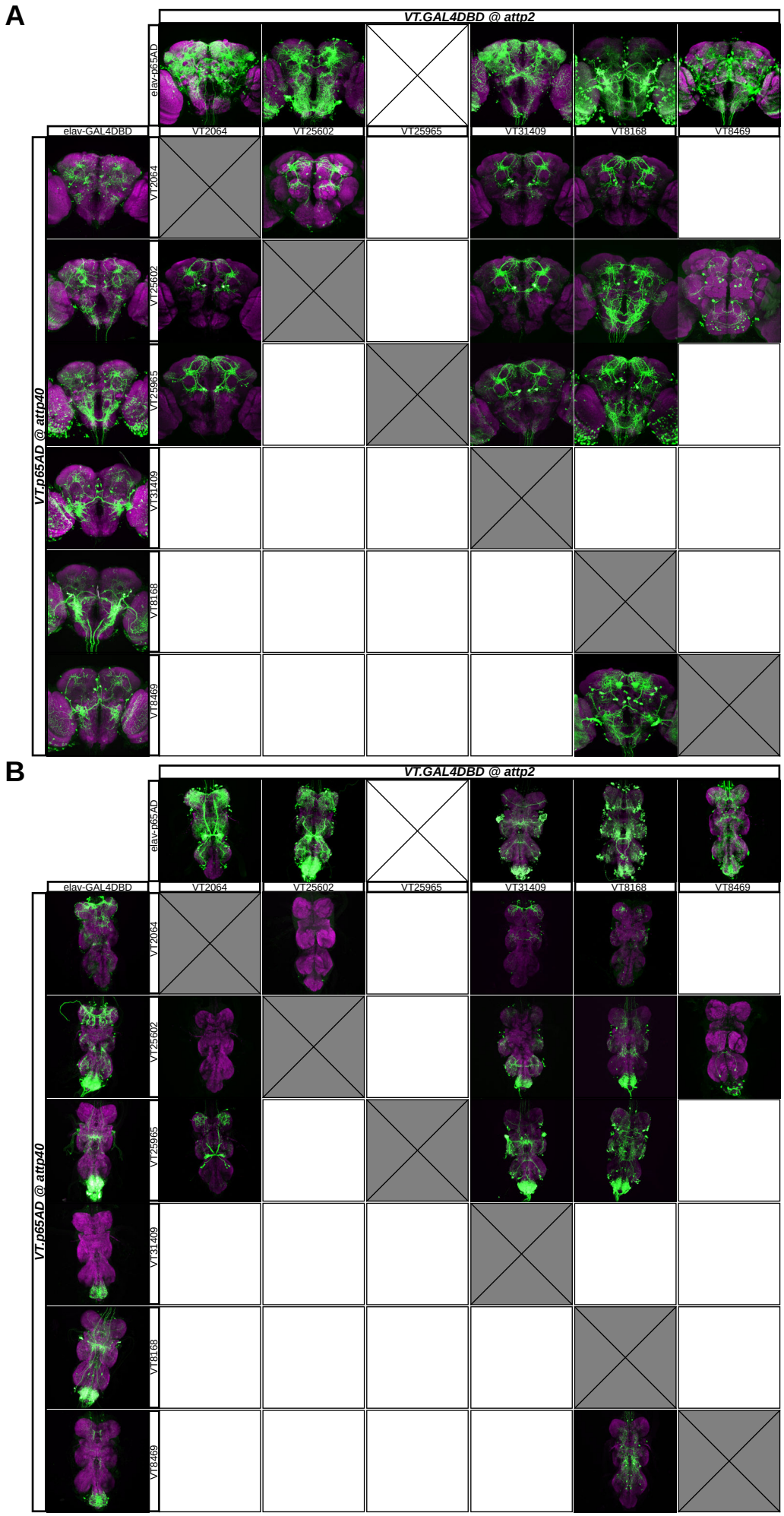

Figure S5 Expression of split-GAL4 combinations for female following

VT25602.p65AD; VT2064.GAL4DBD / UAS-TrpA1

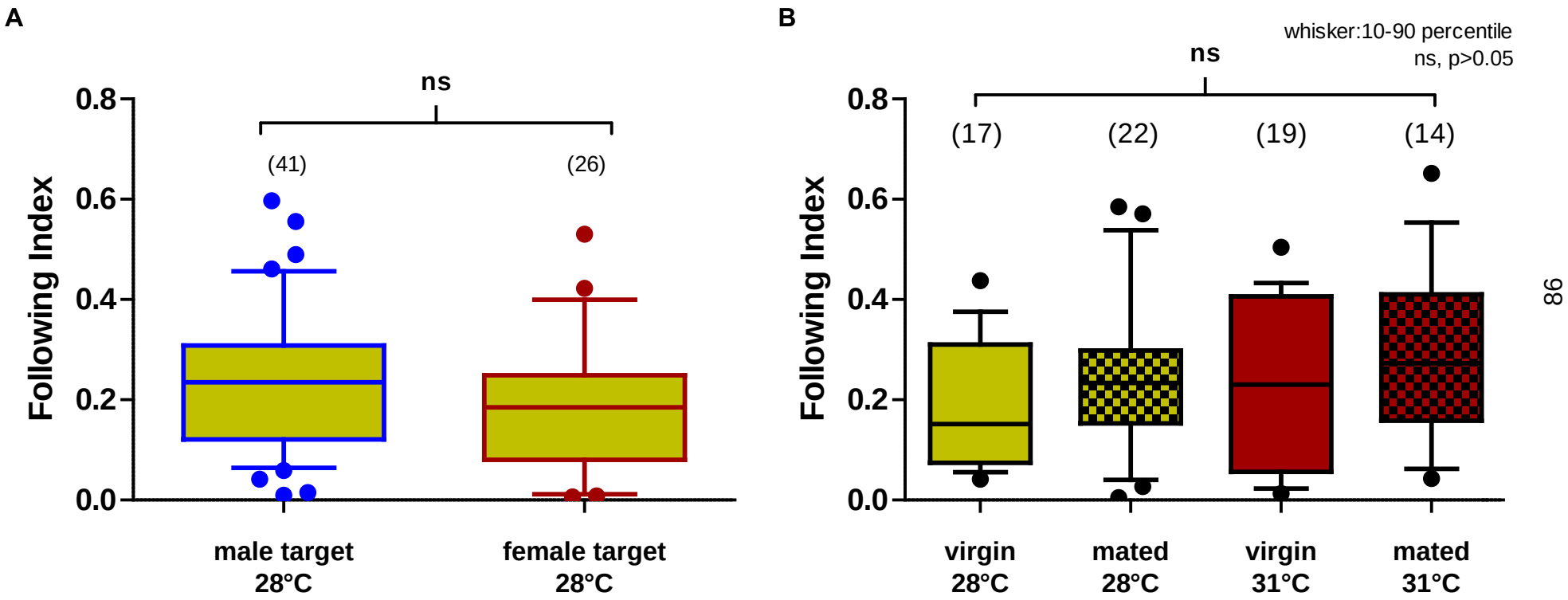

Figure S6 pMP8 activated females follow both male and female targets independently of their mating status

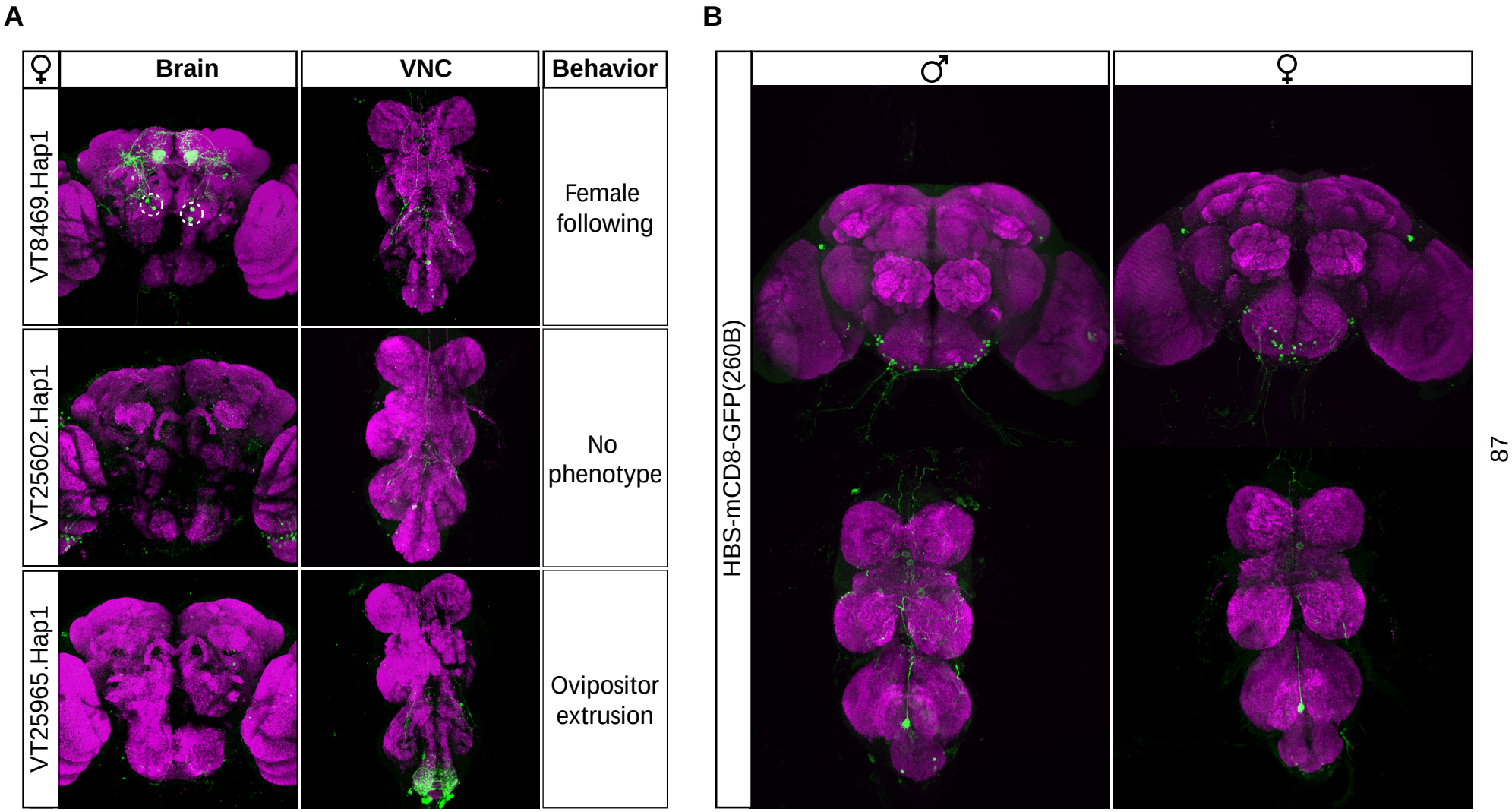

Figure S7 Hap1 lines generated from positve GAL4 tiles and endogenous HBS signal in the VNC

Supplemental figures legends

Figure S1 MARCM expression of female flies showing following

Raw z-projection images of MARCM clones from flies showing following upon TrpA1 activation. Samples were stained with anti-GFP (green) and nc82 (magenta).

Figure S2 MARCM expression of female flies showing no following

Raw z-projection images of MARCM clones from flies showing following upon TrpA1 activation. Samples were stained with anti-GFP (green) and nc82 (magenta).

Figure S3 Neuronal types annotated in MARCM (Neuron 1-10)

Descriptions and segmentations of Neuron 1 to 10 that were observed in the MARCM analysis of *VT2064*. Images with sparse expressions were registered onto a standard brain template. Each of the neurons was segmented manually and shown with the standard brain.

Figure S4 Neuronal types annotated in MARCM (Neuron 11-20)

Descriptions and segmentations of Neuron 11 to 20 that were observed in the MARCM analysis of *VT2064*. Images with sparse expressions were registered onto a standard brain template. Each of the neurons was segmented manually and shown with the standard brain.

Figure S5 Expression of split GAL4 combinations for female following

(A) Matrix of brain stainings from split hemidrivers (first row and column) and split GAL4 combinations that showed female following behavior. Expression of split hemidrivers were obtained by crossing each hemidriver to complementary pan-neuronal driver elav-p65ADZp or elav-ZpGAL4DBD. (B) Matrix of VNC stainings as in (A). Samples were stained with anti-GFP (green) and nc82 (magenta).

Figure S6 pMP8 activated females follow both male and female targets independently of their mating status

(A) Following indexes of *pMP8.split, UAS-TrpA1* females towards male targets and female targets at 28°C (Mann-Whitney test, ns, $p>0.05$). (B) Following indexes of

pMP8.split, UAS-TrpA1 virgin and mated females at 28°C and 31°C (Mann-Whitney test, ns, p>0.05).

Figure S7 Hap1 lines generated from positve GAL4 tiles and endogenous HBS signal in the VNC

(A) Brain and VNC expression and activation-induced behaviors of three Hap1 drivers generated from GAL4 lines showed following behavior in females. (B) Staining of *HBS-mCD8::GFP* reporter alone without any drivers. A few cells in the VNC were observed, suggesting that they are endogenously active in stimulating expression of HBS reporters. Samples were stained with anti-GFP (green) and nc82 (magenta).

References

Aigaki, T., Fleischmann, I., Chen, P.S., and Kubli, E. (1991). Ectopic expression of sex peptide alters reproductive behavior of female D. melanogaster. Neuron *7*, 557-563.

Akerboom, J., Chen, T.W., Wardill, T.J., Tian, L., Marvin, J.S., Mutlu, S., Calderon, N.C., Esposti, F., Borghuis, B.G., Sun, X.R.*, et al.* Optimization of a GCaMP calcium indicator for neural activity imaging. J Neurosci *32*, 13819-13840.

Albert, J.T., and Gopfert, M.C. (2006). A Drosophila gating-spring channel for hearing. Journal of Neurogenetics *20*, 69-69.

Andersson, M. (1994). Sexual selection. Princeton Univ Press, Princeton, NJ.

Bahl, A., Ammer, G., Schilling, T., and Borst, A. (2013). Object tracking in motion-blind flies. Nat Neurosci.

Baines, R.A., Uhler, J.P., Thompson, A., Sweeney, S.T., and Bate, M. (2001). Altered electrical properties in Drosophila neurons developing without synaptic transmission. J Neurosci *21*, 1523-1531.

Bausenwein, B., Dittrich, A.P., and Fischbach, K.F. (1992). The optic lobe of Drosophila melanogaster. II. Sorting of retinotopic pathways in the medulla. Cell Tissue Res *267*, 17-28.

Bausenwein, B., and Fischbach, K.F. (1992). Activity labeling patterns in the medulla of Drosophila melanogaster caused by motion stimuli. Cell Tissue Res *270*, 25-35.

Bello, B., Resendez-Perez, D., and Gehring, W.J. (1998). Spatial and temporal targeting of gene expression in Drosophila by means of a tetracycline-dependent transactivator system. Development *125*, 2193-2202.

Bennet-Clark, H.C., and Ewing, A.W. (1967). Stimuli provided by courtship of male Drosophila melanogaster. Nature *215*, 669-&.

Bennet-Clark, H.C., and Ewing, A.W. (1969). Pulse Interval as a critical parameter in courtship song of Drosophila-melanogaster. Animal Behaviour *17*, 755-&.

Berdnik, D., Chihara, T., Couto, A., and Luo, L. (2006). Wiring stability of the adult Drosophila olfactory circuit after lesion. J Neurosci *26*, 3367-3376.

Berglund, A., Rosenqvist, G., and Svensson, I. (1989). Reproductive Success of Females Limited by Males in 2 Pipefish Species. American Naturalist *133*, 506-516.

Bidaye, S.S. (2012). Neuronal basis for directed waliking in Drosophila melanogaster. Thesis.

Bieschke, E.T., Wheeler, J.C., and Tower, J. (1998). Doxycycline-induced transgene expression during Drosophila development and aging. Mol Gen Genet *258*, 571-579.

Bischof, J., Maeda, R.K., Hediger, M., Karch, F., and Basler, K. (2007). An optimized transgenesis system for Drosophila using germ-line-specific phiC31 integrases. Proc Natl Acad Sci U S A *104*, 3312-3317.

Blondeau, J., and Heisenberg, M. (1982). The 3-dimensional optomotor torque system of Drosophila-melanogaster - studies on wildtype and the mutant optomotor-blind H31. Journal of Comparative Physiology *145*, 321-329.

Bornholdt, R., Oliveira, L.R., and Fabian, M.E. (2008). Sexual size dimorphism in Myotis nigricans (Schinz, 1821) (Chiroptera: Vespertilionidae) from south Brazil. Brazilian Journal of Biology *68*, 897-904.

Borst, A. (2009). Drosophila's view on insect vision. Curr Biol *19*, R36-47.

Borst, A., and Egelhaaf, M. (1989). Principles of visual motion detection. Trends Neurosci *12*, 297-306.

Brand, A.H., and Perrimon, N. (1993). Targeted gene expression as a means of altering cell fates and generating dominant phenotypes. Development *118*, 401-415.

Brent, R., and Ptashne, M. (1985). A eukaryotic transcriptional activator bearing the DNA specificity of a prokaryotic repressor. Cell *43*, 729-736.

Buchner, E. (1976). Elementary movement detectors in an insect visual-system. Biological Cybernetics *24*, 85-101.

Butterworth, F.M. (1969). Lipids of Drosophila: a newly detected lipid in the male. Science *163*, 1356-1357.

Cachero, S., Ostrovsky, A.D., Yu, J.Y., Dickson, B.J., and Jefferis, G.S.X.E. (2010). Sexual dimorphism in the fly brain. Current Biology *20*, 1589-1601.

Camara, N., Whitworth, C., and Van Doren, M. (2008). The creation of sexual dimorphism in the Drosophila soma. Sex Determination and Sexual Development *83*, 65-+.

Chan, Y.B., and Kravitz, E.A. (2007). Specific subgroups of Fru(M) neurons control sexually dimorphic patterns of aggression in Drosophila melanogaster. Proceedings of the National Academy of Sciences of the United States of America *104*, 19577-19582.

Chapman, T., Bangham, J., Vinti, G., Seifried, B., Lung, O., Wolfner, M.F., Smith, H.K., and Partridge, L. (2003). The sex peptide of Drosophila melanogaster: female post-mating responses analyzed by using RNA interference. Proc Natl Acad Sci U S A *100*, 9923-9928.

Chapman, T., Herndon, L.A., Heifetz, Y., Partridge, L., and Wolfner, M.F. (2001). The Acp26Aa seminal fluid protein is a modulator of early egg hatchability in Drosophila melanogaster. Proc Biol Sci *268*, 1647-1654.

Chen, P.S., Stumm-Zollinger, E., Aigaki, T., Balmer, J., Bienz, M., and Bohlen, P. (1988). A male accessory gland peptide that regulates reproductive behavior of female D. melanogaster. Cell *54*, 291-298.

Chen, S., Lee, A.Y., Bowens, N.M., Huber, R., and Kravitz, E.A. (2002). Fighting fruit flies: A model system for the study of aggression. Proceedings of the National Academy of Sciences of the United States of America *99*, 5664-5668.

Cirera, S., and Aguade, M. (1997). Evolutionary history of the sex-peptide (Acp70A) gene region in Drosophila melanogaster. Genetics *147*, 189-197.

Cline, T.W. (1993). The Drosophila sex determination signal - how do flies count to 2. Trends in Genetics *9*, 385-390.

Cook, R. (1975). Lesbian phenotype of Drosophila-melanogaster. Nature *254*, 241-242.

Cook, R. (1981). Courtship-like tracking behavior in wild-type female Drosophila-melanogaster. Zeitschrift Fur Naturforschung C-a Journal of Biosciences *36*, 475-483.

Couto, A., Alenius, M., and Dickson, B.J. (2005). Molecular, anatomical, and functional organization of the Drosophila olfactory system. Current Biology *15*, 1535-1547.

Darwin, C. (1859). On the Origin of Species (1st edition). Chaper 4.

Darwin, C. (1871). The Descent of Man and Selection in Relation to Sex. John Murray, London.

Datta, S.R., Vasconcelos, M.L., Ruta, V., Luo, S., Wong, A., Demir, E., Flores, J., Balonze, K., Dickson, B.J., and Axel, R. (2008). The Drosophila pheromone cVA activates a sexually dimorphic neural circuit. Nature *452*, 473-477.

Demir, E., and Dickson, B.J. (2005). fruitless splicing specifies male courtship behavior in Drosophila. Cell *121*, 785-794.

Dickson, B.J. (2008). Wired for sex: the neurobiology of Drosophila mating decisions. Science *322*, 904-909.

Dierick, H.A., and Greenspan, R.J. (2006). Molecular analysis of flies selected for aggressive behavior. Nature Genetics *38*, 1023-1031.

Donegan, J., and Ewing, A.W. (1980). Duetting in Drosophila and Zaprionus Species. Animal Behaviour *28*, 1289-1289.

Dow, M.A., and Schilcher, F.V. (1975). Aggression and mating success in Drosophila-melanogaster. Nature *254*, 511-512.

Eichner, H., Joesch, M., Schnell, B., Reiff, D.F., and Borst, A. (2011). Internal structure of the fly elementary motion detector. Neuron *70*, 1155-1164.

Ejima, A., Smith, B.P.C., Lucas, C., Van Naters, W.V., Miller, C.J., Carlson, J.R., Levine, J.D., and Griffith, L.C. (2007). Generalization of courtship learning in Drosophila is mediated by cis-vaccenyl acetate. Current Biology *17*, 599-605.

Emlen, S.T., and Oring, L.W. (1977). Ecology, sexual selection, and evolution of mating systems. Science *197*, 215-223.

Ewing, A.W., and Bennet-Clark, H.C. (1968). Courtship songs of Drosophila. Behaviour *31*, 288-+.

Ferveur, J.F., Savarit, F., OKane, C.J., Sureau, G., Greenspan, R.J., and Jallon, J.M. (1997). Genetic feminization of pheromones and its behavioral consequences in Drosophila males. Science *276*, 1555-1558.

Fields, S., and Song, O. (1989). A novel genetic system to detect protein-protein interactions. Nature *340*, 245-246.

Fischer, J.A., Giniger, E., Maniatis, T., and Ptashne, M. (1988). GAL4 activates transcription in Drosophila. Nature *332*, 853-856.

Fisher, R.A. (1930). The Genetical Theory of Natural Selection. Oxford University Press.

Fishilevich, E., and Vosshall, L.B. (2005). Genetic and functional subdivision of the Drosophila antennal lobe. Current Biology *15*, 1548-1553.

Gloor, G.B., Nassif, N.A., Johnson-Schlitz, D.M., Preston, C.R., and Engels, W.R. (1991). Targeted gene replacement in Drosophila via P element-induced gap repair. Science *253*, 1110-1117.

Gohl, D.M., Silies, M.A., Gao, X.J., Bhalerao, S., Luongo, F.J., Lin, C.C., Potter, C.J., and Clandinin, T.R. (2011). A versatile in vivo system for directed dissection of gene expression patterns. Nat Methods *8*, 231-237.

Goodman, C.S., and Doe, C.Q. (1993). Bate, M., Martinez-Arias, A., (Eds.), The Development of Drosophila melanogaster. Cold Spring Harbor Laboratory Press, pp. 1131-1206.

Gopfert, M.C., and Robert, D. (2002). The mechanical basis of Drosophila audition. Journal of Experimental Biology *205*, 1199-1208.

Gotz, K.G. (1964). Optomotory investigation of the visual-system of some eye mutations of the Drosophila fruit-fly. Kybernetik *2*, 77-91.

Griffin, R., Sustar, A., Bonvin, M., Binari, R., del Valle Rodriguez, A., Hohl, A.M., Bateman, J.R., Villalta, C., Heffern, E., Grunwald, D.*, et al.* (2009). The twin spot generator for differential Drosophila lineage analysis. Nat Methods *6*, 600-602.

Grillet, M., Dartevelle, L., and Ferveur, J.F. (2006). A Drosophila male pheromone affects female sexual receptivity. Proc Biol Sci *273*, 315-323.

Grosjean, Y., Rytz, R., Farine, J.P., Abuin, L., Cortot, J., Jefferis, G.S., and Benton, R. (2011). An olfactory receptor for food-derived odours promotes male courtship in Drosophila. Nature *478*, 236-240.

Groth, A.C., Fish, M., Nusse, R., and Calos, M.P. (2004). Construction of transgenic Drosophila by using the site-specific integrase from phage phiC31. Genetics *166*, 1775-1782.

Haag, J., Vermeulen, A., and Borst, A. (1999). The intrinsic electrophysiological characteristics of fly lobula plate tangential cells: III. Visual response properties. J Comput Neurosci *7*, 213-234.

Hall, J.C. (1977). Portions of central nervous-system controlling reproductive-behavior in Drosophila-melanogaster. Behavior Genetics *7*, 291-312.

Hall, J.C. (1994). The mating of a fly. Science *264*, 1702-1714.

Hamada, F.N., Rosenzweig, M., Kang, K., Pulver, S.R., Ghezzi, A., Jegla, T.J., and Garrity, P.A. (2008). An internal thermal sensor controlling temperature preference in Drosophila. Nature *454*, 217-220.

Hanesch, U., Fischbach, K.F., and Heisenberg, M. (1989). Neuronal architecture of the central complex in Drosophila-melanogaster. Cell and Tissue Research *257*, 343-366.

Hasemeyer, M., Yapici, N., Heberlein, U., and Dickson, B.J. (2009). Sensory neurons in the Drosophila genital tract regulate female reproductive behavior. Neuron *61*, 511-518.

Hayssen, V., and Kunz, T.H. (1996). Allometry of litter mass in bats: maternal size, wing morphology, and phylogeny. Journal of Mammalogy *77*, 476-490.

Heinrichs, V., Ryner, L.C., and Baker, B.S. (1998). Regulation of sex-specific selection of fruitless 5 ' splice sites by transformer and transformer-2. Molecular and Cellular Biology *18*, 450-458.

Heinze, S., and Homberg, U. (2007). Maplike representation of celestial E-vector orientations in the brain of an insect. Science *315*, 995-997.

Herculano-Houzel, S. (2009). The human brain in numbers: a linearly scaled-up primate brain. Front Hum Neurosci *3*, 31.

Herndon, L.A., and Wolfner, M.F. (1995). A Drosophila seminal fluid protein, Acp26Aa, stimulates egg laying in females for 1 day after mating. Proc Natl Acad Sci U S A *92*, 10114-10118.

Hoffmann, A.A. (1987). A laboratory study of male territoriality in the sibling species Drosophila-melanogaster and Drosophila-simulans. Animal Behaviour *35*, 807-818.

Horn, C., and Handler, A.M. (2005). Site-specific genomic targeting in Drosophila. Proceedings of the National Academy of Sciences of the United States of America *102*, 12483-12488.

Hoshijima, K., Inoue, K., Higuchi, I., Sakamoto, H., and Shimura, Y. (1991). Control of doublesex alternative splicing by transformer and transformer-2 in Drosophila Science *252*, 833-836.

Inoue, K., Hoshijima, K., Sakamoto, H., and Shimura, Y. (1990). Binding of the Drosophila sex-lethal gene-product to the alternative splice site of transformer primary transcript. Nature *344*, 461-463.

Ito, M., Masuda, N., Shinomiya, K., Endo, K., and Ito, K. (2013). Systematic analysis of neural projections reveals clonal composition of the Drosophila brain. Curr Biol *23*, 644-655.

Jacobs, M.E. (1960). Influence of light on mating of Drosophila-melanogaster. Ecology *41*, 182-188.

Jiggins, F.M., Hurst, G.D.D., and Majerus, M.E.N. (1998). Sex ratio distortion in Acraea encedon (Lepidoptera : Nymphalidae) is caused by a male-killing bacterium. Heredity *81*, 87-91.

Joesch, M., Schnell, B., Raghu, S.V., Reiff, D.F., and Borst, A. (2010). ON and OFF pathways in Drosophila motion vision. Nature *468*, 300-304.

Kamikouchi, A., Inagaki, H.K., Effertz, T., Hendrich, O., Fiala, A., Gopfert, M.C., and Ito, K. (2009). The neural basis of Drosophila gravity-sensing and hearing. Nature *458*, 165-171.

Kamikouchi, A., Shimada, T., and Ito, K. (2006). Comprehensive classification of the auditory sensory projections in the brain of the fruit fly Drosophila melanogaster. J Comp Neurol *499*, 317-356.

Keegan, L., Gill, G., and Ptashne, M. (1986). Separation of DNA binding from the transcription-activating function of a eukaryotic regulatory protein. Science *231*, 699-704.

Keisman, E.L., Christiansen, A.E., and Baker, B.S. (2001). The sex determination gene doublesex regulates the A/P organizer to direct sex-specific patterns of growth in the Drosophila genital imaginal disc. Developmental Cell *1*, 215-225.

Kimura, K., Hachiya, T., Koganezawa, M., Tazawa, T., and Yamamoto, D. (2008). Fruitless and doublesex coordinate to generate male-specific neurons that can initiate courtship. Neuron *59*, 759-769.

Kitamoto, T. (2001). Conditional modification of behavior in Drosophila by targeted expression of a temperature-sensitive shibire allele in defined neurons. J Neurobiol *47*, 81-92.

Koenig, J.H., Saito, K., and Ikeda, K. (1983). Reversible control of synaptic transmission in a single gene mutant of Drosophila melanogaster. J Cell Biol *96*, 1517-1522.

Kohatsu, S., Koganezawa, M., and Yamamoto, D. (2011). Female contact activates male-specific interneurons that trigger stereotypic courtship behavior in Drosophila. Neuron *69*, 498-508.

Kubli, E. (2003). Sex-peptides: seminal peptides of the Drosophila male. Cell Mol Life Sci *60*, 1689-1704.

Kurtovic, A., Widmer, A., and Dickson, B.J. (2007). A single class of olfactory neurons mediates behavioural responses to a Drosophila sex pheromone. Nature *446*, 542-546.

Kyriacou, C.P., and Hall, J.C. (1982). The function of courtship song rhythms in Drosophila. Animal Behaviour *30*, 794-801.

Lai, S.L., and Lee, T. (2006). Genetic mosaic with dual binary transcriptional systems in Drosophila. Nat Neurosci *9*, 703-709.

Lasbleiz, C., Ferveur, J.F., and Everaerts, C. (2006). Courtship behaviour of Drosophila melanogaster revisited. Animal Behaviour *72*, 1001-1012.

Lee, T., and Luo, L. (1999). Mosaic analysis with a repressible cell marker for studies of gene function in neuronal morphogenesis. Neuron *22*, 451-461.

Lee, T., and Luo, L. (2001). Mosaic analysis with a repressible cell marker (MARCM) for Drosophila neural development. Trends Neurosci *24*, 251-254.

Lewis, E.B. (1950). The phenomenon of position effect. Adv Genet *3*, 73-115.

Li, Y., Lu, H., Cheng, P.L., Ge, S., Xu, H., Shi, S.H., and Dan, Y. (2012). Clonally related visual cortical neurons show similar stimulus feature selectivity. Nature *486*, 118-121.

Liang, P., Heitwerth, J., Kern, R., Kurtz, R., and Egelhaaf, M. (2012). Object representation and distance encoding in three-dimensional environments by a neural

circuit in the visual system of the blowfly. Journal of Neurophysiology *107*, 3446-3457.

Liu, H., and Kubli, E. (2003). Sex-peptide is the molecular basis of the sperm effect in Drosophila melanogaster. Proc Natl Acad Sci U S A *100*, 9929-9933.

Liu, T.X. (2012). Anatomical and functional dissection of fruitless positive courtship circuit in Drosophila melanogaster. Thesis.

Lof, M.E., de Gee, M., and Hemerik, L. (2009). Odor-mediated aggregation enhances the colonization ability of Drosophila melanogaster. Journal of Theoretical Biology *258*, 363-370.

Luan, H., Peabody, N.C., Vinson, C.R., and White, B.H. (2006). Refined spatial manipulation of neuronal function by combinatorial restriction of transgene expression. Neuron *52*, 425-436.

Lung, O., and Wolfner, M.F. (2001). Identification and characterization of the major Drosophila melanogaster mating plug protein (vol 31, pg 543, 2001). Insect Biochemistry and Molecular Biology *32*, 109-109.

Manning, A. (1962). A sperm factor affecting receptivity of Drosophila melanogaster females. Nature *194*, 252-&.

Manning, A. (1966). Corpus allatum and sexual receptivity in female Drosophila melanogaster. Nature *211*, 1321-1322.

Manning, A. (1967). The control of sexual receptivity in female Drosophila. Animal Behaviour *15*, 239-250.

Manoli, D.S., Foss, M., Villella, A., Taylor, B.J., Hall, J.C., and Baker, B.S. (2005). Male-specific fruitless specifies the neural substrates of Drosophila courtship behaviour. Nature *436*, 395-400.

Moller, A.P., and Nielsen, J.T. (2006). Prey vulnerability in relation to sexual coloration of prey. Behavioral Ecology and Sociobiology *60*, 227-233.

Muto, A., Ohkura, M., Kotani, T., Higashijima, S., Nakai, J., and Kawakami, K. (2011). Genetic visualization with an improved GCaMP calcium indicator reveals

spatiotemporal activation of the spinal motor neurons in zebrafish. Proc Natl Acad Sci U S A *108*, 5425-5430.

Nagoshi, R.N., Mckeown, M., Burtis, K.C., Belote, J.M., and Baker, B.S. (1988). The control of alternative splicing at genes regulating sexual-differentiation in Drosophila-melanogaster. Cell *53*, 229-236.

Nakai, J., Ohkura, M., and Imoto, K. (2001). A high signal-to-noise Ca(2+) probe composed of a single green fluorescent protein. Nat Biotechnol *19*, 137-141.

Neuser, K., Triphan, T., Mronz, M., Poeck, B., and Strauss, R. (2008). Analysis of a spatial orientation memory in Drosophila. Nature *453*, 1244-U1244.

Nicolai, L.J., Ramaekers, A., Raemaekers, T., Drozdzecki, A., Mauss, A.S., Yan, J., Landgraf, M., Annaert, W., and Hassan, B.A. (2010). Genetically encoded dendritic marker sheds light on neuronal connectivity in Drosophila. Proc Natl Acad Sci U S A *107*, 20553-20558.

Nilsen, S.P., Chan, Y.B., Huber, R., and Kravitz, E.A. (2004). Gender-selective patterns of aggressive behavior in Drosophila melanogaster. Proc Natl Acad Sci U S A *101*, 12342-12347.

North, G., and Greenspan, R.J. (2007). Invertebrate Neurobiology. Cold Spring Harbor Laboratory Press. .

Ohkura, M., Matsuzaki, M., Kasai, H., Imoto, K., and Nakai, J. (2005). Genetically encoded bright Ca2+ probe applicable for dynamic Ca2+ imaging of dendritic spines. Anal Chem *77*, 5861-5869.

Ohtsuki, G., Nishiyama, M., Yoshida, T., Murakami, T., Histed, M., Lois, C., and Ohki, K. (2012). Similarity of visual selectivity among clonally related neurons in visual cortex. Neuron *75*, 65-72.

Oring, L.W., and Lank, D.B. (1986). Polyandry in spotted sandpipers: the impact of environment and experience. (Rubenstein, D. R., Wrangham, R. W. ed) In Ecological aspects of social evolution. Princeton Unverisity Press, Princeton, NJ.

Paradis, S., Sweeney, S.T., and Davis, G.W. (2001). Homeostatic control of presynaptic release is triggered by postsynaptic membrane depolarization. Neuron *30*, 737-749.

Peng, J., Chen, S., Busser, S., Liu, H., Honegger, T., and Kubli, E. (2005). Gradual release of sperm bound sex-peptide controls female postmating behavior in Drosophila. Curr Biol *15*, 207-213.

Penn, J.K.M., Zito, M.F., and Kravitz, E.A. (2010). A single social defeat reduces aggression in a highly aggressive strain of Drosophila. Proceedings of the National Academy of Sciences of the United States of America *107*, 12682-12686.

Pfeiffer, B.D., Jenett, A., Hammonds, A.S., Ngo, T.T., Misra, S., Murphy, C., Scully, A., Carlson, J.W., Wan, K.H., Laverty, T.R.*, et al.* (2008). Tools for neuroanatomy and neurogenetics in Drosophila. Proc Natl Acad Sci U S A *105*, 9715-9720.

Pfeiffer, B.D., Ngo, T.T., Hibbard, K.L., Murphy, C., Jenett, A., Truman, J.W., and Rubin, G.M. (2010). Refinement of tools for targeted gene expression in Drosophila. Genetics *186*, 735-755.

Pfeiffer, B.D., Truman, J.W., and Rubin, G.M. (2012). Using translational enhancers to increase transgene expression in Drosophila. Proc Natl Acad Sci U S A *109*, 6626-6631.

Poeck, B., Triphan, T., Neuser, K., and Strauss, R. (2008). Locomotor control by the central complex in Drosophila - An analysis of the tay bridge mutant. Developmental Neurobiology *68*, 1046-1058.

Potter, C.J., Tasic, B., Russler, E.V., Liang, L., and Luo, L. (2010). The Q system: a repressible binary system for transgene expression, lineage tracing, and mosaic analysis. Cell *141*, 536-548.

Reichardt, W. (1987). Evaluation of optical motion information by movement detectors. J Comp Physiol A *161*, 533-547.

Reichardt, W., and Wenking, H. (1969). Optical detection and fixation of objects by fixed flying flies. Naturwissenschaften *56*, 424-&.

Rideout, E.J., Dornan, A.J., Neville, M.C., Eadie, S., and Goodwin, S.F. (2010). Control of sexual differentiation and behavior by the doublesex gene in Drosophila melanogaster. Nature Neuroscience *13*, 458-U479.

Ringo, J. (1996). Sexual receptivity in insects. Annu Rev Entomol *41*, 473-494.

Ringo, J., Werczberger, R., Altaratz, M., and Segal, D. (1991). Female sexual receptivity is defective in juvenile hormone-deficient mutants of the apterous gene of Drosophila melanogaster. Behav Genet *21*, 453-469.

Ritzenthaler, S., Suzuki, E., and Chiba, A. (2000). Postsynaptic filopodia in muscle cells interact with innervating motoneuron axons. Nat Neurosci *3*, 1012-1017.

Ritzmann, R.E., Ridgel, A.L., and Pollack, A.J. (2008). Multi-unit recording of antennal mechano-sensitive units in the central complex of the cockroach, Blaberus discoidalis. Journal of Comparative Physiology a-Neuroethology Sensory Neural and Behavioral Physiology *194*, 341-360.

Robinett, C.C., Vaughan, A.G., Knapp, J.M., and Baker, B.S. (2010). Sex and the single cell. II. There Is a time and place for xex. Plos Biology *8*.

Root, C.M., Masuyama, K., Green, D.S., Enell, L.E., Nassel, D.R., Lee, C.H., and Wang, J.W. (2008). A presynaptic gain control mechanism fine-tunes olfactory behavior. Neuron *59*, 311-321.

Rosenzweig, M., Kang, K., and Garrity, P.A. (2008). Distinct TRP channels are required for warm and cool avoidance in Drosophila melanogaster. Proc Natl Acad Sci U S A *105*, 14668-14673.

Rubin, G.M., and Spradling, A.C. (1982). Genetic transformation of Drosophila with transposable element vectors. Science *218*, 348-353.

Ruta, V., Datta, S.R., Vasconcelos, M.L., Freeland, J., Looger, L.L., and Axel, R. (2010). A dimorphic pheromone circuit in Drosophila from sensory input to descending output. Nature *468*, 686-U106.

Ryner, L.C., Goodwin, S.F., Castrillon, D.H., Anand, A., Villella, A., Baker, B.S., Hall, J.C., Taylor, B.J., and Wasserman, S.A. (1996). Control of male sexual behavior and sexual orientation in Drosophila by the fruitless gene. Cell *87*, 1079-1089.

Sakurai, A., Koganezawa, M., Yasunaga, K., Emoto, K., and Yamamoto, D. (2012). Select interneuron clusters determine female sexual receptivity in Drosophila. Nat Commun *4*, 1825.

Satokangas, P., Liimatainen, J.O., and Hoikkala, A. (1994). Songs produced by the females of the Drosophila-virilis group of species. Behavior Genetics *24*, 263-272.

Saudan, P., Hauck, K., Soller, M., Choffat, Y., Ottiger, M., Sporri, M., Ding, Z., Hess, D., Gehrig, P.M., Klauser, S*., et al.* (2002). Ductus ejaculatorius peptide 99B (DUP99B), a novel Drosophila melanogaster sex-peptide pheromone. Eur J Biochem *269*, 989-997.

Schmidt, T., Choffat, Y., Schneider, M., Hunziker, P., Fuyama, Y., and Kubli, E. (1993). Drosophila suzukii contains a peptide homologous to the Drosophila melanogaster sex-peptide and functional in both species. Insect Biochem Mol Biol *23*, 571-579.

Schnell, B., Raghu, S.V., Nern, A., and Borst, A. (2012). Columnar cells necessary for motion responses of wide-field visual interneurons in Drosophila. J Comp Physiol A Neuroethol Sens Neural Behav Physiol *198*, 389-395.

Sepp, K.J., and Auld, V.J. (1999). Conversion of lacZ enhancer trap lines to GAL4 lines using targeted transposition in Drosophila melanogaster. Genetics *151*, 1093-1101.

Shorey, H.H. (1962). Nature of sound produced by Drosophila melanogaster during courtship. Science *137*, 677-&.

Siegel, R.W., and Hall, J.C. (1979). Conditioned responses in courtship behavior of normal and mutant Drosophila. Proc Natl Acad Sci U S A *76*, 3430-3434.

Simpson, J.H. (2009). Mapping and manipulating neural circuits in the fly brain. Adv Genet *65*, 79-143.

Sogabe, A., and Yanagisawa, Y. (2007). Sex-role reversal of a monogamous pipefish without higher potential reproductive rate in females. Proceedings of the Royal Society B-Biological Sciences *274*, 2959-2963.

Spieth, H.T. (1974). Courtship behavior in Drosophila. Annual Review of Entomology *19*, 385-405.

Stebbins, M.J., Urlinger, S., Byrne, G., Bello, B., Hillen, W., and Yin, J.C. (2001). Tetracycline-inducible systems for Drosophila. Proc Natl Acad Sci U S A *98*, 10775-10780.

Stebbins, M.J., and Yin, J.C. (2001). Adaptable doxycycline-regulated gene expression systems for Drosophila. Gene *270*, 103-111.

Stockinger, P., Kvitsiani, D., Rotkopf, S., Tirian, L., and Dickson, B.J. (2005). Neural circuitry that governs Drosophila male courtship behavior. Cell *121*, 795-807.

Stowers, R.S. (2011). An efficient method for recombineering GAL4 and QF drivers. Fly (Austin) *5*.

Strauss, R. (2002a). The central complex and the genetic dissection of locomotor behaviour. Curr Opin Neurobiol *12*, 633-638.

Strauss, R. (2002b). The central complex and the genetic dissection of locomotor behaviour. Current Opinion in Neurobiology *12*, 633-638.

Sturtevant, A.H. (1915). A sex-linked character in Drosophila repleta. American Naturalist *49*, 189-192.

Suster, M.L., Seugnet, L., Bate, M., and Sokolowski, M.B. (2004). Refining GAL4-driven transgene expression in Drosophila with a GAL80 enhancer-trap. Genesis *39*, 240-245.

Sweeney, S.T., Broadie, K., Keane, J., Niemann, H., and O'Kane, C.J. (1995). Targeted expression of tetanus toxin light chain in Drosophila specifically eliminates synaptic transmission and causes behavioral defects. Neuron *14*, 341-351.

Tallini, Y.N., Ohkura, M., Choi, B.R., Ji, G., Imoto, K., Doran, R., Lee, J., Plan, P., Wilson, J., Xin, H.B.*, et al.* (2006). Imaging cellular signals in the heart in vivo:

cardiac expression of the high-signal Ca2+ indicator GCaMP2. Proc Natl Acad Sci U S A *103*, 4753-4758.

Terhzaz, S., Rosay, P., Goodwin, S.F., and Veenstra, J.A. (2007). The neuropeptide SIFamide modulates sexual behavior in Drosophila. Biochem Biophys Res Commun *352*, 305-310.

Thistle, R., Cameron, P., Ghorayshi, A., Dennison, L., and Scott, K. (2012). Contact chemoreceptors mediate male-male repulsion and male-female attraction during Drosophila courtship. Cell *149*, 1140-1151.

Thorpe, H.M., and Smith, M.C. (1998). In vitro site-specific integration of bacteriophage DNA catalyzed by a recombinase of the resolvase/invertase family. Proc Natl Acad Sci U S A *95*, 5505-5510.

Tian, L., Hires, S.A., Mao, T., Huber, D., Chiappe, M.E., Chalasani, S.H., Petreanu, L., Akerboom, J., McKinney, S.A., Schreiter, E.R.*, et al.* (2009). Imaging neural activity in worms, flies and mice with improved GCaMP calcium indicators. Nat Methods *6*, 875-881.

Tinette, S., Zhang, L., and Robichon, A. (2004). Cooperation between Drosophila flies in searching behavior. Genes Brain and Behavior *3*, 39-50.

Toda, H., Zhao, X.L., and Dickson, B.J. (2012). The Drosophila female aphrodisiac pheromone activates ppk23(+) sensory neurons to elicit male courtship behavior. Cell Reports *1*, 599-607.

Traven, A., Jelicic, B., and Sopta, M. (2006). Yeast Gal4: a transcriptional paradigm revisited. EMBO Rep *7*, 496-499.

Triphan, T., Poeck, B., Neuser, K., and Strauss, R. (2010). Visual targeting of motor actions in climbing Drosophila. Current Biology *20*, 663-668.

Trivers, R.L. (1972). Parental Investment and Sexual Selection. (Campbell, B. ed.) Sexual Selection and the Descent of Man, 136-179.

Tully, T., and Quinn, W.G. (1985). Classical conditioning and retention in normal and mutant Drosophila melanogaster. J Comp Physiol A *157*, 263-277.

Venken, K.J., Schulze, K.L., Haelterman, N.A., Pan, H., He, Y., Evans-Holm, M., Carlson, J.W., Levis, R.W., Spradling, A.C., Hoskins, R.A., and Bellen, H.J. MiMIC: a highly versatile transposon insertion resource for engineering Drosophila melanogaster genes. Nat Methods *8*, 737-743.

Venken, K.J., Simpson, J.H., and Bellen, H.J. (2011). Genetic manipulation of genes and cells in the nervous system of the fruit fly. Neuron *72*, 202-230.

von Philipsborn, A.C., Liu, T., Yu, J.Y., Masser, C., Bidaye, S.S., and Dickson, B.J. (2011). Neuronal control of Drosophila courtship song. Neuron *69*, 509-522.

von Schilcher, F.V. (1976). Role of auditory stimuli in courtship of Drosophila melanogaster. Animal Behaviour *24*, 18-26.

Vrontou, E., Nilsen, S.P., Demir, E., Kravitz, E.A., and Dickson, B.J. (2006). fruitless regulates aggression and dominance in Drosophila. Nat Neurosci *9*, 1469-1471.

Wang, J., Ma, X., Yang, J.S., Zheng, X., Zugates, C.T., Lee, C.H., and Lee, T. (2004). Transmembrane/juxtamembrane domain-dependent Dscam distribution and function during mushroom body neuronal morphogenesis. Neuron *43*, 663-672.

Wang, L.M., and Anderson, D.J. (2010). Identification of an aggression-promoting pheromone and its receptor neurons in Drosophila. Nature *463*, 227-U114.

Wang, L.M., Han, X.Q., Mehren, J., Hiroi, M., Billeter, J.C., Miyamoto, T., Amrein, H., Levine, J.D., and Anderson, D.J. (2011). Hierarchical chemosensory regulation of male-male social interactions in Drosophila. Nature Neuroscience *14*, 757-U392.

White, J.G., Southgate, E., Thomson, J.N., and Brenner, S. (1986). The structure of the nervous system of the nematode Caenorhabditis elegans. Philos Trans R Soc Lond B Biol Sci *314*, 1-340.

White, K., Grether, M.E., Abrams, J.M., Young, L., Farrell, K., and Steller, H. (1994). Genetic control of programmed cell death in Drosophila. Science *264*, 677-683.

Wilson, C., Bellen, H.J., and Gehring, W.J. (1990). Position effects on eukaryotic gene expression. Annu Rev Cell Biol *6*, 679-714.

Wyatt, G.R., and Davey, K.G. (1996). Cellular and molecular actions of juvenile hormone .2. Roles of juvenile hormone in adult insects. Advances in Insect Physiology, Vol 26 *26*, 1-155.

Yagi, R., Mayer, F., and Basler, K. Refined LexA transactivators and their use in combination with the Drosophila Gal4 system. Proc Natl Acad Sci U S A *107*, 16166-16171.

Yang, C.H., Rumpf, S., Xiang, Y., Gordon, M.D., Song, W., Jan, L.Y., and Jan, Y.N. (2009). Control of the postmating behavioral switch in Drosophila females by internal sensory neurons. Neuron *61*, 519-526.

Yapici, N., Kim, Y.J., Ribeiro, C., and Dickson, B.J. (2008). A receptor that mediates the post-mating switch in Drosophila reproductive behaviour. Nature *451*, 33-37.

Yasuda, R., Nimchinsky, E.A., Scheuss, V., Pologruto, T.A., Oertner, T.G., Sabatini, B.L., and Svoboda, K. (2004). Imaging calcium concentration dynamics in small neuronal compartments. Sci STKE *2004*, pl5.

Yu, H.H., Awasaki, T., Schroeder, M.D., Long, F., Yang, J.S., He, Y., Ding, P., Kao, J.C., Wu, G.Y., Peng, H.*, et al.* (2013). Clonal development and organization of the adult Drosophila central brain. Curr Biol *23*, 633-643.

Yu, H.H., Chen, C.H., Shi, L., Huang, Y., and Lee, T. (2009a). Twin-spot MARCM to reveal the developmental origin and identity of neurons. Nat Neurosci *12*, 947-953.

Yu, H.H., Yang, J.S., Wang, J., Huang, Y., and Lee, T. (2009b). Endodomain diversity in the Drosophila Dscam and its roles in neuronal morphogenesis. J Neurosci *29*, 1904-1914.

Yu, J.Y. (2009). Mapping the courtship neuronal circuit of Drosophila melanogaster. Thesis.

Yu, J.Y., Kanai, M.I., Demir, E., Jefferis, G.S.X.E., and Dickson, B.J. (2010). Cellular organization of the neural circuit that drives Drosophila courtship behavior. Current Biology *20*, 1602-1614.

Yurkovic, A., Wang, O., Basu, A.C., and Kravitz, E.A. (2006). Learning and memory associated with aggression in Drosophila melanogaster. Proc Natl Acad Sci U S A *103*, 17519-17524.

Zars, T. (2000). Behavioral functions of the insect mushroom bodies. Curr Opin Neurobiol *10*, 790-795.

Zhang, Y.Q., Rodesch, C.K., and Broadie, K. (2002). Living synaptic vesicle marker: synaptotagmin-GFP. Genesis *34*, 142-145.

Curriculum Vitae

Yang Wu

EDUCATION

2009~2013 Ph.D., Molecular Biology, University of Vienna, Austria

2007~2009 M.Sc., Biological Sciences, National University of Singapore, Singapore

2001~2005 B.Sc. (Hons.), Biological Sciences, Chu KoChen Honors College, Zhejiang University, China

RESEARCH EXPERIENCE

2009~2013 Neuronal circuitry for social behavior in female *Drosophila melanogaster*
Dr. Barry Dickson
Research Institute of Molecular Biology, Vienna, Austria

2007~2009 Master thesis: Genetic of flowering time in *Arabidopsis thaliana*
Dr. Hao Yu
National University of Singapore, Singapore

2004~2005 Influence of hypoxia on learning and memory in neonatal mice
Dr. Jizeng Du
Zhejiang University, China

CONFERENCE

2011 EMBO conference, Vienna.

ACADEMIC AWARDS

2002, 2004 Dean Scholarship, Zhejiang University, China

2000 1st prize in National High School Students' Contest in Biology and 3rd prize in Computer Programming, Liaoning Province Shiyan High School, China

1998 Honored Student Leader of Shenyang City, No. 82 Junior High School, China

PUBLICATION

Li D, Liu C, Shen L, Wu Y, Chen H, Robertson M, Helliwell CA, Ito T, Meyerowitz EM, Yu H (2008) A repressor complex governs the integration of flowering signals in Arabidopsis. **Developmental Cell** 15: 110-120.